

This dissertation has been 64-200
microfilmed exactly as received

WINNICK, Jack, 1937-

LIQUID-LIQUID PHASE BEHAVIOR OF BINARY
SOLUTIONS AT ELEVATED PRESSURES.

The University of Oklahoma, Ph.D., 1963
Engineering, chemical

University Microfilms, Inc., Ann Arbor, Michigan

THE UNIVERSITY OF OKLAHOMA
GRADUATE COLLEGE

LIQUID-LIQUID PHASE BEHAVIOR OF BINARY
SOLUTIONS AT ELEVATED PRESSURES

A DISSERTATION
SUBMITTED TO THE GRADUATE FACULTY
in partial fulfillment of the requirements for the
degree of
DOCTOR OF PHILOSOPHY

BY
JACK WINNICK
Norman, Oklahoma
1963

LIQUID-LIQUID PHASE BEHAVIOR OF BINARY

SOLUTIONS AT ELEVATED PRESSURES

APPROVED BY

John Powers
Frank B. Cowfield
Stanley E. Babb, Jr.
Shepard D. Christian
Orville K. Crosser

DISSERTATION COMMITTEE

ABSTRACT

Binary liquid mixtures which are miscible at atmospheric temperature and pressure can sometimes be made to separate into two liquid phases by isothermal application of external pressure. Qualitative and quantitative methods of predicting such separations using fundamental thermodynamic data are presented. PVTX and density measurements were made for a binary system and used with available low-pressure solution behavior data to predict the occurrence of phase separation at elevated pressure. The predictions were checked by visual observation of phase separation at pressures up to 90,000 lb./sq. in.

ACKNOWLEDGMENT

The author wishes to thank all the members of the faculty of the Chemical Engineering Department at the University of Oklahoma for their help at various times during the course of the research. He is especially indebted to Professor John E. Powers, without whose help the study would never have begun.

Dr. S. E. Babb of the Physics Department of the University of Oklahoma contributed greatly to the design of several pieces of equipment and aided the progress of the investigation with many timely suggestions on high-pressure technique. Messrs. Gene Scott and Frank Maginnis were responsible not only for the construction of the auxiliary equipment but also for aid in their design.

Dr. Frank Canfield aided greatly near the conclusion of the study with helpful suggestions as to the processing of the data.

Mr. Elton Johnson was, for the last year of the research, always available for long hours in the laboratory.

Special notes of thanks are due Professor W. W. Robertson of the Physics Department at the University of Texas for the use of his visual observation high-pressure cell and to Professor Simon H. Wender of the Chemistry Department of the University of Oklahoma for the use of his cold room for the density determinations.

The study was made possible through use of funds from the National Science Foundation.

TABLE OF CONTENTS

	Page
LIST OF TABLES	vi
LIST OF ILLUSTRATIONS.	vii
Chapter	
I. INTRODUCTION	1
II. THERMODYNAMIC DEVELOPMENT.	4
III. CHOICE OF SYSTEM	19
IV. EQUIPMENT.	27
V. CALIBRATION OF EQUIPMENT	43
VI. PROCEDURE.	49
VII. RESULTS.	56
VIII. TREATMENT OF DATA.	69
IX. CONCLUSIONS.	92
TABLE OF NOMENCLATURE.	94
LITERATURE CITED	98
APPENDIX I	102
APPENDIX II.	109
APPENDIX III	113
APPENDIX IV.	123
APPENDIX V	126
APPENDIX VI.	132

LIST OF TABLES

Table	Page
1. Classification of Binary Liquid System	6
2. Choice of System	21
3. Listing of Balloons.	33
4. Calibration of Bellows	45
5. Results of Density Determinations.	57
6. (V/V^0) vs. P	63
7. Observed Liquid-Liquid Separations	67
8. (V/V^0) vs. X_{ace}	70
9. Molal Change in Volume on Mixing as a Function of Composition.	75
10. $\Delta \underline{V}^m$ vs. X Calculated Directly	79
11. Molal Change in Volume as a Function of Pressure	81
12. Molal Change in Free Energy on Mixing as a Function of Composition	83
13. Activity Data at One Atmosphere.	110
14. Consistency of Activity Data	111
15. Conversion of Free Energy Diagram to 0°C	122
16. Coefficients of Free Energy Polynomials and Activities at 0°C	127

LIST OF ILLUSTRATIONS

Figure	Page
1. Typical Change in Free Energy on Mixing (components miscible)	9
2. Hypothetical Change in Free Energy on Mixing (components partially miscible)	10
3. Unreliable Density Data	28
4. Pycnometer.	29
5. PVT Cell.	31
6. Enlargement of Bellows.	32
7. Measuring Bridge.	35
8. Optical Cell.	37
9. Mercury Reservoir	39
10. Experimental Apparatus.	40
11. Determination of Bellows Linearity.	47
12. Densities at 0°C and One Atmosphere	58
13. Molar Volume and $(\Delta \underline{v}^m)^0$	59
14. Sample R_S vs P.	61
15. Sample (V/V^0) vs. P	62
16. Observed and Extrapolated Separations	68
17. Sample (V/V^0) vs. X	73
18. $\Delta \underline{v}^m$ vs. X.	76
19. $\Delta \underline{v}^m$ vs. X.	77
20. Sample $\Delta \underline{v}^m$ vs. P	82
21. Change in Free Energy on Mixing	85
22. Change in Free Energy on Mixing	86
23. Prediction of Phase Behavior.	88
24. Hypothetical Change in Volume on Mixing	89

LIST OF ILLUSTRATIONS--Continued

Figure	Page
25. Predicted and Observed Phase Behavior	90
26. Isobaric Phase Behavior	91
27. Consistency of Activity Data.	112
28. Heat of Mixing.	114
29. Specific Heats as Functions of Temperature.	116
30. Specific Heats as Functions of Temperature.	117
31. Specific Heats as Functions of X.	118
32. Specific Heats as Functions of X.	119
33. Specific Heats as Functions of X.	120
34. Change in Free Energy from 35.17 to 0°C	121
35. Adiabatic Compressibility	124
36. Unsuccessful Sealing Devices.	133

CHAPTER I

INTRODUCTION

The ability to predict the physical and chemical properties of mixtures is one of the prime objectives of both physical chemists and chemical engineers. In the design of a process which involves the separation of two or more phases in equilibrium it is essential that the equilibrium phase behavior be known. If this behavior can be accurately predicted from other available or more easily obtainable data, it is, of course, highly desirable.

The separation of two liquid phases in equilibrium has been the subject of much study (3), and thus the phase behavior of a large number of binary liquid systems has been examined. While both temperature and pressure affect the phase behavior of such systems, few of the investigations have been concerned with the pressure effect (43). Correspondingly, the prediction of the effect of pressure on liquid-liquid phase behavior has received almost no attention whatever (31).

Previous Investigations

Timmermans (42) was among the first to investigate experimentally the effect of pressure on the mutual solubility of binary liquid mixtures. Subsequent studies of this type have been recently catalogued by Timmermans in a rather comprehensive fashion (43).

The general techniques for the use of thermodynamics in the prediction of the effect of pressure on phase equilibria were elucidated over thirty years ago by Adams (1), and have been used to predict isothermal solubility diagrams of solids in liquids (e.g., 1,2) and the isothermal solid-liquid phase behavior of binary systems which form solid solutions (47). There has, however, been no attempt to use these techniques for the prediction of the pressure effect on the mutual solubilities of liquid pairs.

Necessary Data

The thermodynamic prediction of the pressure effect on phase equilibria is invariably dependent on knowledge of solution behavior data for the system in question at some reference pressure as well as the volumetric properties of the phases as functions of pressure (1). Solution behavior data, usually expressed in terms of activities, has been the object of a large amount of research, especially for binary mixtures of nonelectrolytes (43). The volumetric properties of condensed phases under pressure have not been nearly as well investigated.

Although some cursory investigations of the effect of pressure on the properties of liquids were conducted in the latter part of the 19th century, comprehensive studies of this type began with Bridgman in the early part of this century (7). It was the work of Bridgman which raised the limits of obtainable working pressures to over a million psi. However, his work was devoted exclusively to pure compounds (e.g., 8,9, 11,12,14). The effect of pressure on the physical properties of liquid mixtures has, as would be expected, received less attention. Aside from compressibilities at one atmosphere, calculated from velocity of sound

measurements (e.g., 5,38,44), the works of Gibson (21), Eduljee (18), Reamer (33), and Cutler (17) concerning binary liquid compressions for a total of nine systems stand alone. The prediction of the pressure effect on liquids has been almost completely limited to single component systems (24,28,6).

It was decided to undertake an investigation which would allow visual observation of the effect of pressure on the liquid-liquid phase behavior of a binary mixture of nonelectrolytes and develop a method for predicting such behavior. The data necessary for the prediction would also be obtained and the predicted phase diagram compared with the observed results.

CHAPTER II

THERMODYNAMIC DEVELOPMENT

Qualitative Methods

The solution behavior of liquid mixtures is most readily represented by use of the activity coefficient:

$$\bar{\gamma}_i = \bar{f}_i / f_i^\circ X_i \quad (1)$$

where: $\bar{\gamma}_i$ = activity coefficient of component i in solution.

\bar{f}_i = fugacity of component i in solution.

f_i° = fugacity of pure component i at the temperature and pressure of the system.

X_i = mole fraction of component i.

Mixtures whose components exhibit activity coefficients near unity are classed as near ideal mixtures. Such mixtures will show little or no heat or volume change on mixing and will tend to remain completely mutually soluble over large ranges of temperature and pressure. Those mixtures whose components show activity coefficients substantially greater than unity will usually exhibit positive heat and volume changes on mixing*, while the opposite is true for those mixtures with activity coefficients less than one.

*The rigorous correlation between heat and volume change on mixing is shown by use of the thermodynamic relation derived by Mathieson (25);

Prigogine (32) has classified binary liquid systems as shown in Table 1. Because tendency toward immiscibility is characterized by large values of the activity coefficient the effect of temperature and pressure upon the mutual solubility can be predicted from their effect on the activity coefficients (24);

$$\left(\frac{\partial \ln \bar{\gamma}_i}{\partial T}\right)_P = - \frac{(\bar{H}_i - H_i)}{RT^2} \quad (3)$$

where: \bar{H}_i = partial molal enthalpy of component i in solution.

H_i = pure molal enthalpy of component i at the temperature and pressure of the system.

$$\text{and; } \left(\frac{\partial \ln \bar{\gamma}_i}{\partial P}\right)_T = \frac{\bar{V}_i - V_i}{RT} \quad (4)$$

where: \bar{V}_i = partial molal volume of component i in solution.

V_i = pure molal volume of component i at the temperature and pressure of the system.

Referring to Table 1, systems in classification I will all tend toward immiscibility with decreasing temperature because $\bar{\gamma}_i$ increases, while the opposite is true for those in classification II*. Increasing pres-

$$\left(\frac{\partial \Delta H^M}{\partial X}\right)_{P,T} = \left(\frac{\partial \Delta V^M}{\partial X}\right)_{P,T} \left(\frac{\partial P}{\partial \Delta V^M}\right)_{X,T} \left[\Delta V^M - T \left(\frac{\partial \Delta V^M}{\partial T}\right)_{P,X} \right] + \left(\frac{\partial \Delta H^M}{\partial X}\right)_{\Delta V^M, T} \quad (2)$$

where: ΔH^M = molal change in enthalpy on mixing.
 ΔV^M = molal change in volume on mixing.

who notes that the signs of ΔH^M and ΔV^M are usually the same. He reports further that the shapes of the curves of ΔH^M vs. X and ΔV^M vs. X are generally very similar for any given binary nonelectrolyte mixture.

*It is assumed that the sign of the term $(\bar{H}_i - H_i)$ is the same for each component as the sign of ΔH^M . While some deviations from this rule are known, they are extremely unusual, occurring only over small ranges of composition in very few systems (32).

TABLE 1
CLASSIFICATION OF BINARY LIQUID SYSTEMS

I. Systems with Positive (Endothermic) Heats of Mixing.

Activity Coefficients greater than unity.

A. Those with Positive Volume Changes on Mixing

Example: CS_2 - Acetone

*B. Those with Negative Volume Changes on Mixing

Example: n-hexane - nitrobenzene

II. Systems with Negative (Exothermic) Heats of Mixing.

Activity Coefficients less than unity.

A. Those with Positive Volume Changes on Mixing

None Known

B. Those with Negative Volume Changes on Mixing

Example: CO_2 - o-nitrophenol

*Only relatively few of these systems are known.

sure will bring about mutual insolubility for systems in classifications I.A. and II.A. while increasing solubility for those in I.B. and II.B.*

Quantitative Methods

Using the latter conditions it is possible to predict the effect that increasing external pressure will have upon the mutual solubility of a binary liquid system. In order to determine quantitatively the isothermal liquid-liquid phase diagram, however, a somewhat different attack must be pursued.

At constant pressure and temperature the criterion for equilibrium in any system is that the free energy must be at a minimum (27). Thus, a binary liquid system will separate into two liquid phases only if such a configuration will provide the system with a lower free energy than would be available if the system remained as a single phase. It remains only to provide a relationship which will allow the calculation of the free energy of such a system in terms of thermodynamic quantities which are either available or obtainable in the laboratory.

The molal free energy of mixing, ΔG^m , is defined as the difference between the free energy of a mole of solution and the sum of the free energies of the unmixed components:

$$[\Delta G^m = G_m - \sum(x_i G_i)]_{T,P,x} \quad (5)$$

where: G_m = molal free energy of the solution.

G_i = molal free energy of pure component i at the temperature and pressure of the system.

The molal free energy of the solution can be expressed in terms

*The same argument is true for ΔV^m .

of the partial molal free energies of the components in solution as:

$$[\underline{G}_M = \sum (X_i \bar{G}_i)]_{T,P,X} \quad (6)$$

where: \bar{G}_i = partial molal free energy of component i in solution.

These pure and partial molal free energies of the components, G_i and \bar{G}_i can be expressed in terms of fugacities as:

$$(d\bar{G}_i)_T \equiv (RT d \ln \bar{f}_i)_T \quad (7)$$

$$(\bar{G}_i - G_i)_{T,P} = RT \ln \left(\frac{\bar{f}_i}{f_i^0} \right)_{T,P} \quad (8)$$

Substituting Equations (6) and (8) into (5), the familiar expression is obtained for the free energy change on mixing in terms of the activity, \bar{a}_i :

$$\left[\frac{\Delta G^M}{RT} = \sum (X_i \ln \bar{a}_i) \right]_{T,P,X} \quad (9)$$

where: $\bar{a}_i = \bar{f}_i / f_i^0$

For a binary system Equation (9) reduces to:

$$\left[\frac{\Delta G^M}{RT} = (X_1 \ln \bar{a}_1 + X_2 \ln \bar{a}_2) \right]_{T,P,X} \quad (10)$$

True Free Energy Diagram

If the activities of some binary systems are known at some pressure P^* and temperature T , Equation (10) can be plotted and will appear similar to Figure 1 if substances 1 and 2 are completely miscible. If, instead, a plot such as Figure 2 is obtained, a miscibility gap is indi-

*Pressure cannot actually be held constant in determining the isothermal activity data. However, the small variation involved is disregarded.

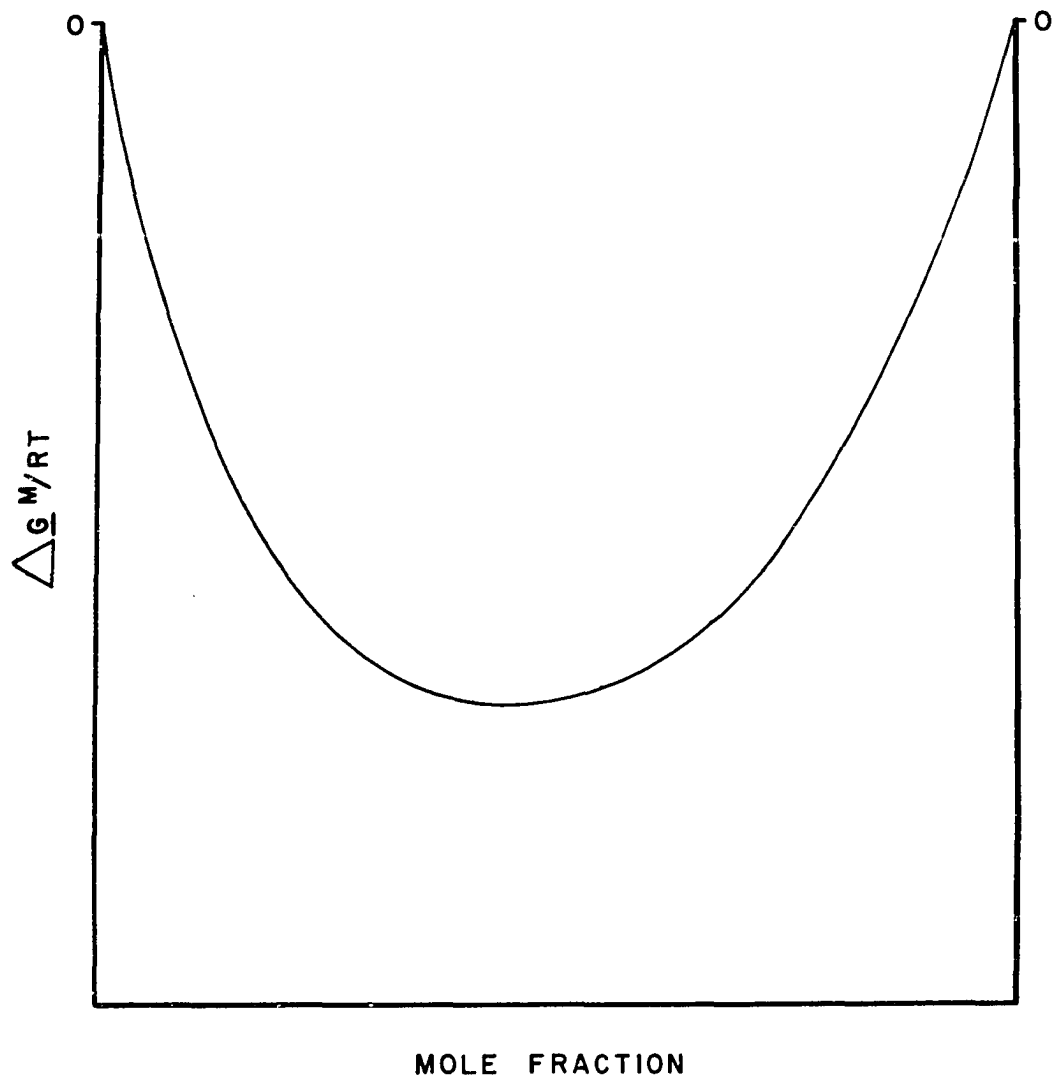


Figure 1.--Typical Change in Free Energy on Mixing
(components miscible)

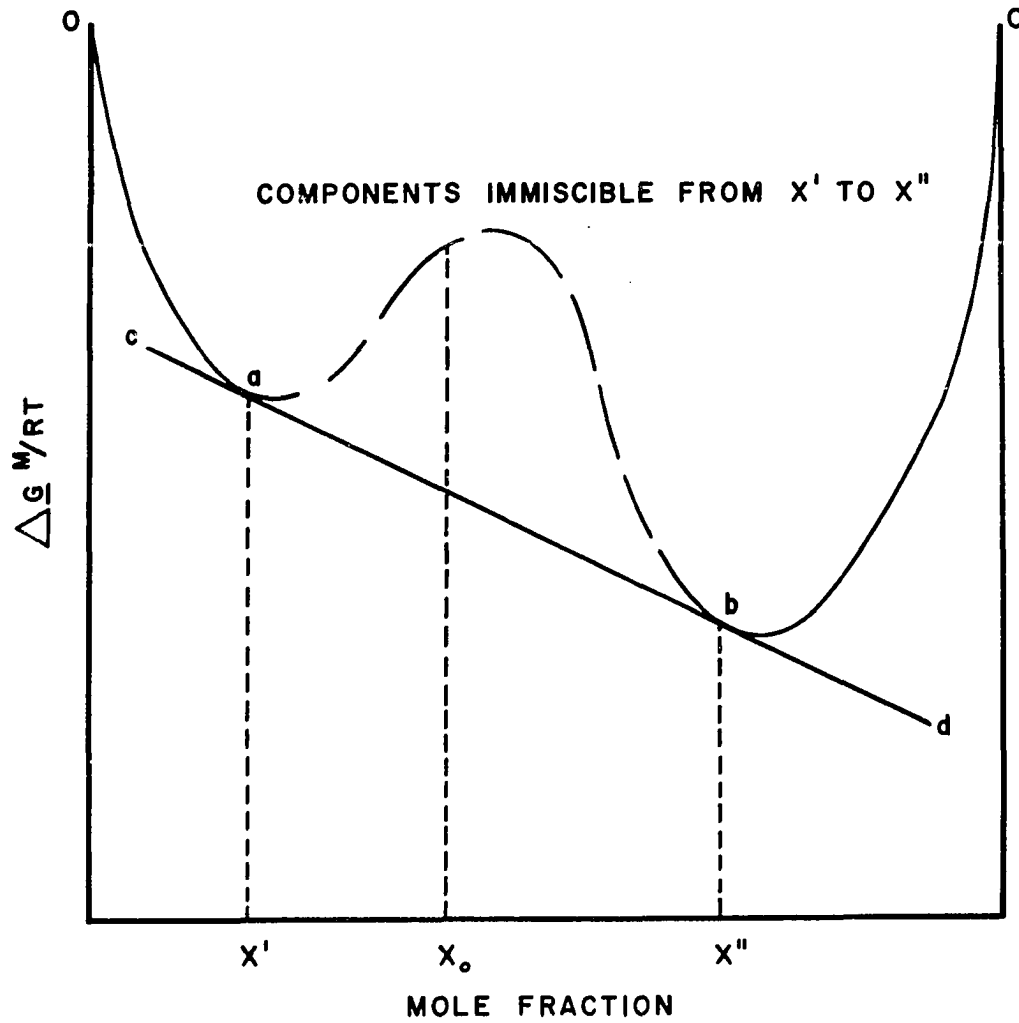


Figure 2.--Hypothetical Change in Free Energy on Mixing (components partially miscible)

cated. Any mixture whose homogeneous* concentration lies between X' and X'' , say at X_0 , will be in equilibrium only when two liquid phases of compositions X' and X'' are present. Points a and b are determined from the points of tangency of a straight line, cd. In this composition range the free energy of two such phases is lower than that resulting from a single phase. The portion of the curve between a and b is dotted because this is a hypothetical region.

With reference to Figure 2 it is now to be shown that: (1) the concentrations of the phases in equilibrium are determined by a straight line drawn tangent to the curve at two points** and (2) the true portion of the curve between these two concentrations is this same straight line.

(1) Equation (5) can be written for a binary mixture as:

$$\left[\Delta \underline{G}^M = X_1 \bar{G}_1 + X_2 \bar{G}_2 - X_1 \underline{G}_1 - X_2 \underline{G}_2 \right]_{T,P,X} \quad (11)$$

and differentiated with respect to X , at constant temperature and pressure:

$$\left(\frac{\partial \Delta \underline{G}^M}{\partial X_1} \right)_{T,P} = \bar{G}_1 - \bar{G}_2 - \underline{G}_1 + \underline{G}_2 + X_1 \left(\frac{\partial \bar{G}_1}{\partial X_1} \right)_{T,P} + X_2 \left(\frac{\partial \bar{G}_2}{\partial X_1} \right)_{T,P} \quad (12)$$

Equation (12) can be simplified by use of the Gibbs-Duhem equation which cancels the last two terms leaving:

$$\left(\frac{\partial \Delta \underline{G}^M}{\partial X_1} \right) = \bar{G}_1 - \bar{G}_2 - \underline{G}_1 + \underline{G}_2 \quad (13)$$

On differentiating Equation (11) again, this time with respect

*That concentration which would result were the mixture a single phase.

**This development is essentially the same as that of Rowlinson (35).

to X_2 , Equation (14) is obtained:

$$\left(\frac{\partial \Delta G^M}{\partial X_2}\right)_{T,P} = \bar{G}_2 - \bar{G}_1 - \underline{G}_2 + \underline{G}_1 \quad (14)$$

Combining Equations (11) and (13):

$$\bar{G}_2 = \Delta G^M - X_1 \left(\frac{\partial \Delta G^M}{\partial X_1}\right)_{T,P} + \underline{G}_2 \quad (15)$$

and combining Equations (11) and (14):

$$\bar{G}_1 = \Delta G^M - X_2 \left(\frac{\partial \Delta G^M}{\partial X_2}\right)_{T,P} + \underline{G}_1 \quad (16)$$

Using the criterion of equilibrium, namely:

$$\bar{G}_1' = \bar{G}_1'' \quad (17)$$

and

$$\bar{G}_2' = \bar{G}_2'' \quad (18)$$

where superscripts refer to phases, the following relationships are obtained:

$$(\Delta G^M)' - X_2' \left(\frac{\partial \Delta G^M}{\partial X_2}\right)'_{T,P} = (\Delta G^M)'' - X_2'' \left(\frac{\partial \Delta G^M}{\partial X_2}\right)''_{T,P} - \underline{G}_1' + \underline{G}_1'' \quad (19)$$

and

$$(\Delta G^M)' + X_1' \left(\frac{\partial \Delta G^M}{\partial X_2}\right)'_{T,P} = (\Delta G^M)'' + X_1'' \left(\frac{\partial \Delta G^M}{\partial X_2}\right)''_{T,P} - \underline{G}_2' + \underline{G}_2'' \quad (20)$$

where; $\underline{G}_1' = \underline{G}_1''$

and $\underline{G}_2' = \underline{G}_2''$

On subtraction of (19) from (20):

$$\left(\frac{\partial \Delta G^M}{\partial X_2}\right)'_{T,P} = \left(\frac{\partial \Delta G^M}{\partial X_2}\right)''_{T,P} \quad (21)$$

from which relation is observed that the slope of the free energy curve is the same at each equilibrium concentration.

Combining (21) with (19):

$$\left(\frac{\partial \Delta \underline{G}^m}{\partial X_2}\right)'_{T,P} = \left(\frac{\partial \Delta \underline{G}^m}{\partial X_2}\right)''_{T,P} = \left[\frac{(\Delta \underline{G}^m)' - (\Delta \underline{G}^m)''}{X_2' - X_2''} \right]_{T,P} \quad (22)$$

from which it is observed that the slope is as drawn in Figure 2, line cd.

(2) If the free energy of the mixture is now expressed in terms of two phases in equilibrium:

$$\Delta \underline{G}^m = X'(\Delta \underline{G}^m)' + X''(\Delta \underline{G}^m)'' \quad (23)$$

where: x' = mole fraction of total mixtures that exists in phase 1.

and: x'' = mole fraction of total mixture that exists in phase 2.

and making use of the mass balance:

$$X'' = 1 - X' \quad (24)$$

substituting (24) into (23):

$$\Delta \underline{G}^m = X'(\Delta \underline{G}^m)' + (1 - X')(\Delta \underline{G}^m)'' \quad (25)$$

and rearranging:

$$\Delta \underline{G}^m = (\Delta \underline{G}^m)'' + X' [(\Delta \underline{G}^m)' - (\Delta \underline{G}^m)''] \quad (26)$$

Since $(\Delta \underline{G}^m)'$ and $(\Delta \underline{G}^m)''$ are constant in the interval from x' to x'' , Equation (26) is that of a straight line between these two points. Thus, the true free energy diagram is as drawn in Figure 2. The reasons for general use of the continuous curve are given by Rowlinson (34) and will not be covered here.

Effect of Pressure

The effect of external pressure on the free energy of mixing of a binary liquid system can be described by starting again at the definition of the free energy change on mixing:

$$\left[\Delta \underline{G}^m = X_1 \bar{G}_1 + X_2 \bar{G}_2 - X_1 \underline{G}_1 - X_2 \underline{G}_2 \right]_{T, P, X} \quad (11)$$

and differentiating with respect to pressure at constant temperature and mole fraction:

$$\left(\frac{\partial \Delta \underline{G}^m}{\partial P} \right)_{T, X} = X_1 \left(\frac{\partial \bar{G}_1}{\partial P} \right)_{T, X} + X_2 \left(\frac{\partial \bar{G}_2}{\partial P} \right)_{T, X} - X_1 \left(\frac{\partial \underline{G}_1}{\partial P} \right)_T - X_2 \left(\frac{\partial \underline{G}_2}{\partial P} \right)_T \quad (27)$$

From basic thermodynamics:

$$\left(\frac{\partial \underline{G}_i}{\partial P} \right)_T = \underline{V}_i \quad (28)$$

and

$$\left(\frac{\partial \bar{G}_i}{\partial P} \right)_T = \bar{V}_i \quad (29)$$

Equations (28) and (29) can be substituted into (27) to obtain:

$$\left(\frac{\partial \Delta \underline{G}^m}{\partial P} \right)_{T, X} = X_1 \bar{V}_1 + X_2 \bar{V}_2 - X_1 \underline{V}_1 - X_2 \underline{V}_2 \quad (30)$$

The right hand side of Equation (30) is recognized as the definition of the change in volume on mixing for a binary system, $\Delta \underline{V}^m$.

Therefore, Equation (30) becomes:

$$\left(\frac{\partial \Delta \underline{G}^m}{\partial P} \right)_{T, X} = \Delta \underline{V}^m \quad (31)$$

Dividing both sides of (31) by RT and integrating between some pressure P_0 and some other pressure P :

$$\left(\frac{\Delta G^M}{RT}\right)_{T,P,X} = \left(\frac{\Delta G^M}{RT}\right)_{T,P_0,X} + \left(\frac{1}{RT} \int_{P_0}^P \Delta V^M dP\right)_{T,X} \quad (32)$$

Equation (10) can be substituted into Equation (32) to obtain:

$$\left(\frac{\Delta G^M}{RT}\right)_{T,P,X} = (x_1 \ln \bar{a}_1 + x_2 \ln \bar{a}_2)_{T,P_0,X} + \left(\frac{1}{RT} \int_{P_0}^P \Delta V^M dP\right)_{T,X} \quad (33)$$

By use of Equation (33), the free energy of mixing for any binary system can be evaluated at any pressure if activity data are known at some pressure P_0 and change in volume on mixing data are available from pressure P_0 to the pressure desired over the entire range of composition. If the system in question is completely miscible at pressure P_0 , but becomes partially immiscible upon application of pressure, this effect will be indicated by a straight line portion in the free energy diagram (See Figure 2) as explained above.

Effect of Temperature

The change in the free energy of mixing with temperature is described by the relation (24):

$$\left[\frac{\partial(\Delta G^M/RT)}{\partial T}\right]_{P,X} = -\frac{\Delta H^M}{RT^2} \quad (34)$$

where: ΔH^M = molal change in enthalpy on mixing.

Over any sizeable range in temperature, the function, ΔH^M , must be considered a variable also (24):

$$\left(\frac{\partial \Delta H^M}{\partial T}\right)_{P,X} = (C_P)_M - \sum [x_i (C_P)_i] \quad (35)$$

where: $(\underline{C}_p)_M$ = molal specific heat of the mixture at constant pressure.

$(\underline{C}_p)_i$ = molal specific heat of pure component i at constant pressure.

The right hand side of Equation (35) is denoted by $\Delta \underline{C}_p^M$, the molal change in specific heat on mixing:

$$\left(\frac{\partial \Delta H^M}{\partial T} \right) = \Delta \underline{C}_p^M \quad (36)$$

Equations (35) and (36) are combined and integrated to yield:

$$\left\{ \left[\frac{\Delta G^M}{RT} \right]_{T_2} - \left[\frac{\Delta G^M}{RT} \right]_{T_1} = - \int_{T_1}^{T_2} \left[\frac{(\Delta H^M)_{T_3} + \int_{T_3}^T \Delta \underline{C}_p^M dT}{RT^2} \right] dT \right\}_{P, X} \quad (37)$$

If an average value of $\Delta \underline{C}_p^M$ can be assumed without serious error,

Equation (37) reduces to

$$\left\{ \left[\frac{\Delta G^M}{RT} \right]_{T_2} - \left[\frac{\Delta G^M}{RT} \right]_{T_1} = - \int_{T_1}^{T_2} \left[\frac{(\Delta H^M)_{T_3} + (\Delta \bar{C}_p^M)(T - T_3)}{RT^2} \right] dT \right\}_{P, X} \quad (38)$$

where: $\Delta \bar{C}_p^M$ = arithmetic average of $\Delta \underline{C}_p^M$ between T and T_3 .

Determination of Activities from Free Energy

If Equation (10) is written on a total moles basis instead of a molal, or per mole basis and differentiated with respect to the number of moles of component one with the moles of component two fixed:

$$\left(\frac{\partial \Delta G^M}{\partial N_1} \right)_{T, P, N_2} = RT \left[\frac{\partial (N_1 \ln \bar{a}_1 + N_2 \ln \bar{a}_2)}{\partial N_1} \right]_{T, P, N_2} \quad (39)$$

where: ΔG^M = total change in free energy on mixing.

N_1 = moles of component 1.

N_2 = moles of component 2.

Carrying out the differentiation:

$$\left(\frac{\partial \Delta G^M}{\partial N_1}\right)_{T,P,N_2} = RT \left[N_1 \frac{\partial \ln \bar{a}_1}{\partial N_1} + \ln \bar{a}_1 + N_2 \frac{\partial \ln \bar{a}_2}{\partial N_1} \right] \quad (40)$$

But the Gibbs-Duhem equation equates the differential terms on the right hand side of Equation (40);

$$N_1 \frac{\partial \ln \bar{a}_1}{\partial N_1} = -N_2 \frac{\partial \ln \bar{a}_2}{\partial N_1} \quad (41)$$

$$\text{So; } \left(\frac{\partial \Delta G^M}{\partial N_1}\right)_{T,P,N_2} = RT \ln \bar{a}_1, \quad (42)$$

$$\text{Because; } \Delta G^M = (N_1 + N_2) \Delta \underline{G}^M; \quad (43)$$

$$\ln \bar{a}_1 = \left\{ \frac{\partial [(N_1 + N_2) \Delta \underline{G}^M / RT]}{\partial N_1} \right\}_{T,P,N_2} \quad (44)$$

If the free energy of mixing diagram is represented by a power series:

$$\frac{\Delta \underline{G}^M}{RT} = \sum [A_i X_2^{(i-1)}] = f(X_2) \quad (45)$$

where: A_i = coefficient of i^{th} term.

X_2 = mole fraction of 2nd component.

Then;

$$\ln \bar{a}_1 = \left\{ \frac{\partial [(N_1 + N_2) f(X_2)]}{\partial N_1} \right\}_{T,P,N_2} \quad (46)$$

$$\text{But, } X_2 = N_2 / (N_1 + N_2) \quad (47)$$

$$\text{So; } \ln \bar{a}_1 = \left\{ \frac{\partial [(N_1 + N_2) f(N_2 / (N_1 + N_2))]}{\partial N_1} \right\}_{T,P,N_2} \quad (48)$$

Carrying out this differentiation:

$$\ln \bar{a}_1 = (N_1 + N_2) \left[\frac{-A_2 N_2}{(N_1 + N_2)^2} - \frac{2A_3 N_2^2}{(N_1 + N_2)^3} - \frac{3A_4 N_2^3}{(N_1 + N_2)^4} - \dots \right] \\ + \left[A_1 + \frac{A_2 N_2}{(N_1 + N_2)} + \frac{A_3 N_2^2}{(N_1 + N_2)^2} + \frac{A_4 N_2^3}{(N_1 + N_2)^3} + \dots \right] \quad (49)$$

Simplifying Equation (49) and replacing X_2 for $N_2/(N_1 + N_2)$:

$$\ln \bar{a}_1 = A_1 - A_3 X_2^2 - 2A_4 X_2^3 - 3A_5 X_2^4 - \dots \quad (50)$$

or;

$$\ln \bar{a}_1 = - \sum_{i=3}^M [(i-2)A_i X_2^{(i-1)}] \quad (51)$$

where; M = number of coefficients in polynomial for $\Delta G^M/RT$

because A_1 is forced to zero in the curve fitting of $\Delta G^M/RT$. So that $\ln \bar{a}_1$ is directly obtained from the coefficients of the polynomial expressing $\Delta G^M/RT$.

Similarly $\ln \bar{a}_2$ can be found:

$$\left(\frac{\partial \Delta G^M}{\partial N_2} \right)_{T, P, N_1} = RT \ln \bar{a}_2 \quad (52)$$

$$\ln \bar{a}_2 = \left\{ \frac{\partial [(N_1 + N_2) f(N_2/(N_1 + N_2))]}{\partial N_2} \right\}_{T, P, N_1} \quad (53)$$

$$\ln \bar{a}_2 = \sum [(i-1)A_i X_2^{(i-2)}] - \sum [(i-2)A_i X_2^{(i-1)}] \quad (54)$$

CHAPTER III

CHOICE OF SYSTEM

Selection

Use of the qualitative tools presented in Chapter II permits the selection of a system which will separate into two liquid phases under isothermally increasing pressures. Three criteria were used in this selection:

1. The system must be a binary nonelectrolyte solution.
2. It must either;
 - a) have been noted to separate under isothermally increasing pressures or
 - b) be expected to do so as a consequence of large activity coefficients at one atmosphere pressure, and positive volume changes on mixing.
3. Solidification must not occur at pressures below those necessary to cause liquid-liquid phase separation.*

To make a quantitative prediction of the phase diagram using Equation (33) it is necessary that the activities at one atmosphere and

*Relations which allow the prediction of solidification of a binary system under pressure have been reported by Adams (1) for eutectic forming mixtures and by Winnick and Powers (47) for solid solution forming mixtures. Such predictions are, however, dependent on knowledge of the behavior of the solid phase under pressure, which is, at present, extremely scarce.

volumetric behavior over the entire range of pressures be known. The latter data are virtually non-existent; however, the existence of the former can be used as a fourth criterion in the choice of the system:

4. The activities must be accurately known at a temperature where phase separation can be induced with pressures within the range of the experimental equipment (90,000 psi).

A large number of systems was considered and Table 2 lists these as to whether they: 1) are known to separate under increasing pressure; 2) possess large values of activity coefficients at one atmosphere; 3) exhibit positive volume changes on mixing and; 4) have accurate activity data available. All of the systems listed show positive enthalpy changes on mixing and hence belong in classification I (See Chapter II).

Of these mixtures, the seven with accurate activity data as well as positive or unknown volume changes on mixing were chosen. These were: carbon tetrachloride-acetonitrile, benzene-acetonitrile, butyl acetate-methanol, n-hexane-chlorobenzene, n-butanol-benzene, carbon disulfide-methylal, and carbon disulfide-acetone. Because, as described in Chapter II, the only type of known binary system which separates into two liquid phases under increasing pressures is an endothermic system with an upper critical solution temperature, these systems will also tend to separate if the temperature is sufficiently lowered isobarically. For this reason, these seven mixtures were cooled slowly to liquid nitrogen temperatures. In all but two of the solutions, carbon disulfide-methylal and carbon disulfide-acetone, freezing occurred before any sign of mutual immiscibility. From these two systems, carbon disulfide-acetone was chosen for study because its activity coefficients were more accurately known.*

*See Appendix II.

TABLE 2
CHOICE OF SYSTEM

System	Reference	Separates Under Increasing Pressure	High Values of Activity Coefficients?	Positive Volume Change On Mixing	Accurate Activity Data?
Methanol-- cyclohexane	65	Yes	Yes	Yes	No
Methanol-- n-hexane	66	Yes	Yes	Yes	No
Carbon tetrachloride-- nitromethane	63	Yes	Yes	Yes	No
Aniline-- cyclohexane	66	Yes	Yes	Yes	No
Acetonitrile-- cyclohexane	63	Yes	Yes	Yes	No
Acetic Anhydride-- cyclohexane	63	Yes	Yes	Yes	No
Nitromethane-- cyclohexane	63	Yes	Yes	Yes	No
Aniline-- n-decane	63	Yes	Yes	Yes	No
Cyclohexane-- methylene iodide	66	Yes	Yes	Yes	No
Benzene-- formic acid	66	Yes	Yes	Yes	No
Ethyl acetate-- i-amyl ether	58	?	Yes	Yes	No
Ethyl acetate-- amyl acetate	58	?	Yes	Yes	No
Benzene-- m-xylol	58	?	Yes	Yes	No

TABLE 2--Continued

System	Reference	Separates Under Increasing Pressure?	High Values of Activity Coefficients?	Positive Volume Change On Mixing?	Accurate Activity Data?
o-xylol-- m-xylol	58	?	Yes	Yes	No
Nitrobenzene-- monoethylaniline	58	?	Yes	Yes	No
Nitrobenzene-- o-toluidine	58	?	Yes	Yes	No
Nitrobenzene-- monoethylaniline	58	?	Yes	Yes	No
Benzene-- m-kresol	58	?	Yes	Yes	No
Toluene-- m-kresol	58	?	Yes	Yes	No
Methanol-- propanol	58	?	Yes	Yes	No
Ethanol-- cyclohexane	56	?	Yes	Yes	No
n-Propanol-- cyclohexane	56	?	Yes	Yes	No
n-Butanol-- cyclohexane	56	?	Yes	Yes	No
Benzene-- i-butanol	56	?	Yes	Yes	No
Carbon disulfide-- ethanol	62	?	Yes	Yes	No
Carbon disulfide-- n-propanol	62	?	Yes	Yes	No
Glutaronitrile-- ethanolamine	61	?	Yes	Yes	No

TABLE 2--Continued

System	Reference	Separates Under Increasing Pressure?	High Values of Activity Coefficients?	Positive Volume Change On Mixing?	Accurate Activity Data?
Glutaronitrile-- n-methylacetamide	61	?	Yes	Yes	No
Glutaronitrile-- ethyl glycol	61	?	Yes	Yes	No
Glutaronitrile-- pyridine	61	?	Yes	Yes	No
Glutaronitrile-- ethylene cyanohydrin	61	?	Yes	Yes	No
Glutaronitrile-- cyclohexane	61	?	Yes	Yes	No
Glutaronitrile-- adiponitrile	61	?	Yes	Yes	No
Glutaronitrile-- formamide	61	?	Yes	Yes	No
Ethyl acetate-- carbon disulfide	62	?	Yes	Yes	No
Hexane-- acetone	62	?	Yes	Yes	No
Carbon disulfide-- hexane	62	?	Yes	Yes	No
Ethanol-- ethyl acetate	62	?	Yes	Yes	No
Benzene-- methyl acetate	62	?	Yes	Yes	No
Carbon tetrachloride-- ethanol	59	?	Yes	?	No
Benzene-- ethanol	52	?	Yes	?	No

TABLE 2--Continued

System	Reference	Separates Under Increasing Pressure?	High Values of Activity Coefficients?	Positive Volume Change On Mixing?	Accurate Activity Data?
Carbon tetrachloride--					
acetonitrile	52	?	Yes	?	Yes
Benzene--					
acetonitrile	54	?	Yes	?	Yes
Ether--					
acetonitrile	57	?	Yes	?	No
Benzene--					
i-propanol	53	?	Yes	?	No
2, 2, 4 Trimethylpentane--					
ethanol	51	?	Yes	?	No
Butyl acetate--					
methanol	64	?	Yes	?	Yes
Ethanol--					
methylcyclohexane	52	?	Yes	Yes	No
Benzene--					
acetic acid	67	?	Yes	Yes	No
Acetone--					
i-propanol	60	?	Yes	Yes	No
Benzene--					
methanol	59	?	Yes	?	Yes
Carbon tetrachloride--					
acetic acid	59	?	Yes	?	No
Carbon tetrachloride--					
trifluoroacetic acid	59	?	Yes	?	No
n-Hexane--					
chlorobenzene	50	?	No	?	Fair
Acetic acid--					
toluene	67	?	Yes	Yes	No

TABLE 2--Continued

System	Reference	Separates Under Increasing Pressure?	High Values of Activity Coefficients?	Positive Volume Change On Mixing?	Accurate Activity Data?
Methanol-- acetonitrile	57	?	Yes	?	No
Methyl acetate-- ethanol	49	?	Yes	?	No
Benzene-- nitromethane	53	No	Yes	No	Yes
n-Butanol-- benzene	55	?	No	Yes	Fair
Carbon disulfide-- methylal	67	?	Yes	Yes	Yes
Carbon disulfide-- acetone	67	?	Yes	Yes	Yes

References are to separation under pressure when observed.

Otherwise, activity coefficient data are referred to where available.

In the absence of either, change in volume on mixing at one atmosphere is noted.

Adjustment of Temperature

Although the activities for the chosen binary liquid system, acetone-carbon disulfide, are known quite accurately at 35.17°C, the pressure needed to cause liquid-liquid phase separation at this temperature would be beyond the range of the equipment. If a prediction of the phase behavior is to be made and compared with that observed, the temperature must be identical. The temperature 0°C was chosen.*

In order to convert the free energy diagram as determined from the data of Zawidzky (48) from 35.17°C to 0°C, the enthalpy of mixing data of Schmidt (36) at 16°C, and the specific heat data of Staveley (41) at 20°, 30° and 40°C were used along with the thermodynamic relations presented in Chapter II. The details of the calculations as well as the results can be found in Appendix III.

To complete the prediction of the pressure-composition liquid-liquid phase diagram then, the volumetric behavior of the system at 0°C over the necessary range in pressure and complete range of composition is all that is yet required.

*While it was originally believed that 0°C would be low enough to allow adequate determination of the observed phase diagram, it was later decided to lower the temperature of these observations to -2°C in order to provide a more complete diagram without jeopardizing the equipment.

CHAPTER IV

EQUIPMENT

Pycnometer

As mentioned in Chapter III, the thermodynamic functions necessary for the prediction of the isothermal phase diagram must be known at a temperature at which phase separation can be induced below 90,000 psi. For the chosen system, acetone-carbon disulfide, this temperature, at which all but the visual measurements were made, was 0°C. (See "Visual Observation" subheading in Chapter VI.)

The density data available for this system at 0°C were found to be unreliable (19,40,45) (See Figure 3). Thus, since the densities of the mixtures need be accurately known in order to determine the P-V-T behavior (see "Treatment of Data"), an investigation toward this end was carried out.

The measurements were made using a 10 ml high-volatility type pycnometer (See Figure 4). In a small room maintained at -2 to 2°C and equipped with a Seederer-Kohlbusch analytical balance, the necessary materials were left for a day in order to bring them as nearly to thermal equilibrium with the surroundings as possible. A 1000 ml beaker filled with clear ice and distilled water served as the constant temperature bath. As testification to the temperature of the room, the distilled water maintained a partly liquid-partly frozen condition over a 5 day period.

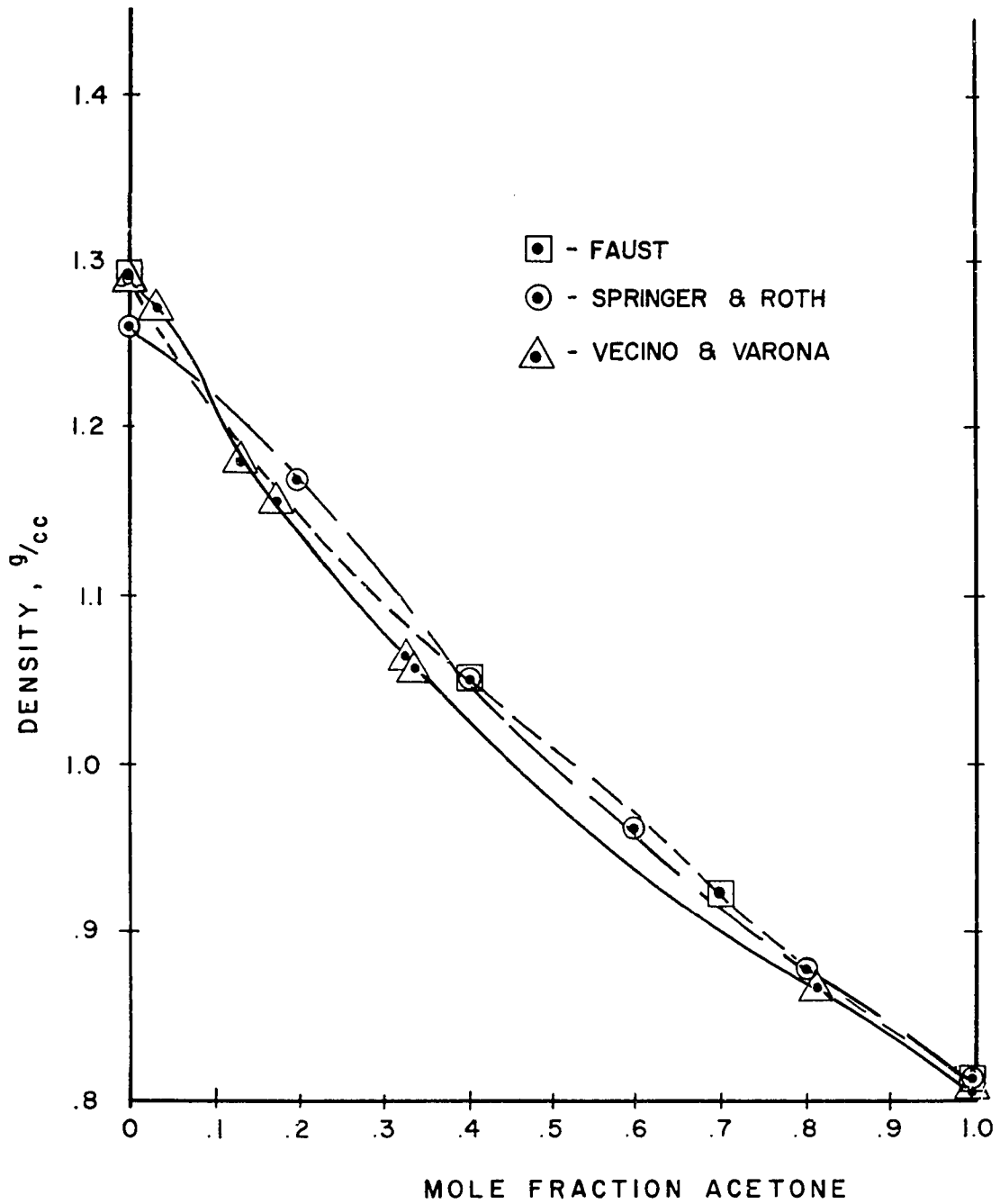


Figure 3.--Unreliable Density Data

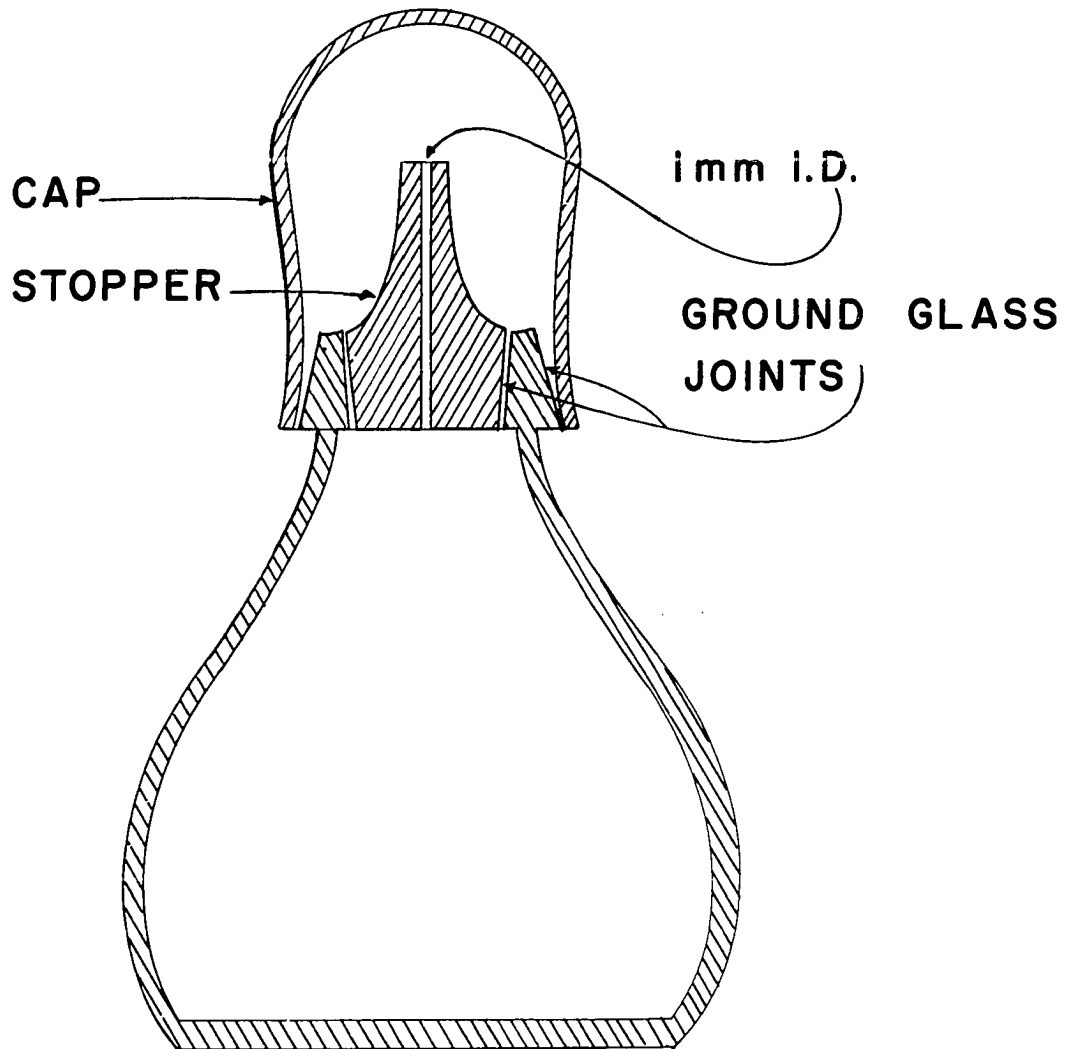


Figure 4.--Pycnometer

P-V-T Cell

In order to ascertain the change in volume on mixing as a function of pressure over the entire range of composition, a piezometer similar to that used by Bridgman (10) was used. Figures 5 and 6 show the piezometer and high pressure enclosure. The cell consists of a four inch diameter hardened steel vessel, 1, with a six inch diameter sleeve, 2, shrunk over it. The pressure seal is made with a rubber "O" ring, 17, a lead washer, 18, and a steel ring, 19.

The mixture under observation is contained in a brass sylphon bellows, 7, which is sealed by means of the cap screw, 3. This bellows is held firmly in place at one end by the retainer, 5, also made of brass. The other end of the bellows is free to move. A piece of Karma wire, 9, is fixed at one end to this free end of the bellows by a set screw, 24, and at the other to two flexible electrical connections, 13. One is a current and the other a potential lead. This orientation eliminates the necessity of correcting for lead wire resistance. The connections are led out of the cell through porcelain insulators, 14. The Karma wire passes across a fixed contact, 25, to which it is firmly pressed by a spring, 11, and Teflon piston, 12. An electrical lead from the fixed contact, 30, as well as the leads from a chromel alumel thermocouple, 33, 34, are brought out of the pressure chamber in the same manner as the Karma wire leads. The thermocouple junction lies in the space to the right of the Teflon piston, 12. The bellows is removed from the cell body by unscrewing the end plug, 21, from the cell body. Three brass set screws, 6, holding the bellows to the retainer, 5, and the screw, 24, holding the Karma wire to the bellows are then removed, releasing the bellows for cleaning and refilling.

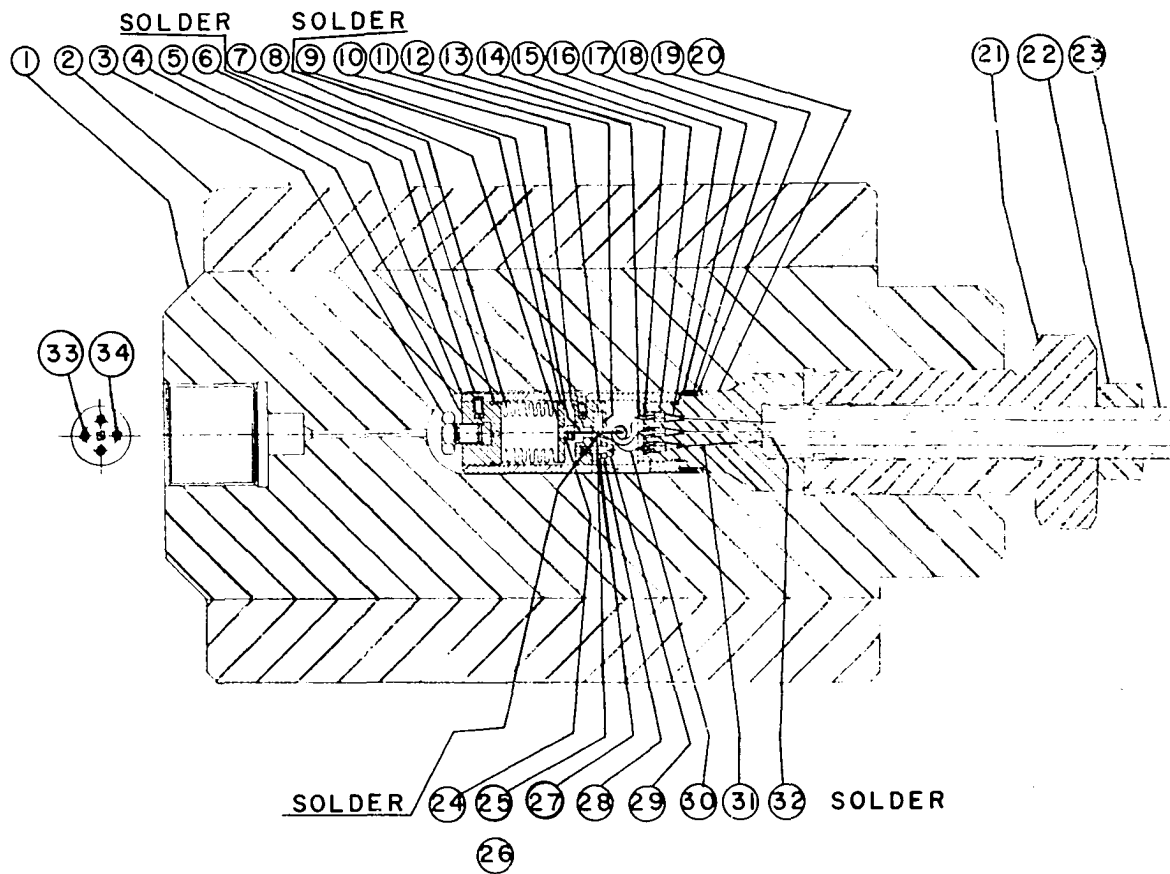


Figure 5.--PVT Cell (Courtesy Harwood Engineering Company)

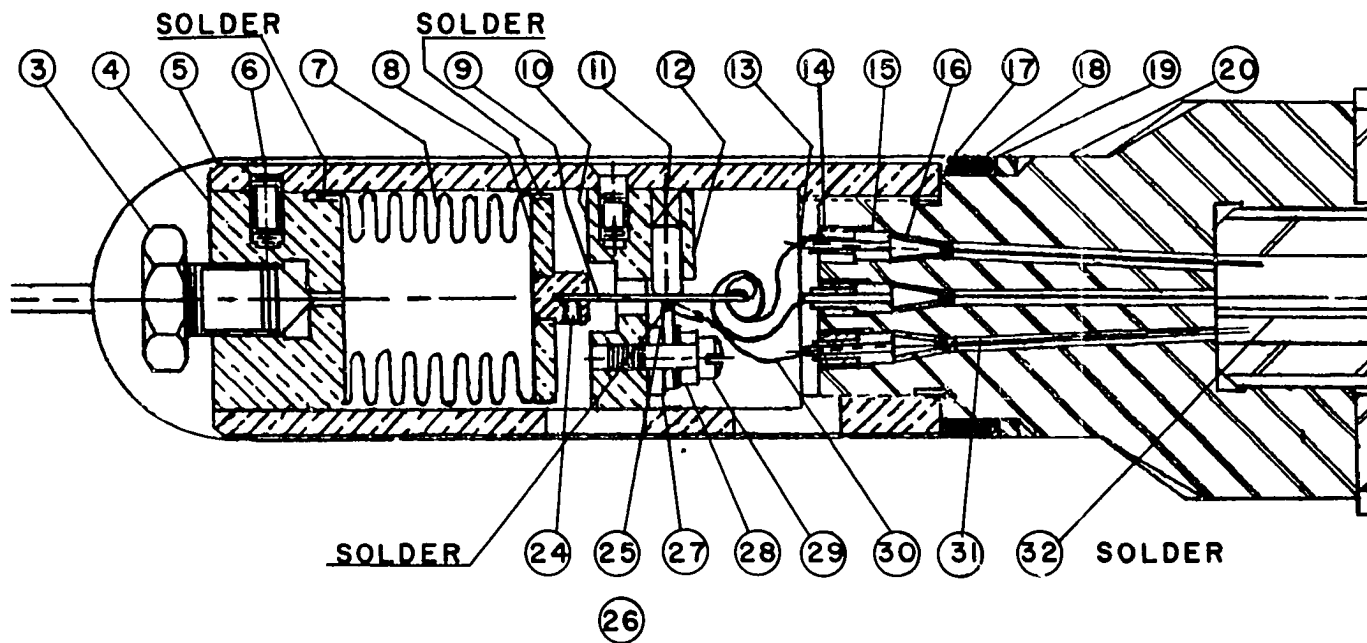


Figure 6.--Enlargement of Bellows (Courtesy Harwood Engineering Company)

TABLE 3

LISTING OF BALLOONS

-
-
- 1 - Vessel
 - 2 - Sleeve
 - 3 - Cap screw
 - 4 - Front bellows end plate
 - 5 - Retainer
 - 6 - Set screws
 - 7 - Syphon bellows
 - 8 - Rear bellows end plate
 - 9 - Karma wire
 - 10 - Fixed connection housing
 - 11 - Spring
 - 12 - Teflon piston
 - 13 - Electrical connection
 - 14 - Porcelain insulator
 - 15 - Unsupported area seal
 - 16 - Unsupported area seal
 - 17 - O-ring
 - 18 - Lead washer
 - 19 - Steel ring
 - 20 - Closure
 - 21 - Drive plug
 - 22 - Nut
 - 23 - Closure bolt
 - 24 - Set screw
 - 25 - Fixed contact
 - 26 - Fixed contact insulator
 - 27 - Insulating spacer
 - 28 - Insulating spacer
 - 29 - Insulating spacer
 - 30 - Electrical leads
 - 31 - Electrical leads
 - 32 - Ground
 - 33 - Thermocouple lead
 - 34 - Thermocouple lead
-
-

The entire cavity around the bellows is filled with the pressure transmission fluid, JP-4 jet fuel. This was chosen for its comparatively low viscosity at high pressures and low temperatures, its low cloud point, and its relatively low cost. As pressure is applied to the pressure transmission fluid, the bellows contracts, equilibrating the pressure within it to that without. This movement occurs along its longitudinal axis due to the design of the bellows (10). The Karma wire is pulled past the fixed contact, and a change in the resistance between either end of the wire and the fixed contact is observed. Suitable calibration yields change in volume to be ascertained as a function of change in resistance (See Chapter V).

The thermocouple potential was measured using a Leeds and Northrup Precision Potentiometer. With it, the temperature could be measured to $\pm 0.2^{\circ}\text{C}$. The small temperature control bath (See "Temperature Control" subheading in this chapter) served as the cold junction. No calibration was carried out.

Measuring Bridge

The electrical bridge used to note this change in resistance is shown as Figure 7. When the slide wire has ceased to move on the fixed contact, the resistance of the segment between the fixed contact and the right hand end of the wire is balanced against the lower section of the bridge by closing the upper DPDT switch to the left, and adjusting the 500 ohm rheostat. A Rubicon Instrument Company Galvanometer indicates the null in the circuit. The upper DPDT switch is then closed to the right and the upper portion of the bridge is balanced against the lower by adjusting the 7 ohm rheostat, $R_w - R_w'$. This configuration eliminates

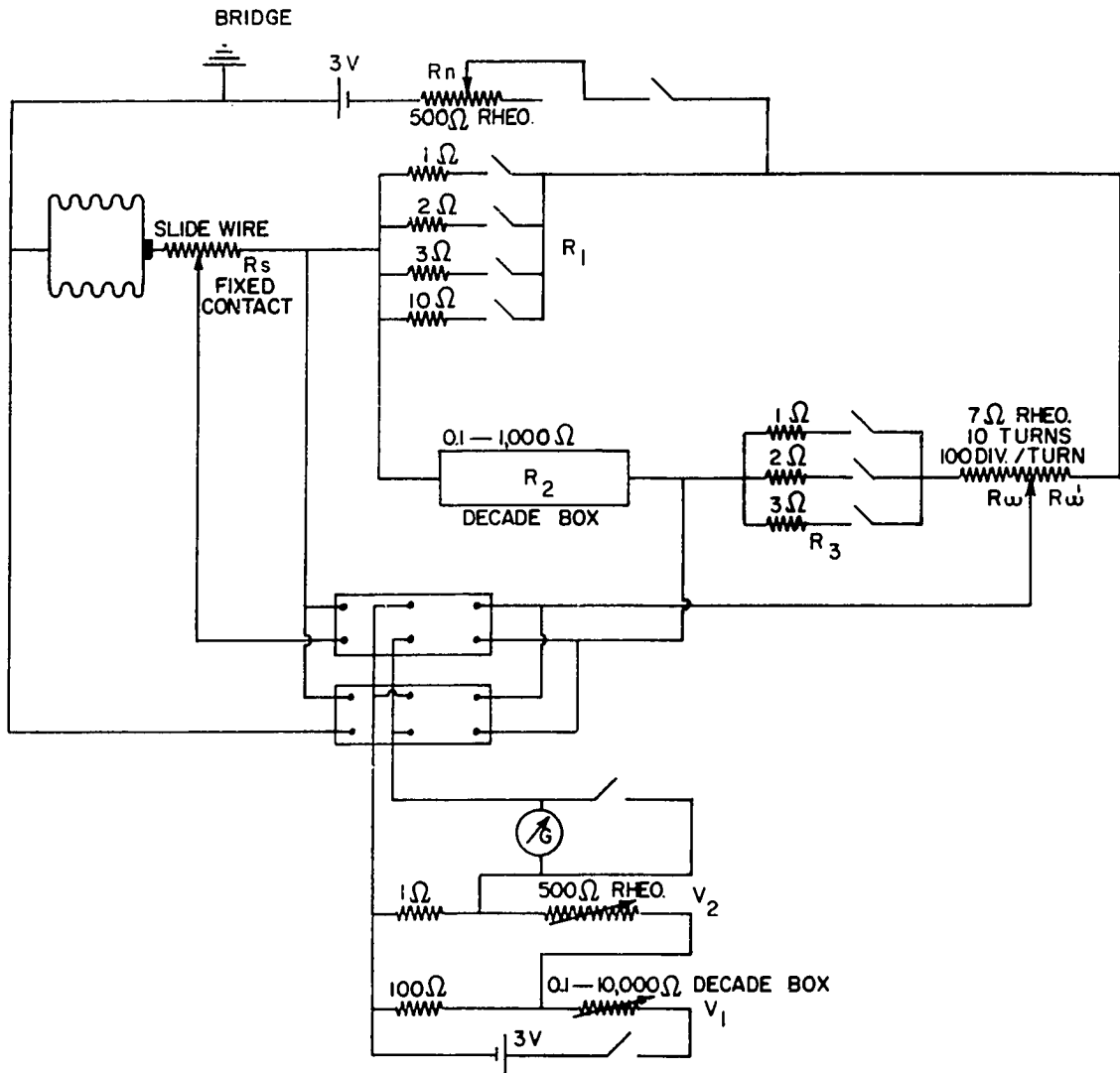


Figure 7.--Measuring Bridge

the need of a standard potential source (See Appendix I). The lower DPDT switch is used in the same manner to measure the resistance of the entire Karma slide wire. The two decade resistors, R_2 and V_1 , are General Radio Company Resistance Boxes. The two 500 ohm rheostats, R_n and V_2 , are Clarostat No. 59-145A "potentiometers." The constant value resistors are standard 0.1% precision wire-wound units.

Visual Cell

The visual observation cell as shown in Figure 8, is constructed of 4340 steel hardened to about 40 Rockwell C. The cell body is ten inches long by four inches in diameter. The two end plugs are $3\frac{1}{2}$ inches long by 2 inches in diameter. The maximum safe pressure for the cell is 90,000 psi. Two $1/32$ inch holes lying on a diameter of the cell midway along its length allow access to the cell interior. The yolk, as pictured with its driving plugs, holds two double ended cones of $5/16$ inch tubing firmly into these holes. Replacement of the top coned tubing with a solid double ended cone resulted in a dead end seal.

The two transparent sapphire windows, which permit visual observation of the experimental mixture in the center of the cell, are 1 inch in diameter by 0.4 inch thick. The pressure seal is made similar to that reported by Poulter (29), where the window is sealed against the face of the end plug using the unsupported area principle of Bridgman (13). Sealing between the end plug and cell is made by a soft steel ring of square cross section which under an applied load, rides up the 45° angle of the end plug and firmly into the cell. In order to seal securely the window to the end plug, both had to be nearly optically flat. The end plugs were first lapped flat by hand using No. 900 wet grit and then polished

with No. 3/o emery polishing paper. However, because the sapphires were found to be dish-shaped to about 5 wavelengths from flatness, a good seal was not obtained until some pressure was applied to the chamber. For this reason, a vacuum was applied to the rear of the windows whenever there was no pressure inside the cell. A silicone rubber "O" ring, as shown in Figure 8 provided an initial seal between the end plug and cell until a pressure high enough to deform the steel ring was obtained.

Mercury Reservoir

To prevent contamination of the sample in the visual observation cell by the pressure transmission fluid, JP-4 jet fuel, an intermediate pressure transmitter had to be used which would act to deliver the pressure into the cell yet not mix with the sample. Mercury was chosen to fulfill this duty. A simple reservoir (Figure 9) was constructed to contain about 10cc of mercury and thus keep the JP-4 from ever reaching the lowest point in the line connected to the optical cell (See Figure 10c) If this occurred, the JP-4 would rise above the remaining column of mercury and contaminate the sample under observation.

Pressure Measurement

Pressures below 50,000 psi were measured using either of two Heise Bourdon Tube gauges of 20,000 and 50,000 psi. maximum. These gauges had been previously calibrated against a dead weight tester and found to be accurate to 0.25% of maximum scale reading (47). High pressure measurement was made using a manganin coil enclosed in a jacketed vessel (23). The resistance of this coil was compared with that of a similar coil mounted outside the vessel. A Foxboro recording potentiometer (23) indicates directly the pressure applied to the inner coil

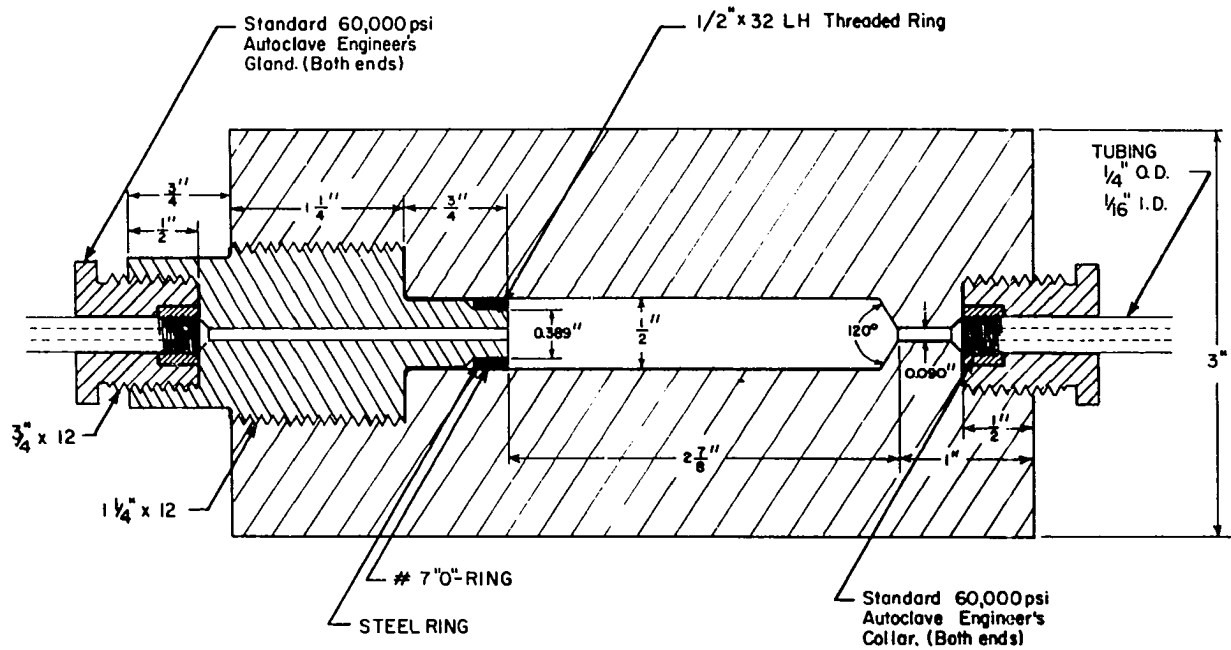


Figure 9.--Mercury Reservoir

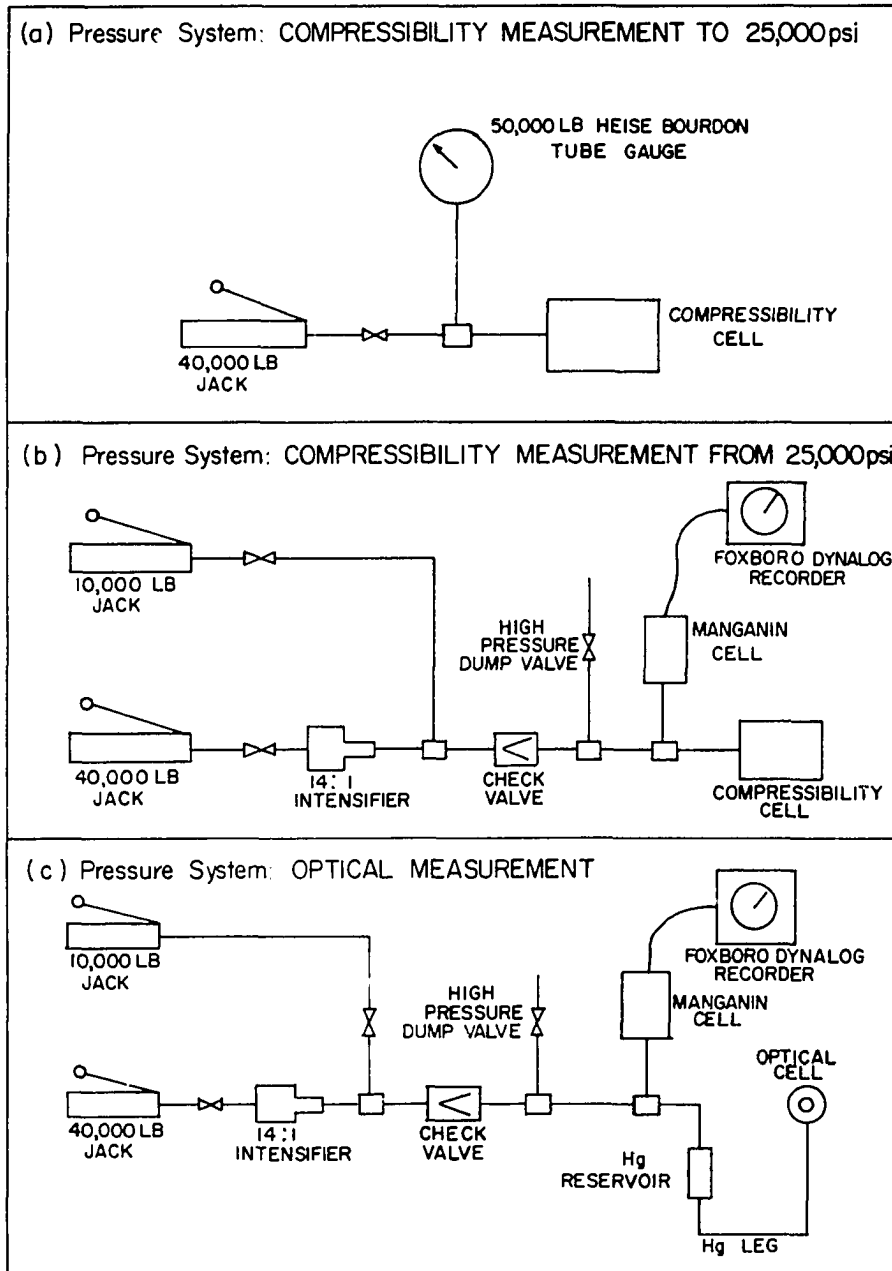


Figure 10.--Experimental Apparatus

after suitable calibration (See Chapter V).

Pressure Application

Pressure was initiated by means of either a 10,000 psi or 40,000 psi maximum Blackhawk hydraulic jack. When higher pressures were necessary a Harwood Engineering Company piston-type intensifier (23) was used. As shown in Figure 10b and c, the piston could be reversed by means of a 10,000 psi jack connected to the high pressure side of the intensifier. A check valve, also supplied by the Harwood Engineering Company (23), retains the pressure on the system as the piston reversal is carried out. A needle valve (23) between the reversing jack and the intensifier protects the jack when high pressures are being applied. Another needle valve acts as a dump, or release, valve from the high pressure side of the apparatus to the atmosphere. The three tees as shown on the high pressure side in Figure 10 are also manufactured by the Harwood Engineering Company (23). All of the Harwood equipment has a maximum pressure limitation of 200,000 psi. The valve between the 40,000 psi jack and the intensifier is a 30,000 psi maximum Autoclave Engineers needle type. The mercury leg seen in Figure 10c is constructed from 100,000 psi. Autoclave Engineers tubing.

Temperature Control

A cascaded temperature control mechanism is used for both the PVT and visual cells. A 35 gallon drum containing an ethylene glycol-water solution is cooled by a $\frac{1}{4}$ h.p. refrigeration unit. This bath is controlled at $-10 \pm 1^{\circ}\text{C}$ by a Honeywell on-off controller in line with the refrigeration unit. A $\frac{1}{3}$ h.p. gear pump circulates the solution continuously through a copper coil immersed in a 5 gallon insulated bucket

containing the same mixture as the drum. The temperature in this bath is controlled within about 0.2°F by a Lux Scientific Company mercury contact thermostat connected to a 100 watt immersion heater. The small and large baths are stirred vigorously at all times with a Precision Scientific Co. Laboratory Stirrer and a $\frac{1}{4}$ h.p. "Lightnin" mixer respectively. To control the temperatures of the high-pressure vessels, the fluid from the small bath is pumped through coils of copper tubing wrapped around them using a $\frac{1}{8}$ h.p. centrifugal pump. These coils are covered with fiberglass insulation held down with heavy-duty cloth-backed tape. "Thermon" high-conductivity cement is used to achieve effective heat transfer between the PVT cell and its cooling coil. The coil surrounding the visual cell is soldered to the yolk over about 50% of its surface. About 20 ft. of $\frac{3}{8}$ in. tubing is used for the PVT cell and about the same length of $\frac{1}{4}$ in. tubing for the visual cell.

Safety

All the pressure equipment was contained behind a $\frac{1}{4}$ " thick steel barricade reinforced on the inside with 2" x 4" wood beams. Only valve handles, pressure gauges and hydraulic jacks protruded.

CHAPTER V

CALIBRATION OF EQUIPMENT

P-V-T-Cell

The measurements made during compression of the liquid samples in the sylphon bellows were of the resistance of the section of Karma wire between the fixed contact and flexible leads (See Figure 6) and of the applied pressure. In order to obtain the fractional volume change of the samples with pressure, three things must be known:

- 1) The initial volume of the bellows;
- 2) The relationship between the change in length of the bellows and its change in volume;
- 3) The relationship between the change in resistance of the Karma wire and its length, and hence, the length of the bellows.

The first of these, the initial volume of the bellows, was calculated from the weight of the sample within it and the density at one atmosphere.

Instead of determining the other two relations separately, it was decided to carry out a calibration incorporating both.

If a linear relationship is assumed between the change in volume of the bellows with pressure and the change in resistance of the Karma wire segment with length then:

$$\Delta_p V = K (\Delta_p R_s) \quad (55)$$

where: $\Delta_p V$ = change in bellows volume during pressure change ΔP , cc .

$\Delta_p R_s$ = change in resistance of Karma wire segment during same pressure change, ΔP , ohms.

K = bellows constant, cc/ohm.

then, dividing by V^0 , the initial volume of the bellows:

$$\Delta_p (V/V^0) = \frac{K}{V^0} (\Delta_p R_s) \quad (56)$$

where; $\Delta_p (V/V^0)$ = fractional change in volume during pressure change ΔP .

A relationship is obtained which describes the fractional volume change of a sample with pressure. The constant K is determined by making use of the literature data (37) for CS_2 at $0^\circ C$ and modifying Equation (56):

$$K = \frac{[\Delta_p (V/V^0)]' V^0}{\Delta_p R_s} \quad (57)$$

where: $\Delta_p (V/V^0)'$ = fractional change in volume of pure CS_2 at $0^\circ C$ during pressure change ΔP , as reported (37).

The constant K can then be evaluated by superimposing the end points (at one atmosphere and 15,000 psi) of the resistance versus pressure readings on the $(V/V^0)'$ versus pressure plot. This operation was carried out and the bellows constant found to be 7.0232 cc/ohm. Also, the data were found to be congruent within .0002 cc/cc* as shown in Table 4. The values in the last column were calculated using the above constant. This agreement indicates that the assumption of linearity Equation (55) is valid at least to the limit of the calibration, 15,000 psi.

*At all but 50 atmospheres.

TABLE 4
CALIBRATION OF BELLOWS

$$K = \frac{\Delta_p (V/V^0)'}{V^0 \Delta_p R_s} = 7.0232 \text{ cc/ohm}$$

$$P, \text{atm} \quad \left[(V/V^0)' \right]^* \quad (V/V^0) = 1 - \left(\frac{K \Delta_p R_s}{V^0} \right)$$

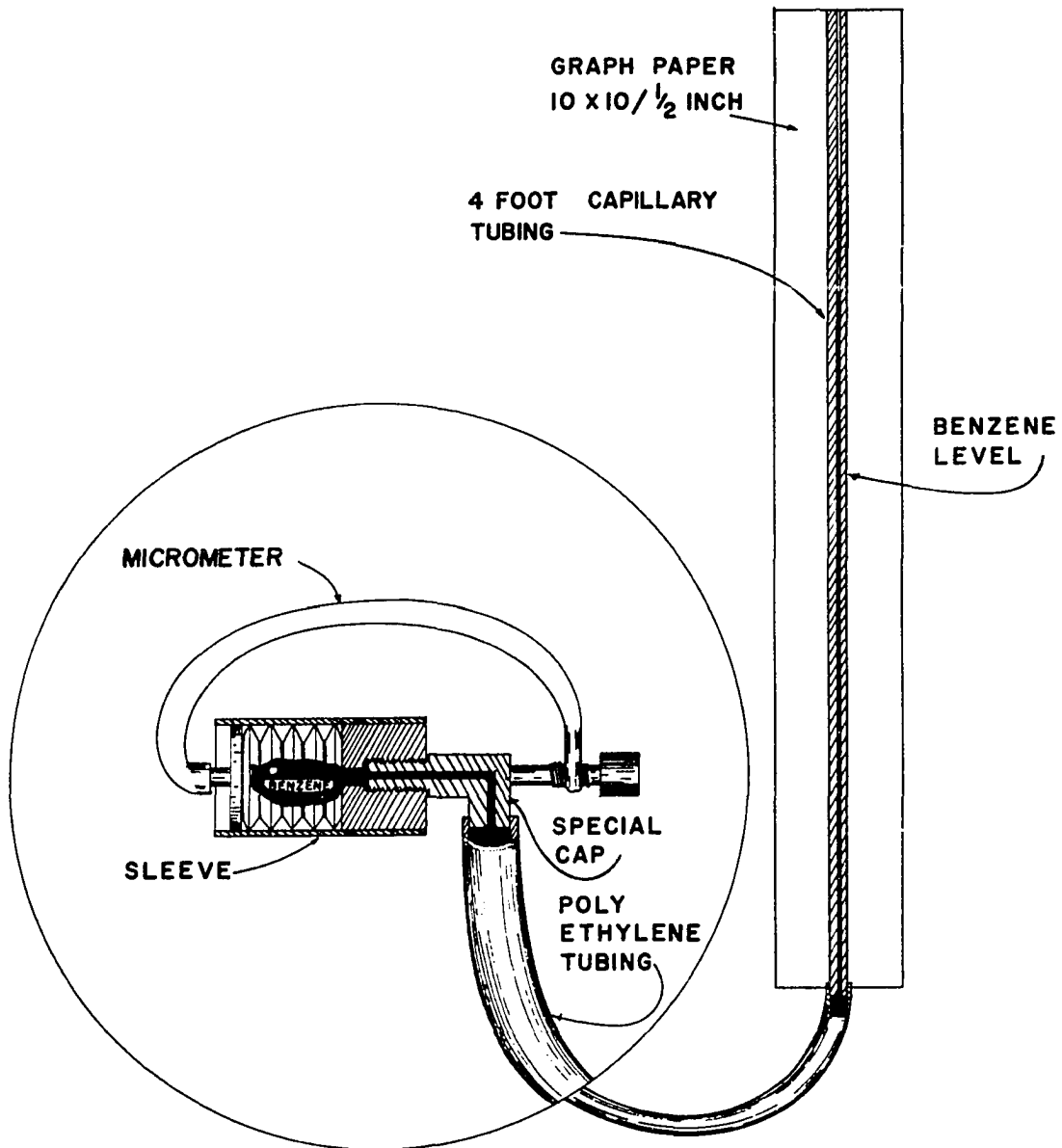
1	1.0000	1.0000
50	.9967	.9963
100	.9925	.9925
150	.9889	.9889
200	.9855	.9854
250	.9822	.9821
300	.9790	.9789
350	.9759	.9758
400	.9729	.9728
450	.9700	.9699
500	.9672	.9671
550	.9645	.9644
600	.9619	.9617
650	.9593	.9592
700	.9567	.9565
750	.9542	.9541
800	.9518	.9517
850	.9494	.9494
900	.9470	.9470
950	.9447	.9447
1000	.9425	.9425

*Seitz, W. and Lechner, G. Annalen der Physik, XLIX, 1916, p. 93.

To evaluate the effect of higher pressures on the linearity assumption, two tests were carried out: First, the change in bellows volume with length was determined over a large range in volume and second, the resistance of the Karma wire was measured as a function of pressure. These tests are described below:*

In order to determine whether the volume change on the bellows remained linear with its change in length, the bellows was removed and placed in a close fitting but nonbinding sleeve. (See Figure 11.) A 4 foot capillary tube was calibrated using a serological pipette of 0.001 ml resolution and found to be linear to this degree with a capacity of 0.0276 ml/in. Ten by ten to the half inch graph paper allowed reading of the level in the capillary to 0.2 divisions or 0.01 inch. The liquid level could thus be measured within 0.0003 ml. By means of a specially constructed cap, the bellows was filled with benzene and connected to the capillary. Thick-walled polyethylene tubing was used to make this connection so as to avoid stretching during the subsequent operation. By compressing the bellows with a micrometer directly along its axis, the change in level in the capillary was measured against the change in length of the bellows. The results showed the bellows to be as linear as was able to be determined using this technique ($\pm 0.5\%$ during a compression of 10%) (See Appendix I). Bridgman has found, however, with bellows' of much more crude construction, that the linearity is better than 0.1% (10). Also, because any small non-linearity would not cause a measureable error in the volume change on mixing values (these being determined by relative and not absolute compressibilities), no

*The tests for linearity were essentially the same as those used by Bridgman (10) and also by Cutler (17).



DETERMINATION OF BELLOWS LINEARITY

Figure 11.--Determination of Bellows Linearity

further attempts at calibration were carried out.

The exact absolute resistivity* of the Karma wire was never measured. However, the resistance of the entire wire was measured at various pressures (See Chapter IV) and found not to change enough to be measurable.

The bellows constant, K, as determined to 15,000 psi, was used unaltered over the entire range of pressures.

Manganin Pressure Gauge

The manganin pressure gauge and recorder were calibrated simultaneously by use of another manganin coil previously calibrated by means of the freezing points of mercury (24). The two coils were attached to the same pressure apparatus, the resistance of the standard coil being measured on a Mueller bridge. The results showed the recorder reading to be a linear function of applied pressure, reproducible on each scale to .25% of the maximum scale reading of 50,000, 100,000, and 200,000 psi.

Measuring Bridge

The only part of the measuring bridge which was calibrated was the slide wire rheostat, $R_w - R_w'$, as it was the only variable which affected the calculation of the resistance of the Karma wire section. (See Appendix I.) This calibration was carried out using a Mueller bridge accurate to 2×10^{-4} ohms. The variation from linearity was found to be about 1.7×10^{-3} ohms. No calibration curve was drawn, however, as this precision is approximately the same as that allowed by the vernier.

*It was found to be approximately 8 ohms per foot..

CHAPTER VI

PROCEDURE

Density Determinations

The pycnometer described in Chapter IV was used to determine the density-composition diagram of the system acetone-carbon disulfide at 0°C.

Samples of known mole fraction of acetone-carbon disulfide were made using the method of Powers (30), whereby samples of the pure liquids are injected into a pre-weighed, rubber covered glass bottle using a hypodermic needle and syringe.

The pycnometer was filled with the liquid in question and placed in the ice bath up to the neck. After 20 minutes, the stopper was inserted rather abruptly so as to cause a jet of liquid to be ejected through the hole in its center. The stopper and outer ground glass joint on the pycnometer body were then carefully dried so as to leave the level of liquid exactly even with the top of the stopper and the cap firmly pressed in place. Any vaporization then taking place does not cause a weight loss as the vapor is trapped in the cap. The pycnometer was then weighed, disassembled, and refilled with the same sample, the procedure then being repeated. The density of each sample was measured at least four times, or until three readings of the weight agreed within 1 mg. The pycnometer was then dried and weighed and the procedure

repeated for the next sample. In all, ten samples were run: doubly distilled water serving as a calibration, pure acetone, pure carbon disulfide, and seven mixtures of varying mole fractions (See Chapter VII).

P-V-T Measurements

For determination of the isotherms of various mole fractions of acetone-carbon disulfide mixtures the vessel shown as Figure 5 was used in combination with the measuring bridge (Figure 7). The cell was maintained at 0°C at all times by means of the temperature control described in Chapter IV. In preparation for the determination of an isotherm, a sample was prepared in the same manner as for the density measurements. The bellows was removed from the Karma wire and retainer, cleaned thoroughly with acetone and then ether, dried by vacuum and weighed along with the screw cap. The sample was then inserted by alternately compressing the bellows and then slowly filling with a hypodermic needle and syringe as the bellows was allowed to expand. When no air bubbles were seen during the compressions, the bellows was assumed full of liquid. An excess of liquid was allowed to remain which was then forced out as the cap was screwed in. The bellows was then rinsed in ether and vacuum dried. Special care was exercised in drawing out liquid which remained in the threads of the opening. When the bellows ceased to lose weight on standing, the weight was recorded and the bellows reinserted into the retainer, the Karma wire fixed into its housing on the bellows, and the entire assembly replaced into the cell. About three hours were allowed to assure temperature equilibrium. Although the thermocouple potential would stabilize after about twenty minutes, the bellows and its contents were not assumed to be at temperature equilibrium until no change in

resistance with time was noted on the measuring bridge. This indicated the bellows was no longer contracting. Pressure was then applied in an increment of 2500 psi and after thermal equilibrium was again attained the resistance of the section of Karma wire between the fixed contact and the flexible leads was recorded. About 20 minutes was usually sufficient to assure this equilibrium. The change in the resistance during a pressure change of 2500 psi was about 0.005 ohms.

Seventeen samples of different mole fractions were investigated. Eleven of these were examined from 1 atmosphere to 30,000 psi, the pressure limit for the needle valve between the jack and the PVT cell, using the arrangement shown in Figure 10a. The other six were examined from 1 atmosphere to 100,000 psi using the arrangement shown in Figure 10b. The measurements were divided into these two groups in order to obtain the best possible accuracy in pressure measurement in the low pressure range where the compressibilities are high. The Heise Bourdon Tube Gauge allowed pressure measurement to ± 50 psi. Using the manganin gauge and recorder, the precision dropped to ± 250 psi. However, in the high pressure range, the compressibility is lowered, so the precision in the calculation of relative volume is not greatly affected.

The freezing point of pure acetone is believed to be about 90,000 psi at 0°C (58) and that of carbon disulfide 150,000 psi (15) at this same temperature. No studies have been made on the freezing pressures of mixtures of the two. Because freezing may permanently distort the bellows and render it useless, samples of high acetone concentrations were taken no higher than 85,000 psi. The samples richer in carbon disulfide were compressed up to 100,000 psi and pure carbon disulfide up to 125,000 psi.

Visual Observation

The visual observation cell is shown as Figure 5. Before assembly, all parts of the cell were thoroughly cleaned with acetone. A nylon bristle brush was used to clean the threads in the cell and on the end plugs. The faces of the end plugs were scrupulously cleaned and wiped dry with lens tissue until no dust was apparent. The sapphires were then pressed on firmly. When the interference pattern caused by the air space between sapphire and end plug ceased to change when hand pressure was removed, the sapphire was assumed in place. At this time, vigorous shaking would not dislodge the sapphire. Using a Cenco vacuum pump, a vacuum was pulled behind both sapphires to assure that they remained in position. The steel rings were then set in place and the silicone rubber "O" rings were slipped on above them. The cell was set into position in the yolk and the bottom driving plug and cone were threaded in until the cell was firmly pressed against the top underside of the yolk. This arrangement made a temporary seal at the bottom so that the liquid sample could be inserted. The end plugs were then carefully inserted after all threads were coated with molybdenum disulfide grease. The vacuum was maintained behind the sapphires at all times (See Figure 8). The mercury leg and reservoir were cleaned with acetone, filled with mercury and placed into position. The first liquid sample was then injected using a hypodermic syringe and a length of 0.5 mm I.D. stainless steel tubing. The top cone and driving plug were screwed in tightly using a 16 inch smooth-jawed wrench. Because carbon disulfide attacks all known elastomer "O" rings, including silicone rubber, the pressure was raised rather rapidly so as to set the steel rings before the "O" rings dissolved enough to fail. About 60,000 psi was sufficient. The pressure was then

slowly released and the sample left in for 24 hours to allow it to dissolve out as much of the "O" rings as possible, and thus prevent contamination of subsequent samples. The cell was then drained and the procedure repeated. Rinsing was carried out with acetone, using the hypodermic syringe and tubing, and the experimental trials begun. As long as the end plugs were not moved, the steel rings provided a seal over the entire pressure range. If, however, they had to be removed, the entire sealing procedure had to be repeated using new steel and rubber rings. On removal, the "O" rings were found to be ragged, soft and rather lifeless. On immersion in carbon disulfide no further dissolution was apparent.*

Each experimental sample was prepared according to the method of Powers (30). The sample was inserted in the same manner as the first and the pressure raised to about 20,000 psi. After fiberglass insulation was wrapped around the cell, cooling was begun and about 12 hours were allowed to assure thermal equilibrium. The vacuum was removed from behind the sapphires and a mercury-in-glass thermometer was placed into one end plug with its bulb resting against the sapphire, a rubber stopper at the outer end of the plug acting as an insulator. The temperature read on the thermometer was essentially the same** as that of a copper-constantan thermocouple lying between the yolk and cell. The pressure was increased until cloudiness occurred. It was held there and the

*The "O" rings were left in a beaker of carbon disulfide for about an hour and removed, the carbon disulfide then being allowed to evaporate. At dryness, no residue was noted. When the same experiment was carried out with a new silicone "O" ring, a visible film of sediment was observed.

**To within 0.2°C, or as accurately as the thermocouple potential was measured using the same Leeds and Northrup Potentiometer as was used with the PVT cell.

temperature allowed to restabilize. The pressure was then lowered until the solution cleared, and then raised again to the translucent pressure. These two pressures, that necessary to cause cloudiness and that to cause clearing coincided within about 500 psi.

That no JP-4 entered the cell during the experimentation was known on the basis of two observations: First, at all times there was a slight leak at the fitting at the bottom of the mercury reservoir. As long as mercury was leaking, it could be safely assumed that no JP-4 could reach the cell. If JP-4 were leaking, it was possible that the column of JP-4 had reached the low point in the mercury leg and could rise into the cell. Second, when JP-4 did enter the cell it was evidenced by streams of high viscosity having an index of refraction much different from the experimental mixture.

Nine mixtures ranging in composition from 14.79 to 93 percent acetone were examined at -2°C . This temperature was used instead of 0°C , where the PVT and density measurements were made, in order to obtain a more complete phase diagram. This was the case since the range of pressures where separation occurred was uncomfortably near the limit of the equipment. In order to estimate the effect of temperature on the separation pressure, three samples were allowed to warm slightly, while the pressure was raised sufficient to maintain cloudiness. (See Chapter VII.)

At the conclusion of each trial, the cell was warmed by pumping 30°C water through the copper tubing. This was done to prevent any water from condensing inside the pressure chamber during the time the cell was open for rinsing and sample insertion.

Reagents

The reagents used exclusively in the study were Fischer Reagent Grade acetone and Baker Reagent Grade carbon disulfide. Each was distilled with the first 10 and last 40% being discarded. The acetone accepted had an observed boiling point range from 132.5 - 133°F. The carbon disulfide ranged from 113.5 - 114°F.

Although the samples had some exposure to the atmosphere during preparation and insertion into the slyphon bellows and also into the visual observation cell, no appreciable contamination of the acetone with water was believed to have taken place. Griswold and Buford (22) report excellent accuracy in vapor-liquid equilibrium studies using approximately the same purification and handling techniques for their acetone.

CHAPTER VII

RESULTS

Density Determinations

The densities of the nine different composition acetone-carbon disulfide mixtures were calculated directly from the weight of the sample and volume of the pycnometer obtained from the water calibration. These results are shown as Figure 12 and column 2 in Table 5.

The molal volume of each sample was calculated from the density and mole fraction of the sample:

$$\bar{V}_M^0 = \left[\frac{X_{\text{acc}} (MW)_{\text{acc}} + X_{\text{CS}_2} (MW)_{\text{CS}_2}}{\rho^0} \right] \text{ cc/mole} \quad (58)$$

where: $(MW)_{\text{acc}}$ = molecular weight of acetone.

$(MW)_{\text{CS}_2}$ = molecular weight of CS_2 .

These results were fit to a 5th order polynomial using a least squares routine on an IBM 1410 Data Processing System, using twenty decimal accuracy.* The resultant polynomial is shown above Table 5 with the values listed in column 3. The curve is drawn in Figure 13.

The molal change in volume on mixing at 0°C and one atmosphere,

*The program used for all smoothing operations was the IBM No. 7.0.002 least square routine for the 1620 Data Processing System. However, it was found that for polynomials of 4th order and higher that the eight digit capacity of the 1620 caused large cumulative errors, actually worsening the fit with increasing order. Thus, for the 5th order polynomials, the program was altered so as to be used on the 1410 and make use of the 20 decimal accuracy.

TABLE 5

RESULTS OF DENSITY DETERMINATIONS

Acetone - CS₂ 0°C 1 Atmosphere

$$\underline{V}_M^{\circ} = 58.8741 + 16.0970x - 1.1526x^2 - 9.8920x^3 + 15.9456x^4 - 8.4328x^5$$

X _{acet}	ρ°	\underline{V}_M°	$(\Delta \underline{V}_M)^{\circ}$
0.00000	1.29339	58.871	0.0000
0.08742	1.23702	60.277	0.3072
0.10000			0.3333
0.17477	1.18488	61.598	0.5303
0.20000			0.6040
0.26538	1.13310	62.962	0.7554
0.30000			0.7974
0.40000			0.9174
0.40644	1.06024	64.892	0.9124
0.50000			0.9748
0.55761	0.98805	66.870	0.9904
0.60000			0.9783
0.70000			0.9258
0.76863	0.89741	69.377	0.8451
0.80000			0.7911
0.87559	0.85600	70.457	0.5807
0.90000			0.5162
1.00000	0.81299	71.440	0.0000

Density of pure acetone literature (46) = 0.81248

Density of pure CS₂ literature (46) = 1.29319

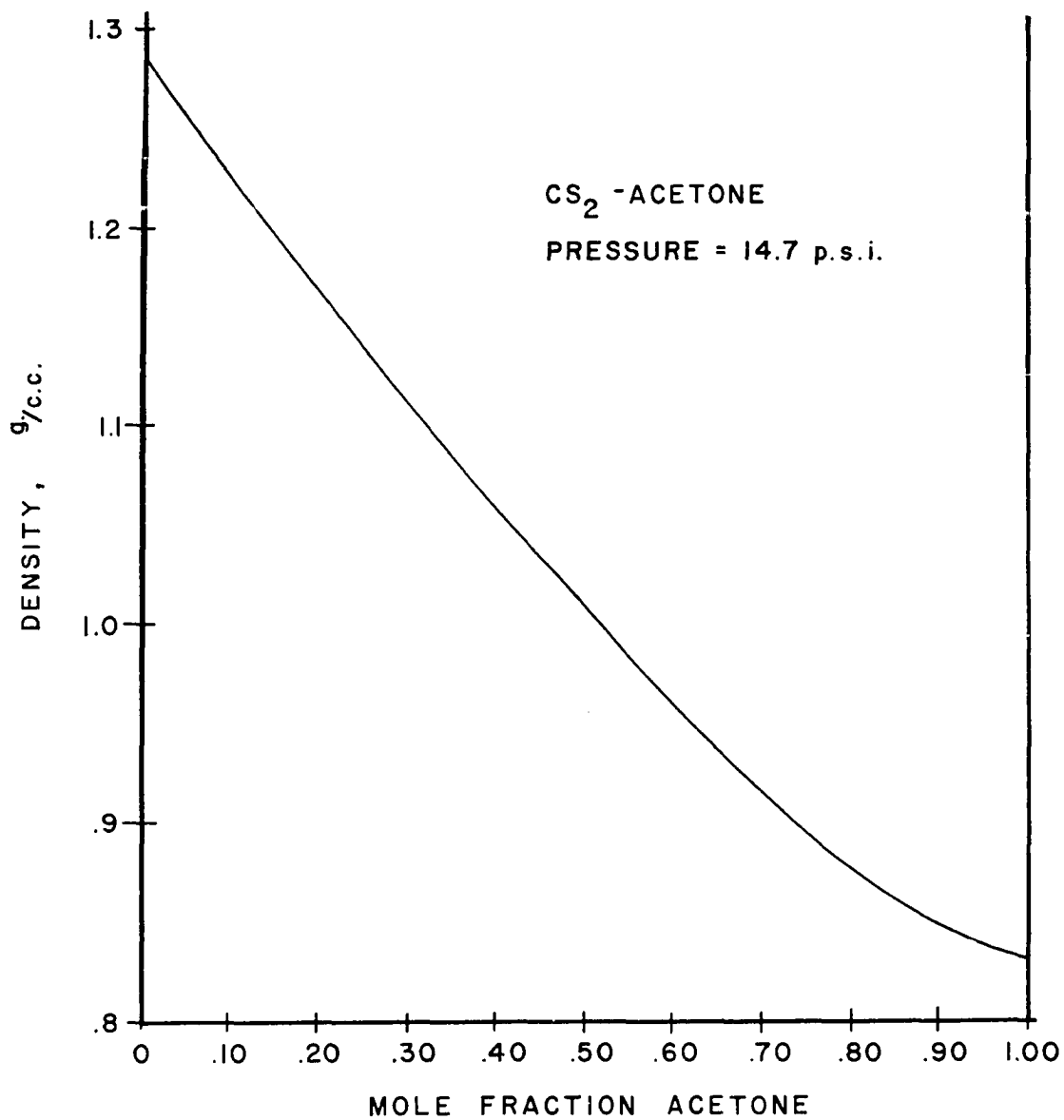


Figure 12.--Densities at 0°C and One Atmosphere

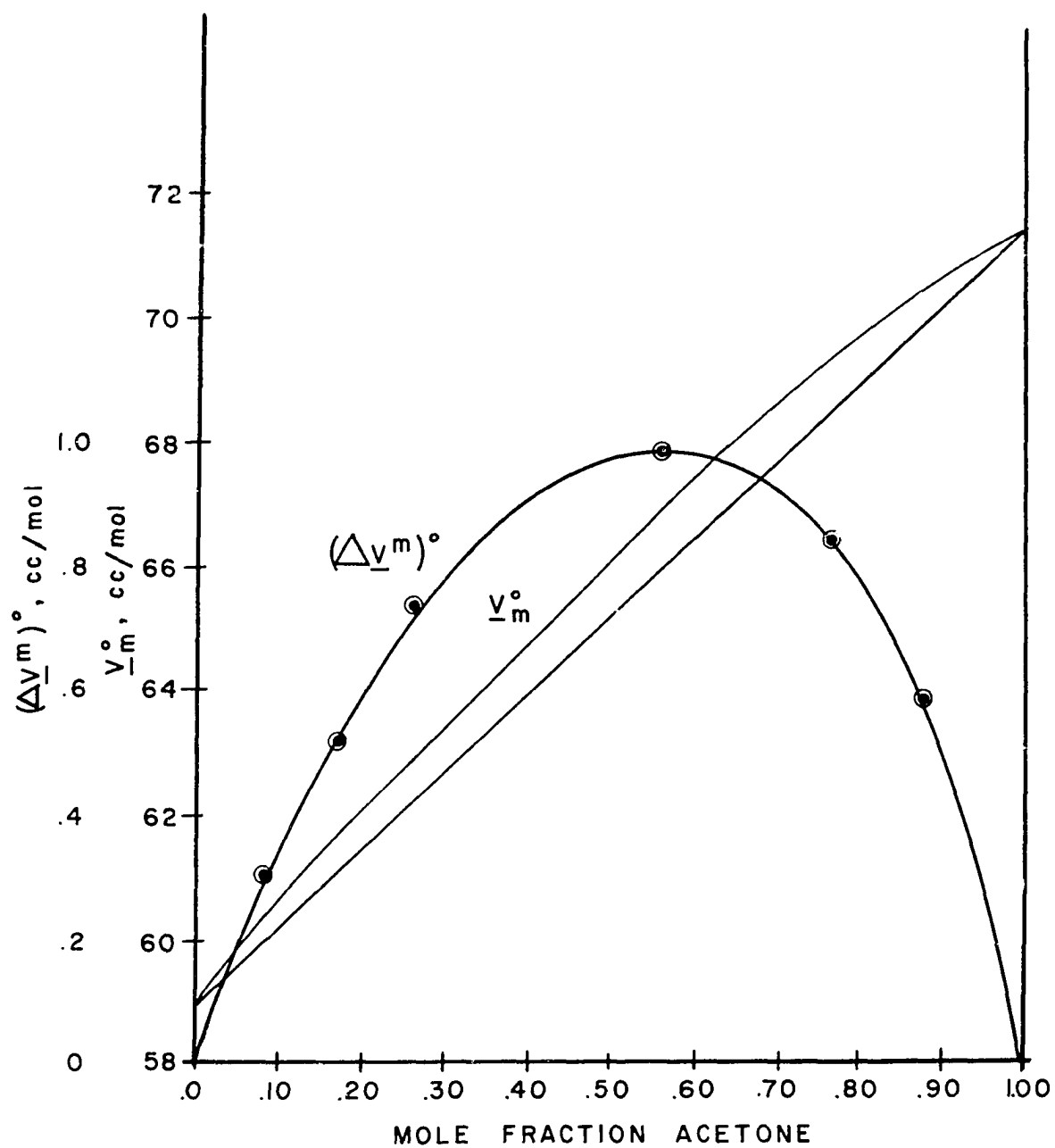


Figure 13.--Molar Volume and $(\Delta \underline{V}^m)^0$

$(\Delta \underline{V}^M)^\circ$, was calculated from the results of the smoothing and the definition of $\Delta \underline{V}^M$:

$$\Delta \underline{V}^M \equiv \underline{V}_M - \sum x_i \underline{V}_i^\circ \quad (59)$$

For the system in question:

$$(\Delta \underline{V}^M)^\circ = \underline{V}_M^\circ + X_{\text{acet}} (\underline{V}_{\text{CS}_2}^\circ - \underline{V}_{\text{acet}}^\circ) - \underline{V}_{\text{CS}_2}^\circ \quad (60)$$

These results are listed as column 4 in Table 5 and the curve drawn in Figure 13.

Compression Measurements

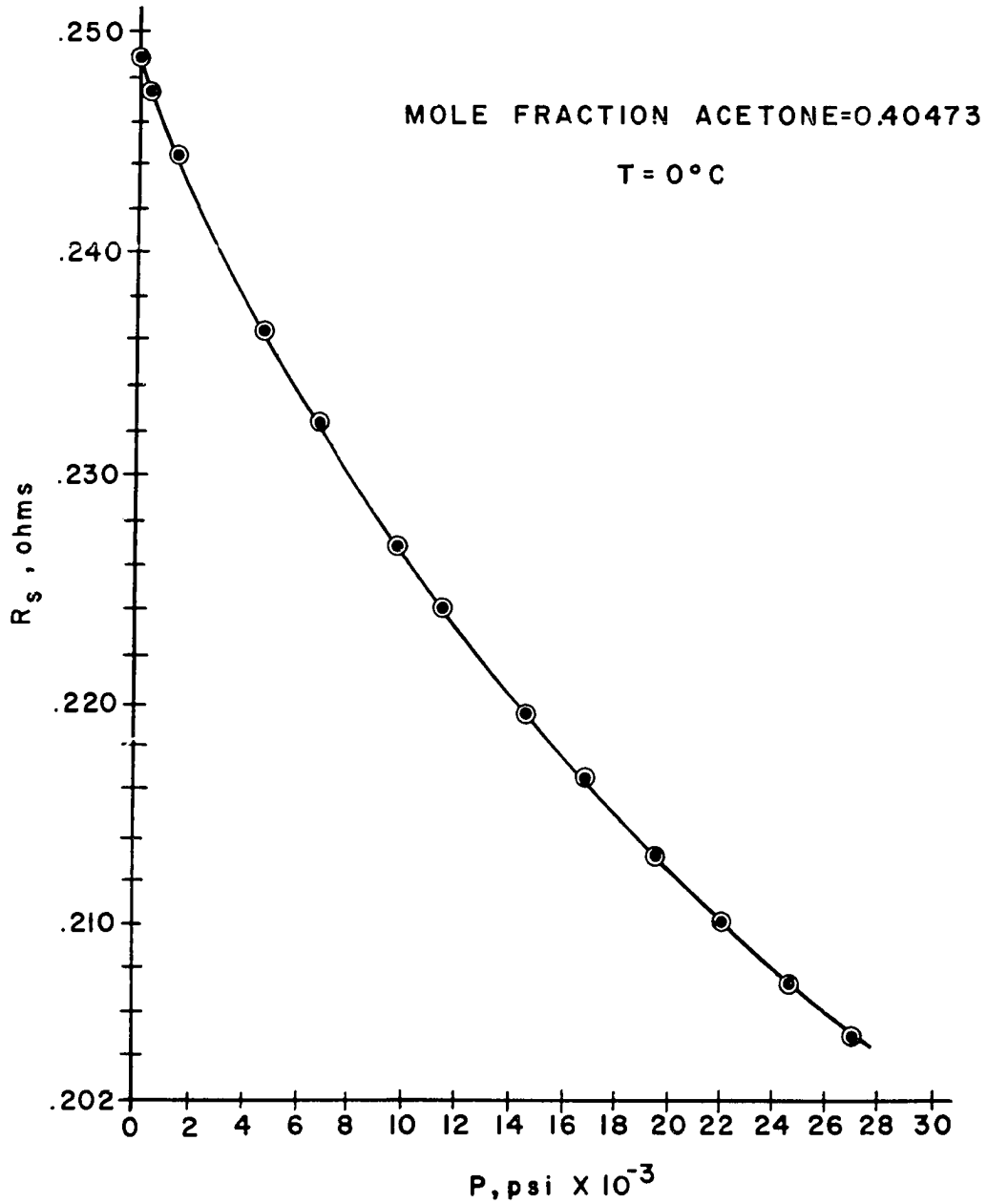
The resistance versus pressure data from the PVT cell were smoothed in the same manner as \underline{V}_M° , this time using third order polynomials. A sample curve is shown as Figure 14. These data were converted to (V/V°) vs. pressure values using Equation (56) and the initial volumes of the bellows calculated from the densities of the mixtures and the weight of samples in the bellows:

$$\left(\frac{V}{V^\circ}\right) = 1 - \Delta_p \left(\frac{V}{V^\circ}\right) = 1 - \frac{K}{V^\circ} (\Delta_p R_s) \quad (61)$$

One result is shown as Figure 15. The complete results are tabulated as Table 6.

Observed Separations

The results of the visual observations are listed as Table 7. The resultant curve at -2°C and that envisioned at 0°C are shown as Figure 16. The points at 0°C were extrapolated on the basis of the apparent effect of temperature on the separation pressures of four samples.

Figure 14.--Sample R_s vs P

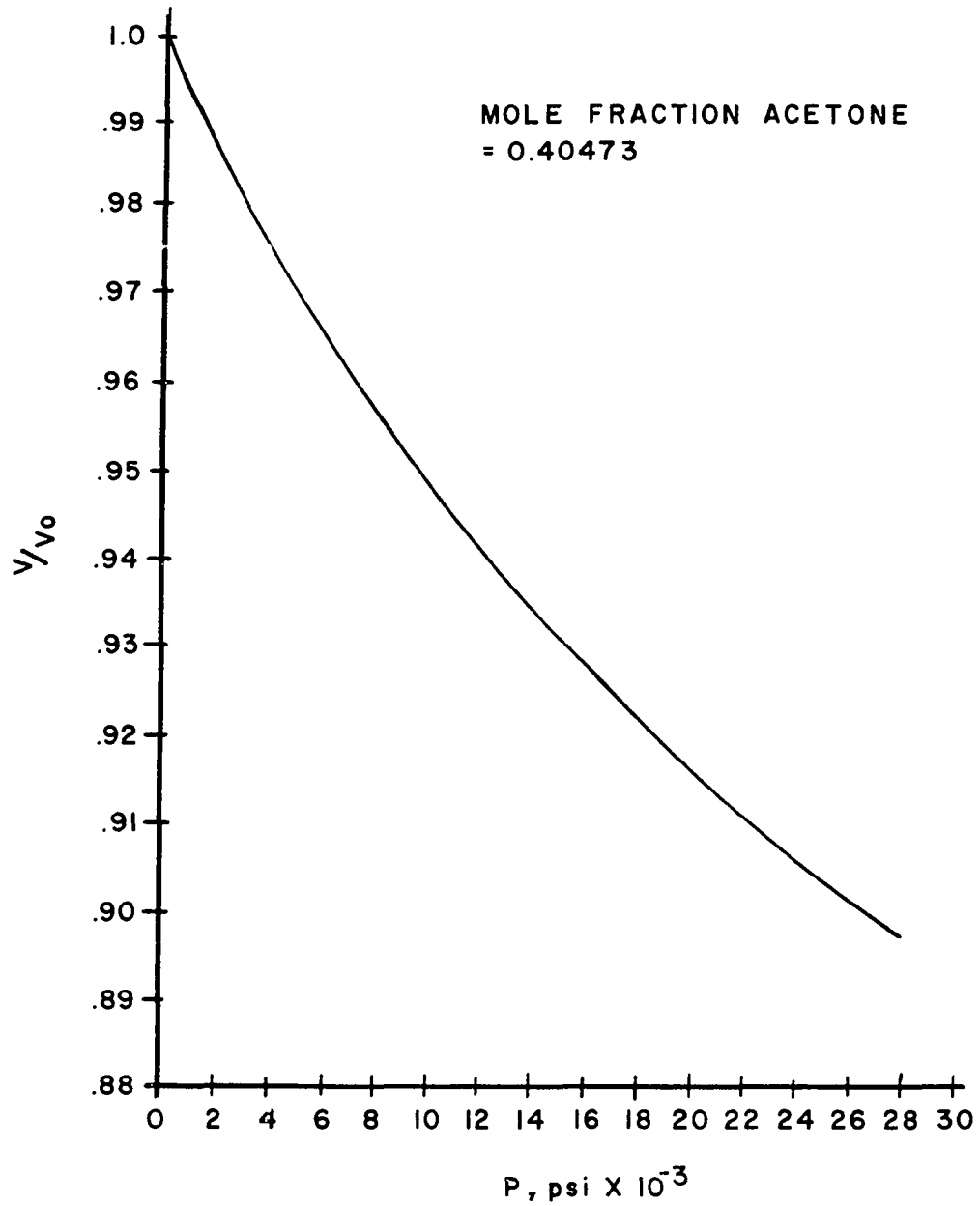


Figure 15.--Sample (V/V⁰) vs. P

TABLE 6
(V/V⁰) vs P

A. X _{ace} = 0.00000		B. X _{ace} = 1.00000	
<u>(V/V⁰)</u>	<u>P,psi</u>	<u>(V/V⁰)</u>	<u>P,psi</u>
1.0000	14.7	1.0000	14.7
0.9948	1,000	0.9937	1,000
0.9572	10,000	0.9485	10,000
0.9418	15,000	0.9304	15,000
0.9288	20,000	0.9150	20,000
0.9172	25,000	0.9039	25,000
0.9070	30,000	0.8919	30,000
0.8977	35,000	0.8817	35,000
0.8890	40,000	0.8727	40,000
0.8811	45,000	0.8647	45,000
0.8737	50,000	0.8575	50,000
0.8669	55,000	0.8509	55,000
0.8606	60,000	0.8449	60,000
0.8549	65,000	0.8389	65,000
0.8495	70,000	0.8335	70,000
0.8445	75,000	0.8281	75,000
0.8398	80,000	0.8239	80,000
0.8354	85,000	0.8196	85,000
C. X _{ace} = 0.10401		D. X _{ace} = .15436	
<u>(V/V⁰)</u>	<u>P,psi</u>	<u>(V/V⁰)</u>	<u>P,psi</u>
1.0000	14.7	1.0000	14.7
0.9948	1,000	0.9947	1,000
0.9759	5,000	0.9756	5,000
0.9562	10,000	0.9557	10,000
0.9399	15,000	0.9394	15,000
0.9262	20,000	0.9257	20,000
0.9142	25,000	0.9138	25,000

TABLE 6--Continued

E. $X_{ace} = 0.25778$

(V/V^0)	P, psi
1.0000	14.7
0.9941	1,000
0.9733	5,000
0.9520	10,000
0.9349	15,000
0.9208	20,000
0.9084	25,000

G. $X_{ace} = 0.50608$

(V/V^0)	P, psi
1.0000	14.7
0.9942	1,000
0.9730	5,000
0.9512	10,000
0.9335	15,000
0.9190	20,000
0.9064	25,000

I. $X_{ace} = 0.60187$

(V/V^0)	P, psi
1.0000	14.7
0.9937	1,000
0.9714	5,000
0.9492	10,000
0.9318	15,000
0.9174	20,000
0.9044	25,000

F. $X_{ace} = 0.40473$

(V/V^0)	P, psi
1.0000	14.7
0.9942	1,000
0.9733	5,000
0.9520	10,000
0.9348	15,000
0.9205	20,000
0.9070	25,000

H. $X_{ace} = 0.51046$

(V/V^0)	P, psi
1.0000	14.7
0.9940	1,000
0.9722	5,000
0.9500	10,000
0.9323	15,000
0.9178	20,000
0.9057	25,000

J. $X_{ace} = 0.75209^*$

(V/V^0)	P, psi
1.0000	14.7
0.9933	1,000
0.9700	5,000
0.9474	10,000
0.9301	15,000
0.9160	20,000
0.9027	25,000

TABLE 6--Continued

K. $X_{ace} = 0.89391$

(V/V^0)	P, psi
1.0000	14.7
0.9935	1,000
0.9707	5,000
0.9480	10,000
0.9304	15,000
0.9157	20,000
0.9026	25,000

L. $X_{ace} = 0.22262$

(V/V^0)	P, psi
0.9001	30,000
0.8899	35,000
0.8807	40,000
0.8722	45,000
0.8645	50,000
0.8575	55,000
0.8510	60,000
0.8451	65,000
0.8396	70,000
0.8345	75,000
0.8296	80,000
0.8250	85,000

M. $X_{ace} = 0.42235$

(V/V^0)	P, psi
0.8955	30,000
0.8851	35,000
0.8758	40,000
0.8673	45,000
0.8598	50,000
0.8530	55,000
0.8466	60,000
0.8408	65,000
0.8353	70,000
0.8299	75,000
0.8247	80,000
0.8198	85,000

N. $X_{ace} = 0.60720$

(V/V^0)	P, psi
0.8930	30,000
0.8827	35,000
0.8734	40,000
0.8649	45,000
0.8571	50,000
0.8500	55,000
0.8436	60,000
0.8376	65,000
0.8321	70,000
0.8269	75,000
0.8220	80,000
0.8173	85,000

TABLE 6--Continued

O. $X_{ace} = 0.75209^*$

<u>(V/V⁰)</u>	<u>P,psi</u>
0.8919	30,000
0.8816	35,000
0.8722	40,000
0.8637	45,000
0.8560	50,000
0.8489	55,000
0.8423	60,000
0.8364	65,000
0.8309	70,000
0.8258	75,000
0.8209	80,000
0.8158	85,000

*Both runs made with same sample in bellows.

TABLE 7
OBSERVED LIQUID-LIQUID SEPARATIONS

Acetone - CS ₂		
X _{ace}	T, °C	P, psi
.1479	-2	> 82,000*
.2022	-2	76,000
.2022	-1.75	75,500
.2494	-2	72,500
.2971	-2	73,600
.2971	-1	76,000
.40	-7	64,000
.40	-2	73,000
.4717	-2	74,500
.5267	-2	78,000
.5267	-1.25	79,500
.6422	-2	> 85,000*
.93	-2	> 77,500*

*No separation was noted to this pressure.

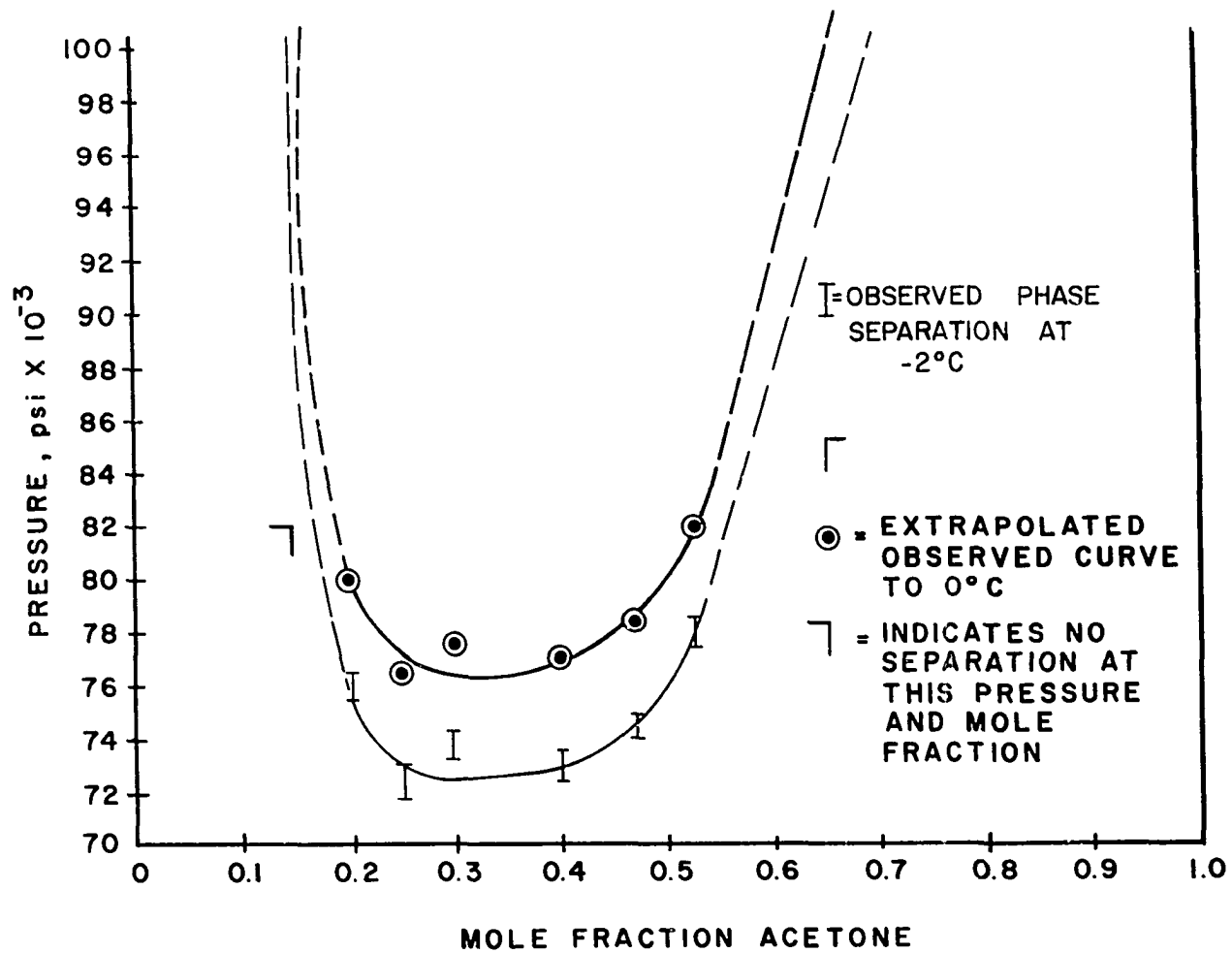


Figure 16.--Observed and Extrapolated Separations

CHAPTER VIII

TREATMENT OF DATA

Calculation of ΔV^M

In order to obtain the change in volume on mixing for mixtures of acetone-carbon disulfide over the range of pressure necessary to integrate Equation (33) and hence predict the isothermal phase diagram, it was necessary to perform four operations on the volume-pressure data:

- 1) The (V/V^0) data were smoothed as functions of mole fraction at 5000 psi increments in pressure using the "least squares" method.
- 2) The change in volume on mixing (ΔV^M) was calculated from 1) at each mole fraction and each pressure.
- 3) The results of 2) were smoothed as a function of mole fraction at each pressure using the "least squares" method.
- 4) The results of 3) were smoothed as a function of pressure at each mole fraction using the "least squares" method.

Each of these operations is described in greater detail below:

- 1) The (V/V^0) data were smoothed with respect to mole fraction at each 5000 psi increment in pressure using a 3rd order polynomial. These results are also shown in Table 8. The curve at 10,000 psi is drawn as Figure 17. These results should be able to be compared, at least qualitatively, with the isothermal

TABLE 8

 (V/V^0) vs X_{ace} (SMOOTHED)

Pressure = 1,000 psi		Pressure = 5,000 psi	
X_{ace}	(V/V^0)	X_{ace}	(V/V^0)
0.00000	0.99482	0.00000	0.97628
0.10000	0.99474	0.10000	0.97575
0.20000	0.99460	0.20000	0.97499
0.30000	0.99438	0.30000	0.97408
0.40000	0.99414	0.40000	0.97312
0.50000	0.99391	0.50000	0.97220
0.60000	0.99370	0.60000	0.97142
0.70000	0.99355	0.70000	0.97084
0.80000	0.99349	0.80000	0.97057
0.90000	0.99354	0.90000	0.97065
1.00000	0.99373	1.00000	0.97117

Pressure = 10,000 psi		Pressure = 15,000 psi	
X_{ace}	(V/V^0)	X_{ace}	(V/V^0)
0.00000	0.95726	0.00000	0.94180
0.10000	0.95595	0.10000	0.93970
0.20000	0.95449	0.20000	0.93767
0.30000	0.95301	0.30000	0.93585
0.40000	0.95158	0.40000	0.93421
0.50000	0.95028	0.50000	0.93282
0.60000	0.94921	0.60000	0.93171
0.70000	0.94842	0.70000	0.93090
0.80000	0.94798	0.80000	0.93041
0.90000	0.94795	0.90000	0.93022
1.00000	0.94837	1.00000	0.93034

Pressure = 20,000 psi		Pressure = 25,000 psi	
X_{ace}	(V/V^0)	X_{ace}	(V/V^0)
0.00000	0.92884	0.00000	0.91721
0.10000	0.92615	0.10000	0.91442
0.20000	0.92372	0.20000	0.91179
0.30000	0.92163	0.30000	0.90894
0.40000	0.91986	0.40000	0.90739
0.50000	0.91841	0.50000	0.90569
0.60000	0.91731	0.60000	0.90439
0.70000	0.91652	0.70000	0.90352
0.80000	0.91605	0.80000	0.90310
0.90000	0.91584	0.90000	0.90309
1.00000	0.91581	1.00000	0.90349

TABLE 8--Continued

Pressure = 30,000 psi		Pressure = 35,000 psi	
X_{ace}	(V/V^0)	X_{ace}	(V/V^0)
0.00000	0.90705	0.00000	0.89769
0.10000	0.90369	0.10000	0.89390
0.20000	0.90066	0.20000	0.89059
0.30000	0.89812	0.30000	0.88785
0.40000	0.89597	0.40000	0.88562
0.50000	0.89427	0.50000	0.88390
0.60000	0.89303	0.60000	0.88268
0.70000	0.89220	0.70000	0.88193
0.80000	0.89179	0.80000	0.88157
0.90000	0.89170	0.90000	0.88150
1.00000	0.89188	1.00000	0.88168
Pressure = 40,000 psi		Pressure = 45,000 psi	
X_{ace}	(V/V^0)	X_{ace}	(V/V^0)
0.00000	0.88903	0.00000	0.88106
0.10000	0.88497	0.10000	0.87683
0.20000	0.88145	0.20000	0.87316
0.30000	0.87857	0.30000	0.87016
0.40000	0.87625	0.40000	0.86775
0.50000	0.87450	0.50000	0.86596
0.60000	0.87330	0.60000	0.86475
0.70000	0.87258	0.70000	0.86409
0.80000	0.87232	0.80000	0.86393
0.90000	0.87238	0.90000	0.86414
1.00000	0.87267	1.00000	0.86465
Pressure = 50,000 psi		Pressure = 55,000 psi	
X_{ace}	(V/V^0)	X_{ace}	(V/V^0)
0.00000	0.87368	0.00000	0.86689
0.10000	0.86938	0.10000	0.86256
0.20000	0.86562	0.20000	0.85873
0.30000	0.86253	0.30000	0.85558
0.40000	0.86005	0.40000	0.85303
0.50000	0.85820	0.50000	0.85114
0.60000	0.85700	0.60000	0.84991
0.70000	0.84637	0.70000	0.84932
0.80000	0.85632	0.80000	0.84934
0.90000	0.85668	0.90000	0.84985
1.00000	0.85743	1.00000	0.85081

TABLE 8--Continued

Pressure = 60,000 psi		Pressure = 65,000 psi	
X_{ace}	(V/V^0)	X_{ace}	(V/V^0)
0.00000	0.86062	0.00000	0.85484
0.10000	0.85626	0.10000	0.85043
0.20000	0.85239	0.20000	0.84651
0.30000	0.84919	0.30000	0.84329
0.40000	0.84660	0.40000	0.84068
0.50000	0.84468	0.50000	0.83874
0.60000	0.84345	0.60000	0.83751
0.70000	0.84288	0.70000	0.83694
0.80000	0.84286	0.80000	0.83703
0.90000	0.84362	0.90000	0.83764
1.00000	0.84476	1.00000	0.83874
Pressure = 70,000 psi		Pressure = 75,000 psi	
X_{ace}	(V/V^0)	X_{ace}	(V/V^0)
0.00000	0.84946	0.00000	0.84446
0.10000	0.84499	0.10000	0.83986
0.20000	0.84103	0.20000	0.83582
0.30000	0.83777	0.30000	0.83252
0.40000	0.83513	0.40000	0.82989
0.50000	0.83319	0.50000	0.82797
0.60000	0.83197	0.60000	0.82677
0.70000	0.83143	0.70000	0.82624
0.80000	0.83156	0.80000	0.82637
0.90000	0.83222	0.90000	0.82699
1.00000	0.83339	1.00000	0.82805
Pressure = 80,000 psi		Pressure = 85,000 psi	
X_{ace}	(V/V^0)	X_{ace}	(V/V^0)
0.00000	0.83978	0.00000	0.83534
0.10000	0.83504	0.10000	0.83060
0.20000	0.83089	0.20000	0.82636
0.30000	0.82751	0.30000	0.82189
0.40000	0.82482	0.40000	0.82006
0.50000	0.82290	0.50000	0.81802
0.60000	0.82174	0.60000	0.81680
0.70000	0.82131	0.70000	0.81636
0.80000	0.82160	0.80000	0.81672
0.90000	0.82245	0.90000	0.81774
1.00000	0.82381	1.00000	0.81942

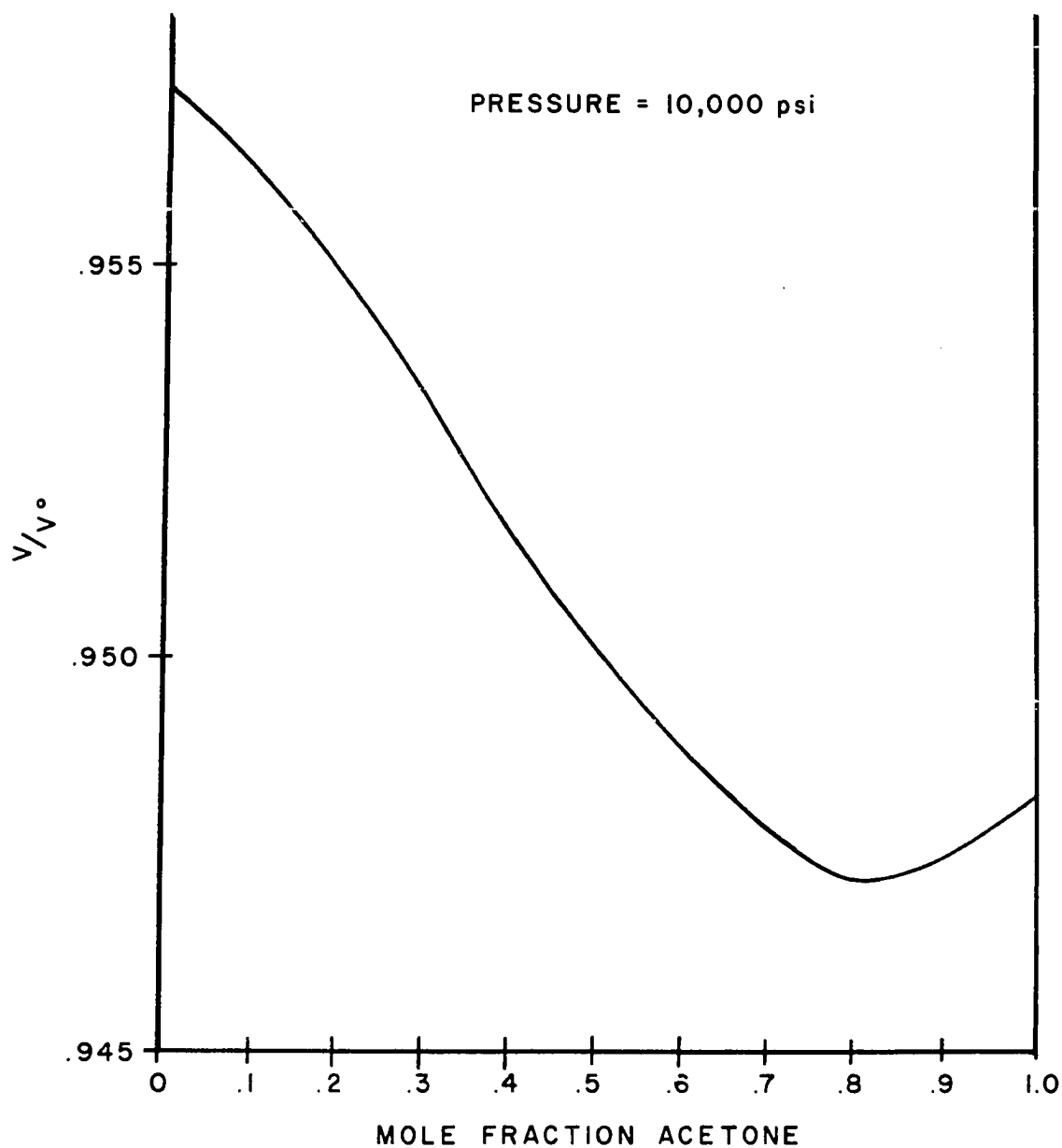


Figure 17.--Sample (V/V°) vs. X

compressibilities of this mixture determined at 1 atmosphere (See Appendix IV).

- 2) The changes in volume on mixing for each 0.1 increment in mole fraction and 5000 psi increments in pressure were calculated using the smoothed (V/V^0) data from operation 1), and molal volumes at one atmosphere:

$$\Delta \underline{V}^m = \left(\frac{V}{V^0}\right) \underline{V}_m^0 - X_{\text{acet}} \left(\frac{V}{V^0}\right)_{\text{acet}} \underline{V}_{\text{acet}}^0 - X_{\text{CS}_2} \left(\frac{V}{V^0}\right)_{\text{CS}_2} \underline{V}_{\text{CS}_2}^0 \quad (62)$$

where: $\Delta \underline{V}^m$ = molal change in volume on mixing for mixture of composition X at pressure P.

$\left(\frac{V}{V^0}\right)$ = volume occupied at pressure P by that mass of sample of composition X which occupied unit volume at one atmosphere.

$\left(\frac{V}{V^0}\right)_{\text{acet}}$ = volume occupied at pressure P by that mass of acetone which occupied unit volume at one atmosphere.

$\left(\frac{V}{V^0}\right)_{\text{CS}_2}$ = volume occupied at pressure P by that mass of carbon disulfide which occupied unit volume at one atmosphere.

- 3) These results were smoothed with respect to mole fraction at each pressure using a 5th order polynomial, as was used in constructing the change in volume on mixing curve at one atmosphere. Table 9 shows the results of this procedure. Figures 18 and 19 illustrate the curves from 5000 psi to 70,000 psi. The curves above 70,000 psi are not shown as they are probably not representative of the true behavior. (See Appendix IV).

The data points shown on the alternate curves are calculated from the (V/V^0) vs P curves and Equation (62). Thus, the deviation of these points from the smooth curves shows the

TABLE 9
 MOLAL CHANGE IN VOLUME ON MIXING AT 0°C AS A FUNCTION OF
 COMPOSITION (SMOOTHED)
 ACETONE-CARBON DISULFIDE

$$\Delta \underline{V}^m = Ax_{ace}^5 + Bx_{ace}^4 + Cx_{ace}^3 + Dx_{ace}^2 + Ex_{ace}$$

$P \times 10^{-3}$ psi	A	B	C	D	E
0	-8.433	15.946	-9.892	-1.153	3.532
1	-8.433	15.946	-9.555	-1.551	3.592
5	-8.433	15.946	-8.810	-2.333	3.629
10	-8.433	15.946	-8.827	-2.006	3.319
15	-8.433	15.946	-9.278	-1.104	2.869
20	-8.433	15.946	-9.579	- .448	2.513
25	-8.433	15.946	-9.100	- .929	2.516
30	-8.433	15.946	-9.507	- .154	2.149
35	-8.433	15.946	-9.710	+ .331	1.865
40	-8.433	15.946	-9.731	+ .542	1.676
45	-8.433	15.946	-9.637	+ .577	1.546
50	-8.433	15.946	-9.481	+ .493	1.473
55	-8.433	15.946	-9.314	+ .368	1.433
60	-8.433	15.946	-9.192	+ .294	1.385
65	-8.433	15.946	-9.221	+ .366	1.342
70	-8.433	15.946	-9.204	+ .408	1.283

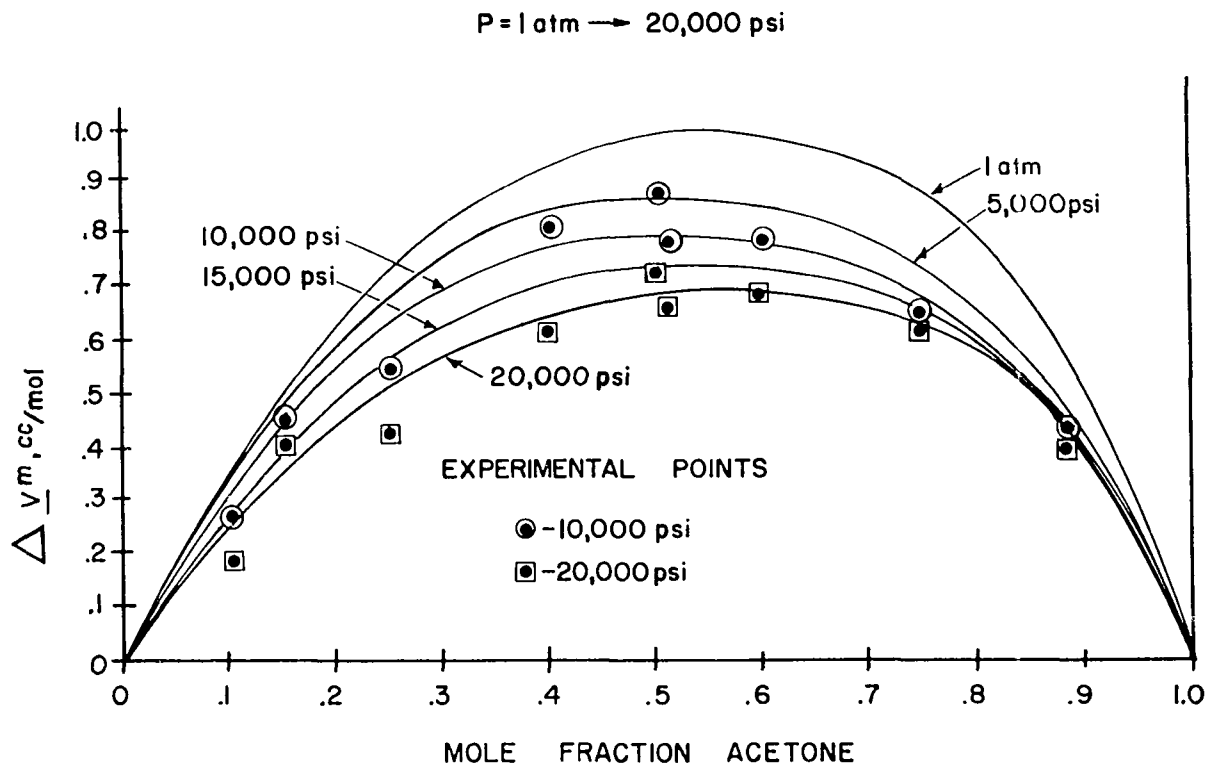


Figure 18.-- ΔV_m vs. X

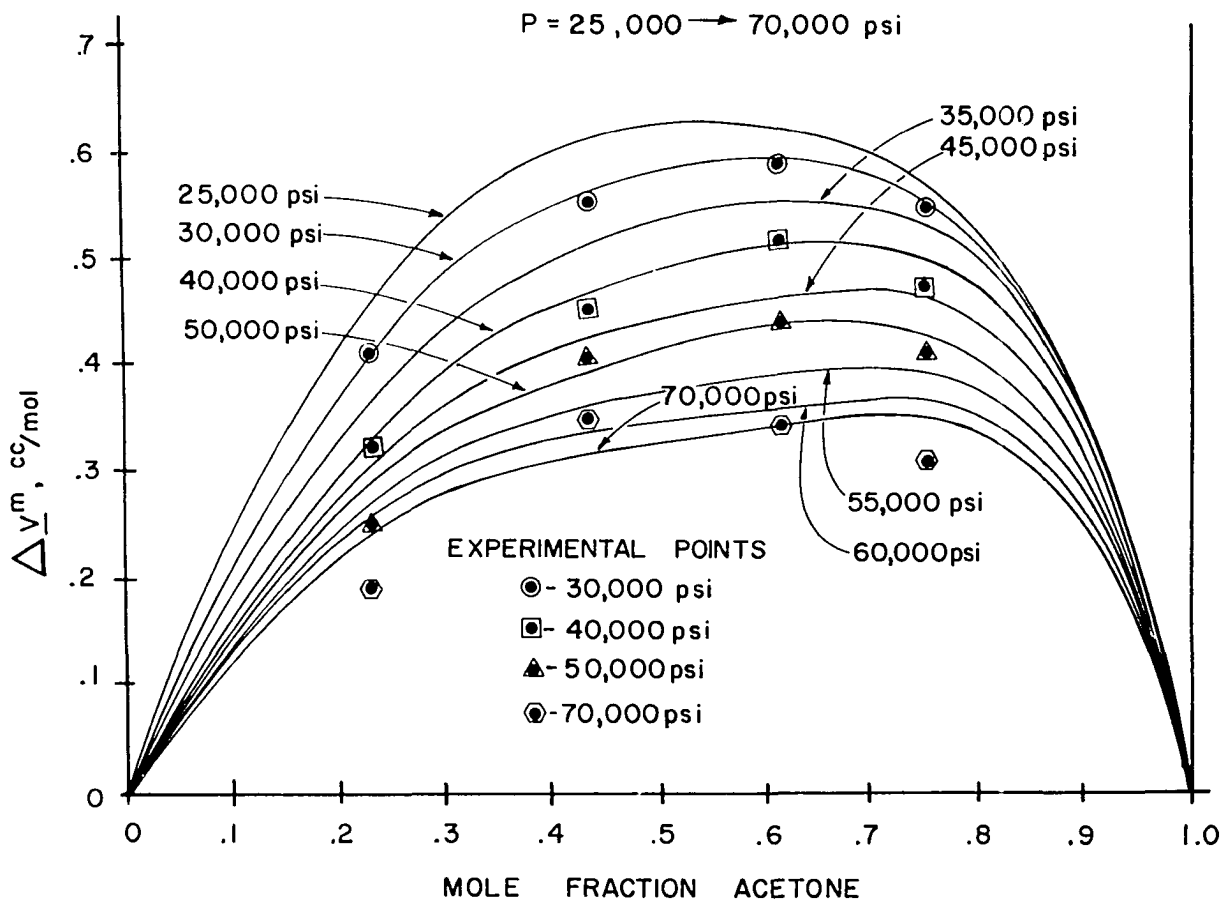


Figure 19.-- $\Delta \underline{V}^m$ vs. X

effect of smoothing operations 1) and 2) and offer a good representation of the experimental error. Table 10 lists the points calculated to 75,000 psi at each 5000 psi.

- 4) In order to integrate Equation (33) and hence predict the isothermal carbon disulfide-acetone liquid-liquid phase diagram, the results of operation 2) were smoothed with respect to pressure at each 0.02 increment in mole fraction from 10 percent to 80 percent acetone. These polynomials are listed as Table 11. One sample curve is shown as Figure 20. The curves were extrapolated to 100,000 psi, permitting graphical integration to this pressure.

Prediction of Phase Behavior

The third order polynomials expressing ΔV^m as a function of pressure at each 0.02 increment in mole fraction were integrated to pressures of 25,000, 50,000, 60,000 and 70,000 psi. The extrapolated regions were used to graphically integrate to 75,000, 80,000, 90,000 and 100,000 psi. These areas were then divided by RT and substituted into Equation (33):

$$\left(\frac{\Delta G^m}{RT}\right)^P = \left(\frac{\Delta G^m}{RT}\right)^{P_0} + \frac{1}{RT} \int_{P_0}^P \Delta V^m dP \quad (63)$$

and thus added to the free energy curve at 0°C and 1 atmosphere (See Appendix III). The results are shown as Table 12. The shape of the free energy diagrams at each pressure is shown as Figures 21 and 22.

Using the method outlined in Chapter II tangents were drawn to the curves at two points where possible. At pressures below 75,000 psi, the free energy diagram exhibits no inflection point and hence, separa-

TABLE 10

 ΔV^m VS X CALCULATED DIRECTLY

P = 14.7 psi		P = 5,000psi		P = 10,000psi		P = 15,000psi	
<u>X</u>	<u>ΔV^m</u>	<u>X</u>	<u>ΔV^m</u>	<u>X</u>	<u>ΔV^m</u>	<u>X</u>	<u>ΔV^m</u>
0.00000	0.0000	0.00000	0.0000	0.0000	0.0000	0.00000	0.0000
0.08742	0.3072	0.10401	0.3535	0.10401	0.2628	0.10401	0.2938
0.17477	0.5303	0.15436	0.4904	0.15436	0.4684	0.15436	0.4369
0.26538	0.7554	0.25778	0.6298	0.25778	0.5435	0.25778	0.4748
0.40644	0.9124	0.40473	0.8516	0.40473	0.7941	0.40473	0.7426
0.55761	0.9904	0.50608	0.9168	0.50608	0.8539	0.50608	0.7869
0.76863	0.8451	0.51046	0.8649	0.51046	0.7740	0.51046	0.7030
0.87559	0.5807	0.60180	0.8381	0.60180	0.7728	0.60180	0.7323
1.00000	0.0000	0.75209	0.6804	0.75209	0.6230	0.75209	0.6221
		0.89391	0.4518	0.89391	0.4244	0.89391	0.4248
		1.00000	0.0000	1.00000	0.0000	1.00000	0.0000
P = 20,000psi		P = 25,000psi					
<u>X</u>	<u>ΔV^m</u>	<u>X</u>	<u>ΔV^m</u>				
0.00000	0.0000	0.00000	0.0000				
0.10401	0.1891	0.10401	0.2340				
0.15436	0.4037	0.15436	0.3846				
0.25778	0.4190	0.25778	0.3722				
0.40473	0.6902	0.40473	0.6309				
0.50608	0.7226	0.50608	0.6613				
0.51046	0.6496	0.51046	0.6176				
0.60187	0.6892	0.60187	0.6042				
0.75209	0.6081	0.75209	0.5080				
0.89391	0.3947	0.89391	0.3134				
1.00000	0.0000	1.00000	0.0000				

TABLE 10--Continued

	P = 30,000psi	P = 35,000psi	P = 40,000psi
<u>X</u>	<u>Δv^m</u>	<u>Δv^m</u>	<u>Δv^m</u>
0.00000	0.0000	0.0000	0.0000
0.22262	0.4017	0.3588	0.3223
0.42235	0.5508	0.5015	0.4608
0.60720	0.5971	0.5620	0.5218
0.75209	0.5563	0.5278	0.4887
1.00000	0.0000	0.0000	0.0000
	P = 45,000psi	P = 50,000psi	P = 55,000psi
<u>X</u>	<u>Δv^m</u>	<u>Δv^m</u>	<u>Δv^m</u>
0.00000	0.0000	0.0000	0.0000
0.22262	0.2870	0.2603	0.2366
0.42235	0.4218	0.4031	0.3851
0.60720	0.4777	0.4372	0.4026
0.75209	0.4449	0.4024	0.3648
1.00000	0.0000	0.0000	0.0000
	P = 60,000psi	P = 65,000psi	P = 70,000psi
<u>X</u>	<u>Δv^m</u>	<u>Δv^m</u>	<u>Δv^m</u>
0.00000	0.0000	0.0000	0.0000
0.22262	0.2164	0.2046	0.1958
0.42235	0.3698	0.3664	0.3509
0.60720	0.3730	0.3670	0.3485
0.75209	0.3291	0.3287	0.3142
1.00000	0.0000	0.0000	0.0000
	P = 75,000psi		
<u>X</u>	<u>Δv^m</u>		
0.00000	0.0000		
0.22262	0.1890		
0.42235	0.3335		
0.60720	0.3404		
0.75209	0.3106		
1.00000	0.0000		

TABLE 11

MOLAL CHANGE IN VOLUME AT 0°C AS A FUNCTION OF PRESSURE (SMOOTHED)

$$\Delta \underline{V}^m = A + BP + CP^2 + DP^3$$

X	A	Bx10 ³	Cx10 ⁵	Dx10 ⁷
0.10	0.3463	-5.3662	1.6227	2.1109
0.12	0.4074	-6.3214	2.0513	2.3125
0.14	0.4652	-7.2359	2.5066	2.4496
0.16	0.5196	-8.1090	2.9850	2.5259
0.18	0.5706	-8.9404	3.4844	2.5443
0.20	0.6182	-9.7290	3.9987	2.5106
0.22	0.6622	-10.4752	4.5286	2.4253
0.24	0.7028	-11.1774	5.0670	2.2953
0.26	0.7400	-11.8354	5.6117	2.1233
0.28	0.7738	-12.4489	6.1605	1.9121
0.30	0.8043	-13.0173	6.7098	1.6656
0.32	0.8316	-13.5398	7.2553	1.3884
0.34	0.8559	-14.0156	7.7935	1.0842
0.36	0.8772	-14.4449	8.3227	0.7556
0.38	0.8957	-14.8265	8.8384	0.4072
0.40	0.9115	-15.1597	9.3360	0.0437
0.42	0.9247	-15.4443	9.8141	-0.3327
0.44	0.9355	-15.6799	10.2693	-0.7183
0.46	0.9440	-15.8656	10.6974	-1.1086
0.48	0.9503	-16.0011	11.0958	-1.5006
0.50	0.9544	-16.0854	11.4602	-1.8896
0.52	0.9566	-16.1184	11.7882	-2.2727
0.54	0.9567	-16.0992	12.0758	-2.6458
0.56	0.9550	-16.0272	12.3193	-3.0047
0.58	0.9513	-15.9018	12.5152	-3.3454
0.60	0.9457	-15.7229	12.6620	-3.6661
0.62	0.9380	-15.4895	12.7547	-3.9613
0.64	0.9284	-15.2020	12.7932	-4.2305
0.66	0.9165	-14.8577	12.7671	-4.4633
0.68	0.9022	-14.4576	12.6784	-4.6610
0.70	0.8854	-14.0014	12.5240	-4.8199
0.72	0.8657	-13.4877	12.2987	-4.9349
0.74	0.8428	-12.9162	11.9997	-5.0025
0.76	0.8164	-12.2864	11.6235	-5.0189
0.78	0.7860	-11.5974	11.1662	-4.9799
0.80	0.7512	-10.8492	10.6260	-4.8832

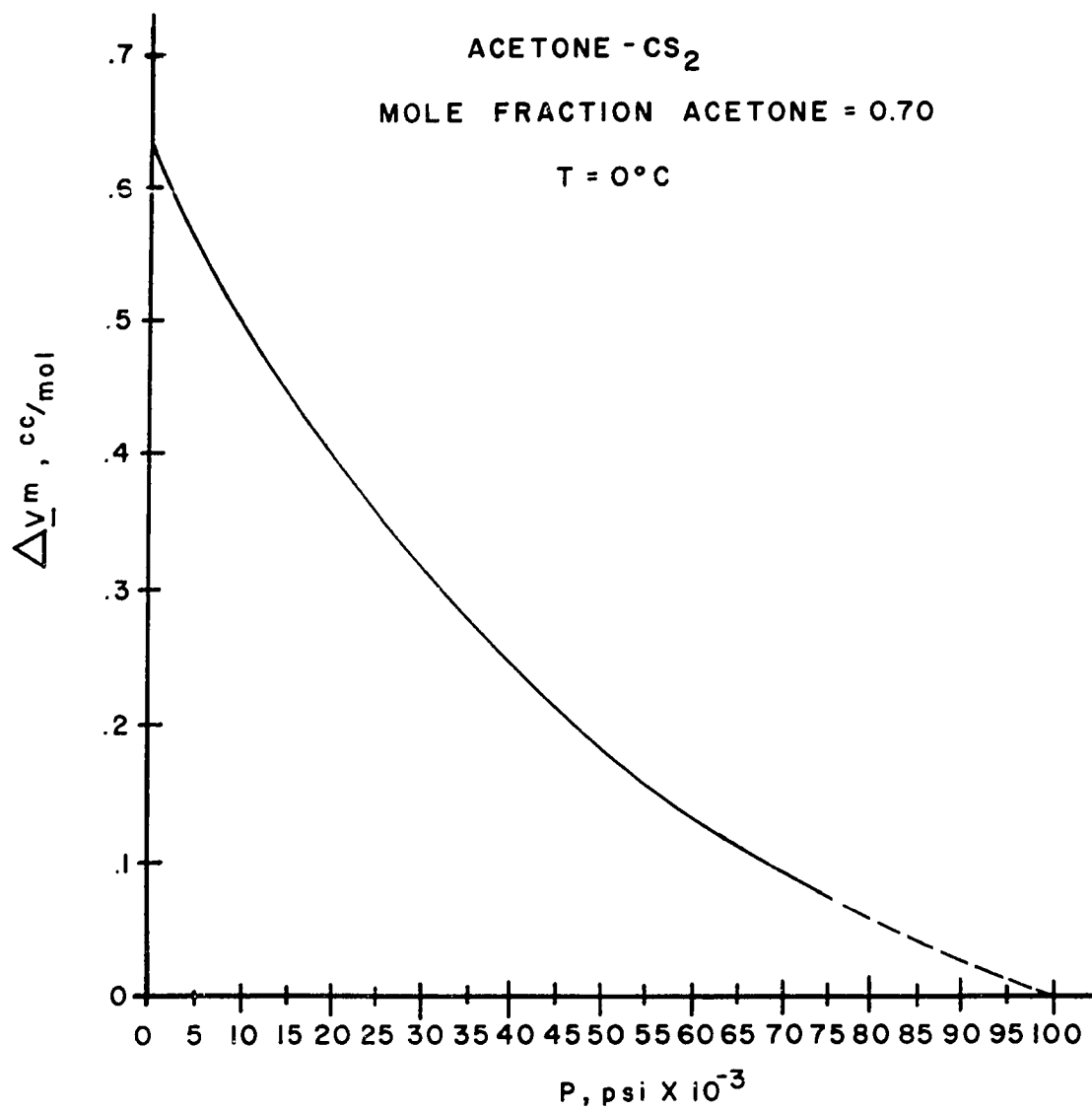


Figure 20.--Sample $\Delta \underline{V}^m$ vs. P

TABLE 12

MOLAL CHANGE IN FREE ENERGY ON MIXING AT 0°C AS A FUNCTION
OF COMPOSITION
ACETONE-CARBON DISULFIDE

x_{ace}	$-\Delta G^m/RT$			
	P = 25,000psi	50,000psi	60,000psi	70,000psi
0.00	0.0000	0.0000	0.0000	0.0000
0.10	0.0855	0.0717	0.0676	0.0638
0.12	0.0923	0.0760	0.0712	0.0667
0.14	0.0983	0.0797	0.0741	0.0690
0.16	0.1041	0.0833	0.0770	0.0713
0.18	0.1096	0.0868	0.0799	0.0736
0.20	0.1150	0.0899	0.0824	0.0759
0.22	0.1198	0.0932	0.0852	0.0779
0.24	0.1245	0.0963	0.0878	0.0801
0.26	0.1289	0.0992	0.0903	0.0822
0.28	0.1333	0.1023	0.0930	0.0845
0.30	0.3174	0.1052	0.0955	0.0867
0.32	0.1410	0.1078	0.0977	0.0887
0.34	0.1445	0.1103	0.1000	0.0908
0.36	0.1478	0.1127	0.1022	0.0927
0.38	0.1509	0.1152	0.1044	0.0948
0.40	0.1538	0.1174	0.1064	0.0966
0.42	0.1567	0.1197	0.1086	0.0986
0.44	0.1594	0.1218	0.1105	0.1004
0.46	0.1615	0.1237	0.1122	0.1020
0.48	0.1637	0.1255	0.1139	0.1036
0.50	0.1657	0.1272	0.1155	0.1051
0.52	0.1677	0.1289	0.1170	0.1066
0.54	0.1696	0.1306	0.1187	0.1081
0.56	0.1712	0.1320	0.1200	0.1093
0.58	0.1728	0.1334	0.1214	0.1105
0.60	0.1741	0.1347	0.1224	0.1116
0.62	0.1752	0.1357	0.1233	0.1124
0.64	0.1757	0.1362	0.1238	0.1127
0.66	0.1763	0.1369	0.1244	0.1132
0.68	0.1767	0.1373	0.1248	0.1135
0.70	0.1764	0.1373	0.1248	0.1135
0.72	0.1761	0.1373	0.1247	0.1134
0.74	0.1750	0.1367	0.1242	0.1129
0.76	0.1730	0.1353	0.1229	0.1116
0.78	0.1706	0.1338	0.1215	0.1104
0.80	0.1668	0.1311	0.1191	0.1081
1.00	0.0000	0.0000	0.0000	0.0000

TABLE 12--Continued

X_{ace}	$-\Delta G^m/RT$			
	75,000psi	80,000psi	90,000psi	100,000psi
0.00	0.0000	0.0000	0.0000	0.0000
0.10	0.0620	0.0603	0.0569	0.0536
0.12	0.0646	0.0623	0.0585	0.0545
0.14	0.0666	0.0642	0.0597	0.0554
0.16	0.0686	0.0659	0.0608	0.0558
0.18	0.0706	0.0676	0.0618	0.0564
0.20	0.0724	0.0693	0.0632	0.0573
0.22	0.0745	0.0711	0.0646	0.0583
0.24	0.0764	0.0729	0.0660	0.0593
0.26	0.0785	0.0746	0.0673	0.0604
0.28	0.0805	0.0766	0.0691	0.0617
0.30	0.0826	0.0785	0.0707	0.0631
0.32	0.0844	0.0803	0.0723	0.0646
0.34	0.0864	0.0822	0.0740	0.0661
0.36	0.0882	0.0839	0.0754	0.0672
0.38	0.0903	0.0858	0.0772	0.0687
0.40	0.0920	0.0875	0.0788	0.0704
0.42	0.0939	0.0894	0.0806	0.0720
0.44	0.0957	0.0911	0.0823	0.0731
0.46	0.0972	0.0926	0.0836	0.0750
0.48	0.0988	0.0942	0.0852	0.0765
0.50	0.1002	0.0955	0.0865	0.0779
0.52	0.1017	0.0970	0.0882	0.0798
0.54	0.1021	0.0984	0.0895	0.0812
0.56	0.1043	0.0996	0.0907	0.0825
0.58	0.1055	0.1007	0.0917	0.0833
0.60	0.1066	0.1018	0.0927	0.0843
0.62	0.1073	0.1025	0.0934	0.0850
0.64	0.1076	0.1027	0.0937	0.0853
0.66	0.1080	0.1031	0.0940	0.0856
0.68	0.1083	0.1033	0.0940	0.0855
0.70	0.1083	0.1033	0.0941	0.0856
0.72	0.1082	0.1032	0.0938	0.0853
0.74	0.1076	0.1026	0.0932	0.0846
0.76	0.1064	0.1014	0.0921	0.0836
0.78	0.1052	0.1002	0.0910	0.0826
0.80	0.1050	0.0981	0.0889	0.0804
1.00	0.0000	0.0000	0.0000	0.0000

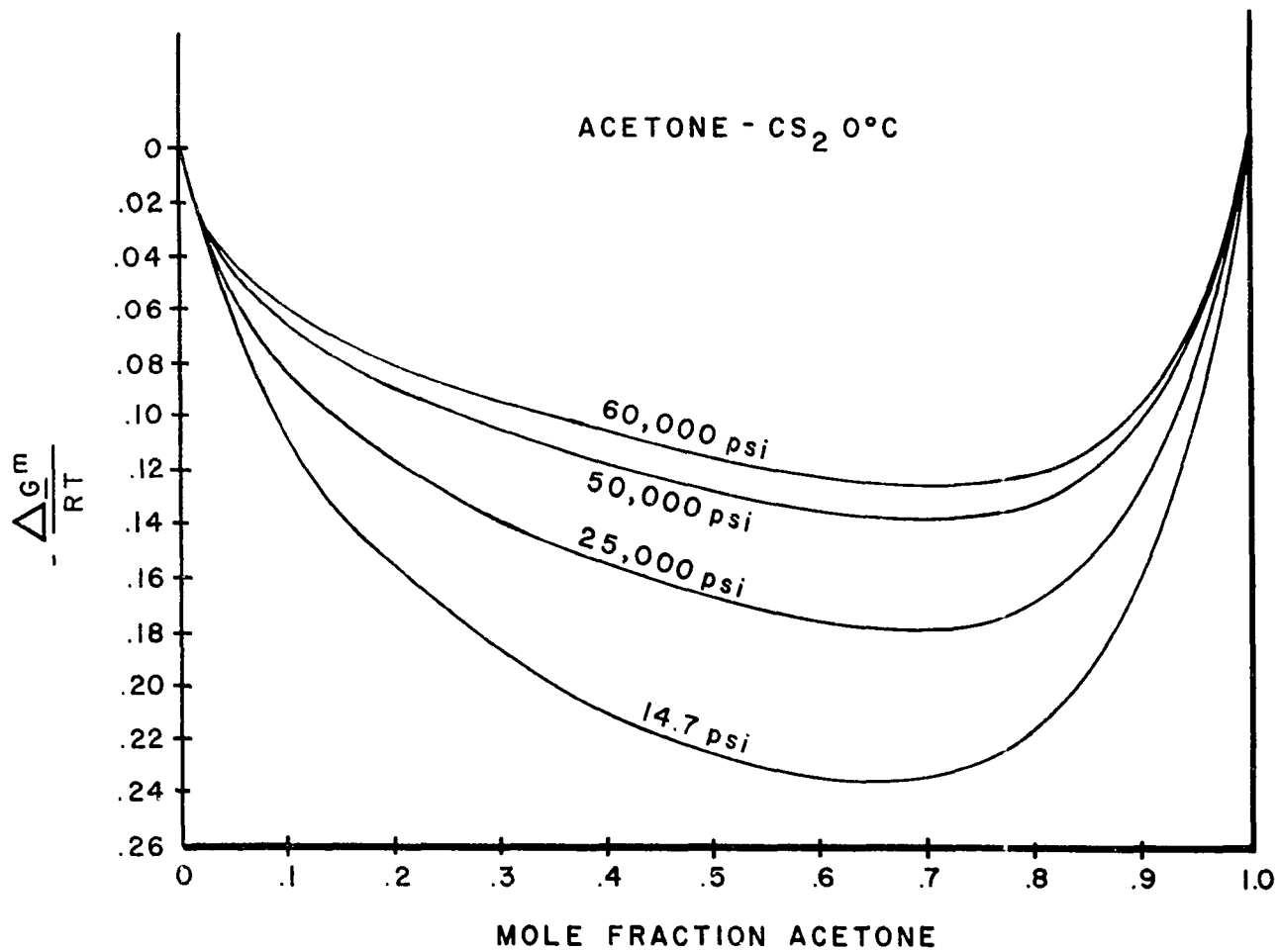


Figure 21.--Change in Free Energy on Mixing

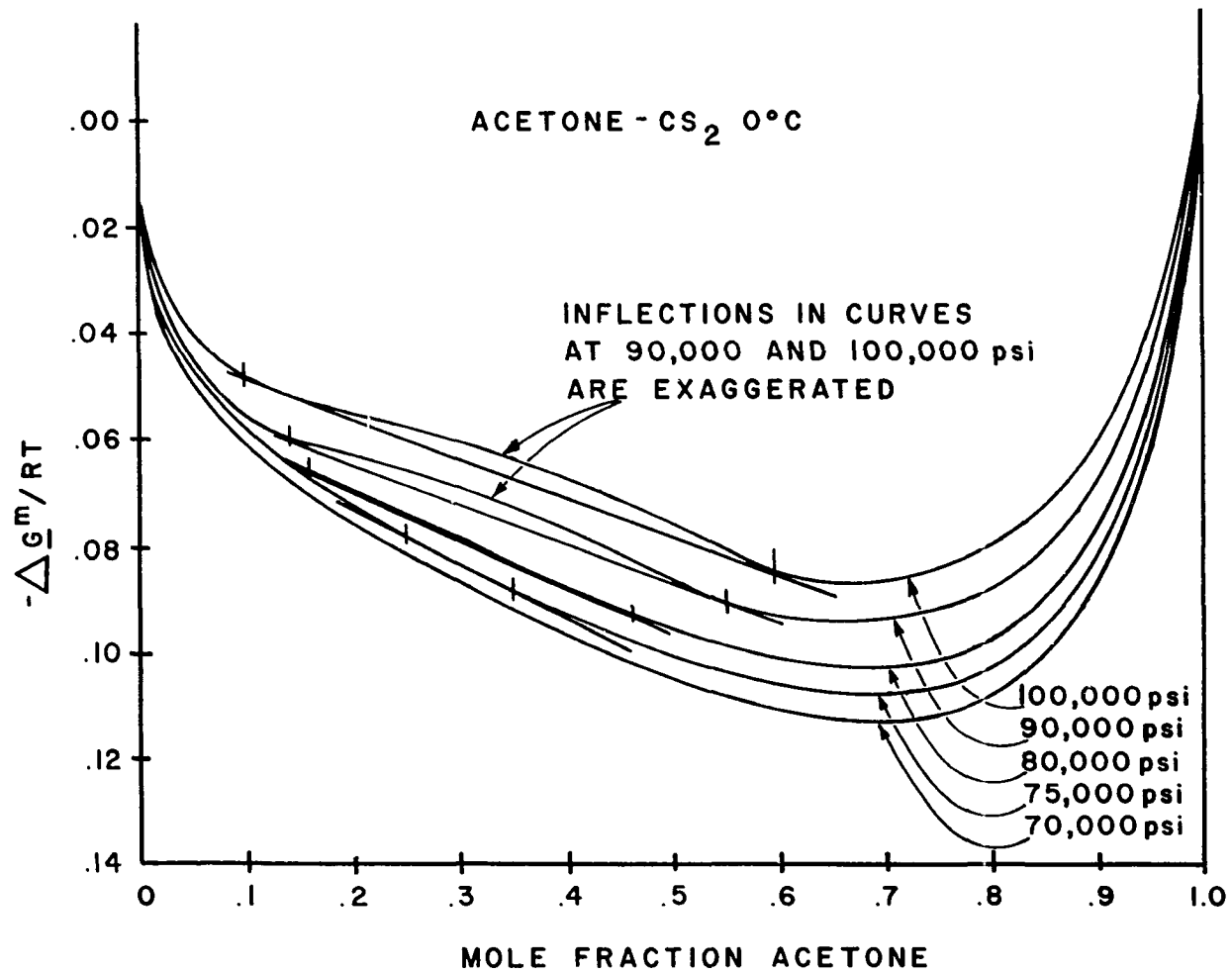


Figure 22.--Change in Free Energy on Mixing

tion into two liquid phases is predicted only at pressures above this at 0°C. The compositions of the phases in equilibrium at high pressures as determined by the tangents are shown as Figure 23.

It should be noted here that the free energy diagrams as shown in Figure 22 exhibit "humps" or regions of metastable and unstable conditions instead of straight lines between the compositions in equilibrium (See Chapter II). This occurs because of the smoothing operations on the PVT data. If the data were accurate enough to show discontinuities when they occurred, as pictured diagrammatically as Figure 24, the true free energy curve would be obtained. Instead, the smoothing operations tend to round off these discontinuities and the continuous free energy curves are obtained. Also, if these changes in volume on mixing data were this accurate, prediction of the isothermal liquid-liquid phase diagram could be made directly from such figures without need for the change in free energy on mixing diagrams.

The predicted and observed phase diagrams are reproduced as Figure 25. The shapes are markedly similar to the isobaric results of Clusius and Ringer (16) at one atmosphere (Figure 26).

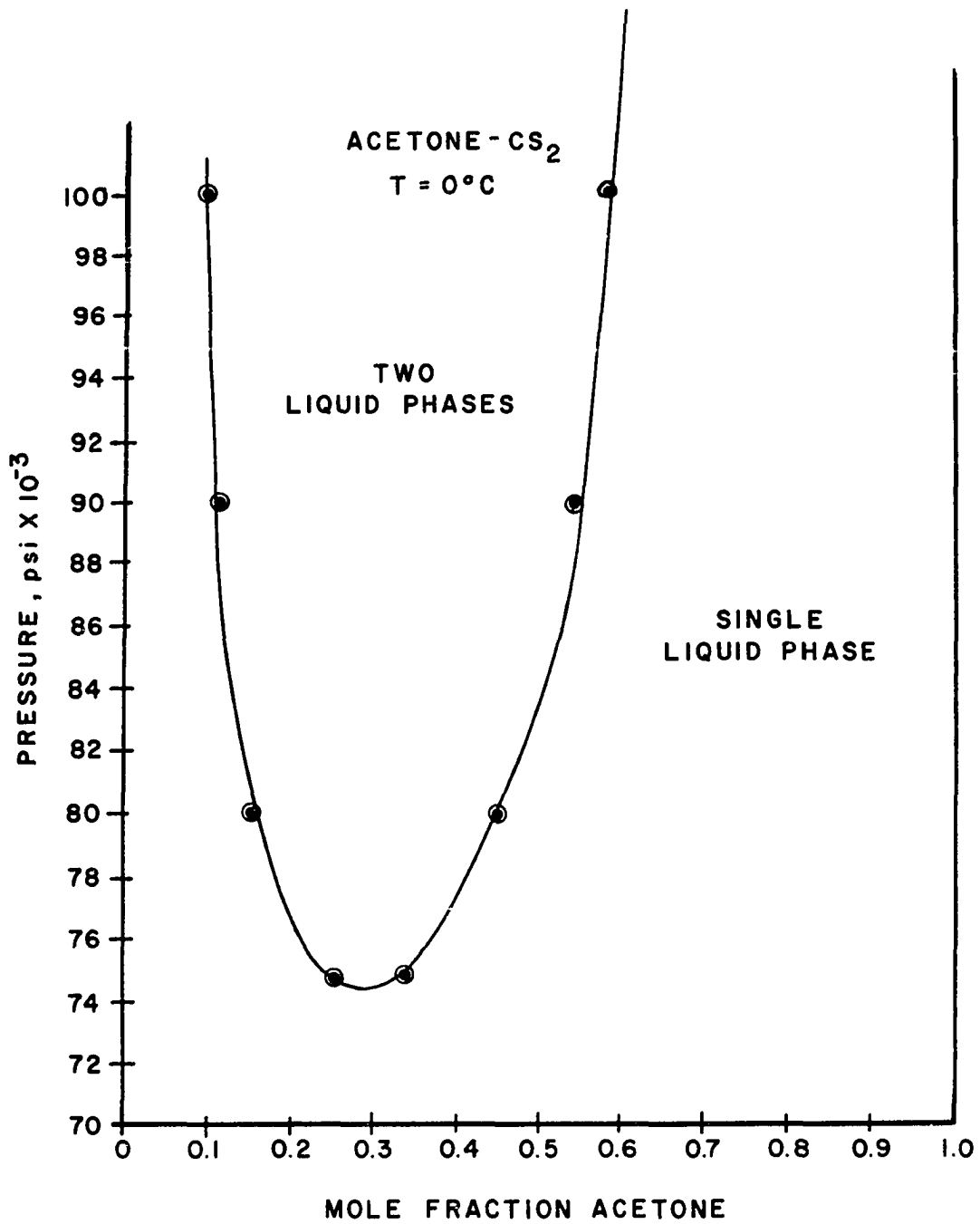


Figure 23.--Prediction of Phase Behavior

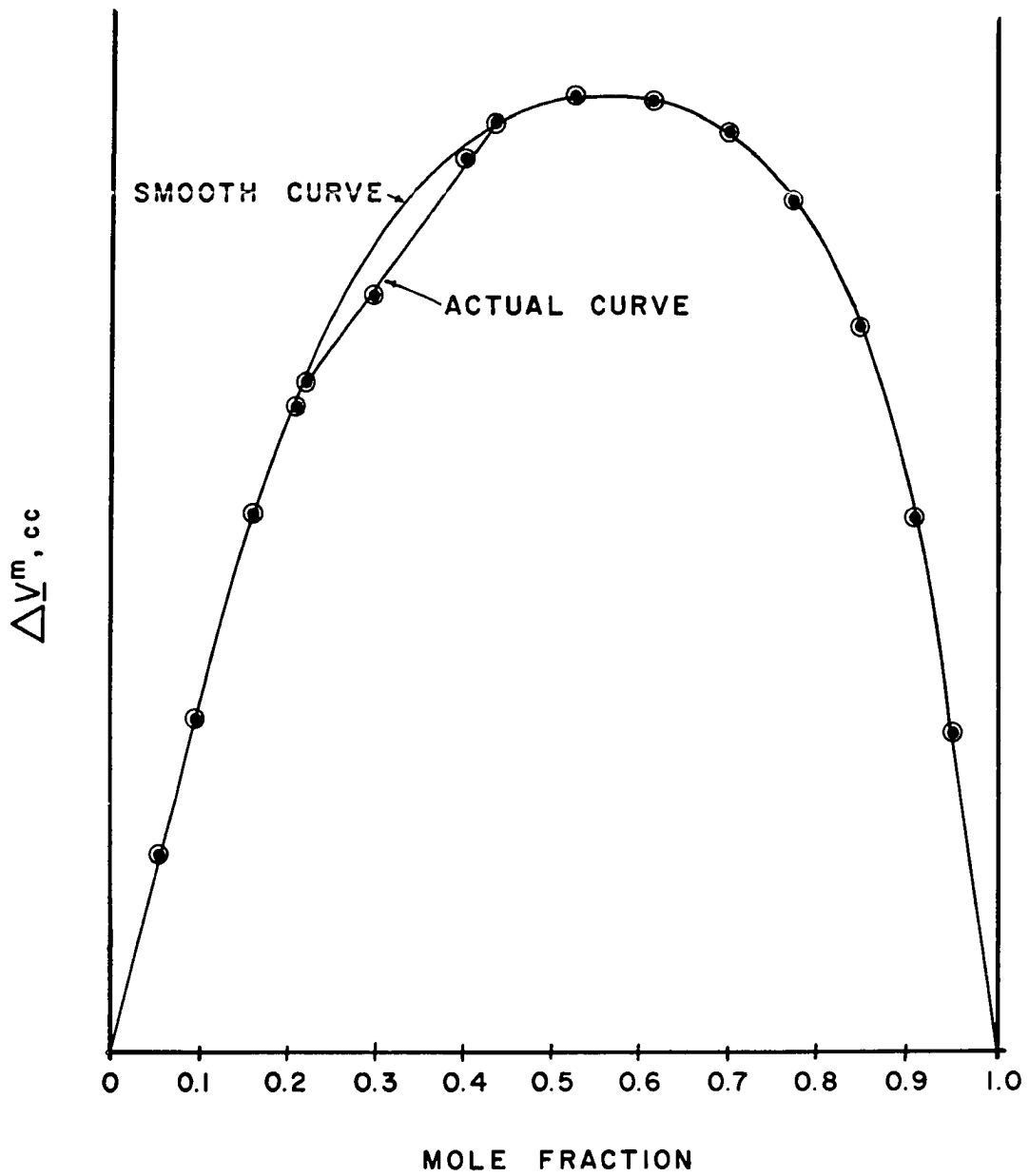


Figure 24.--Hypothetical Change in Volume on Mixing

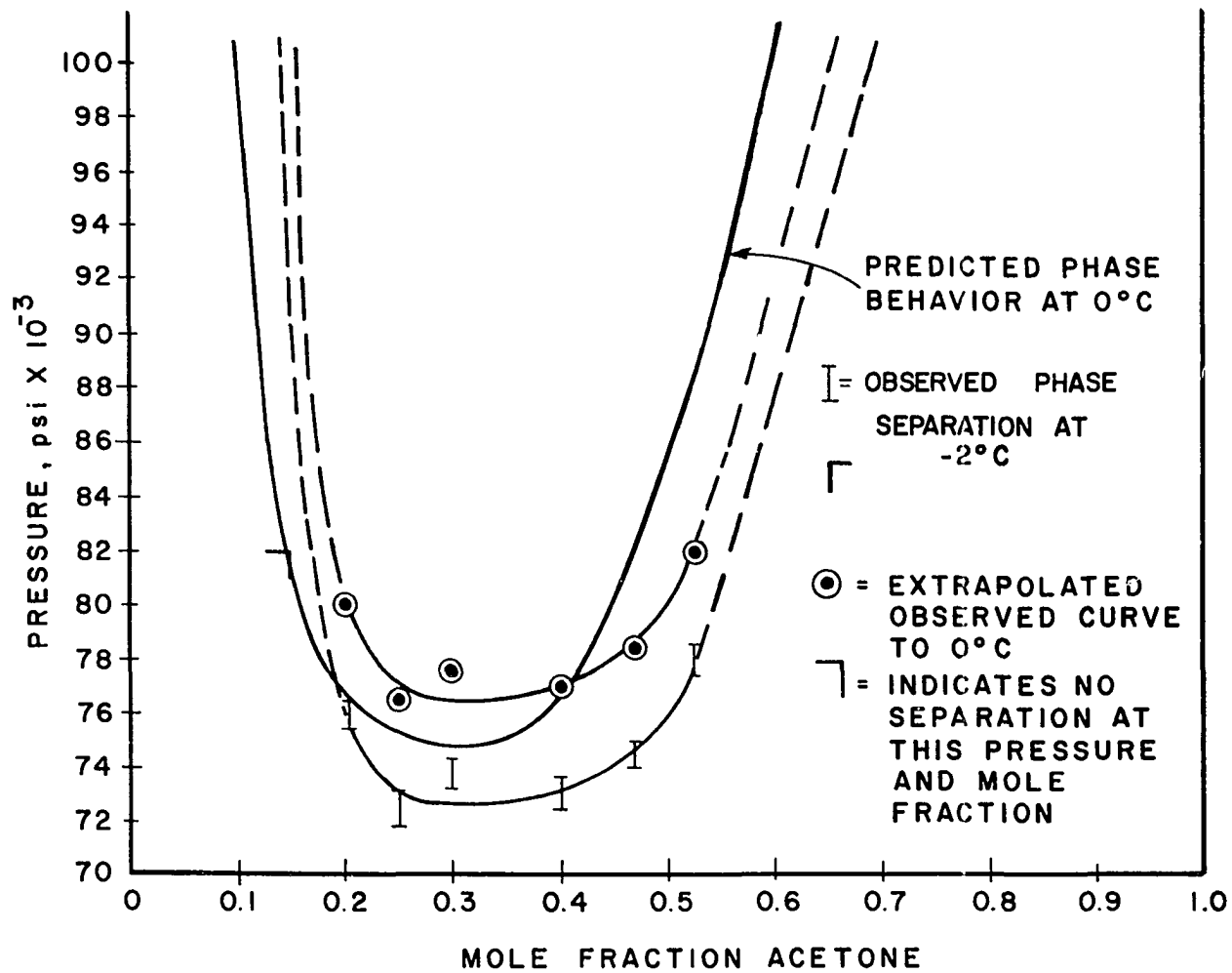


Figure 25.--Predicted and Observed Phase Behavior

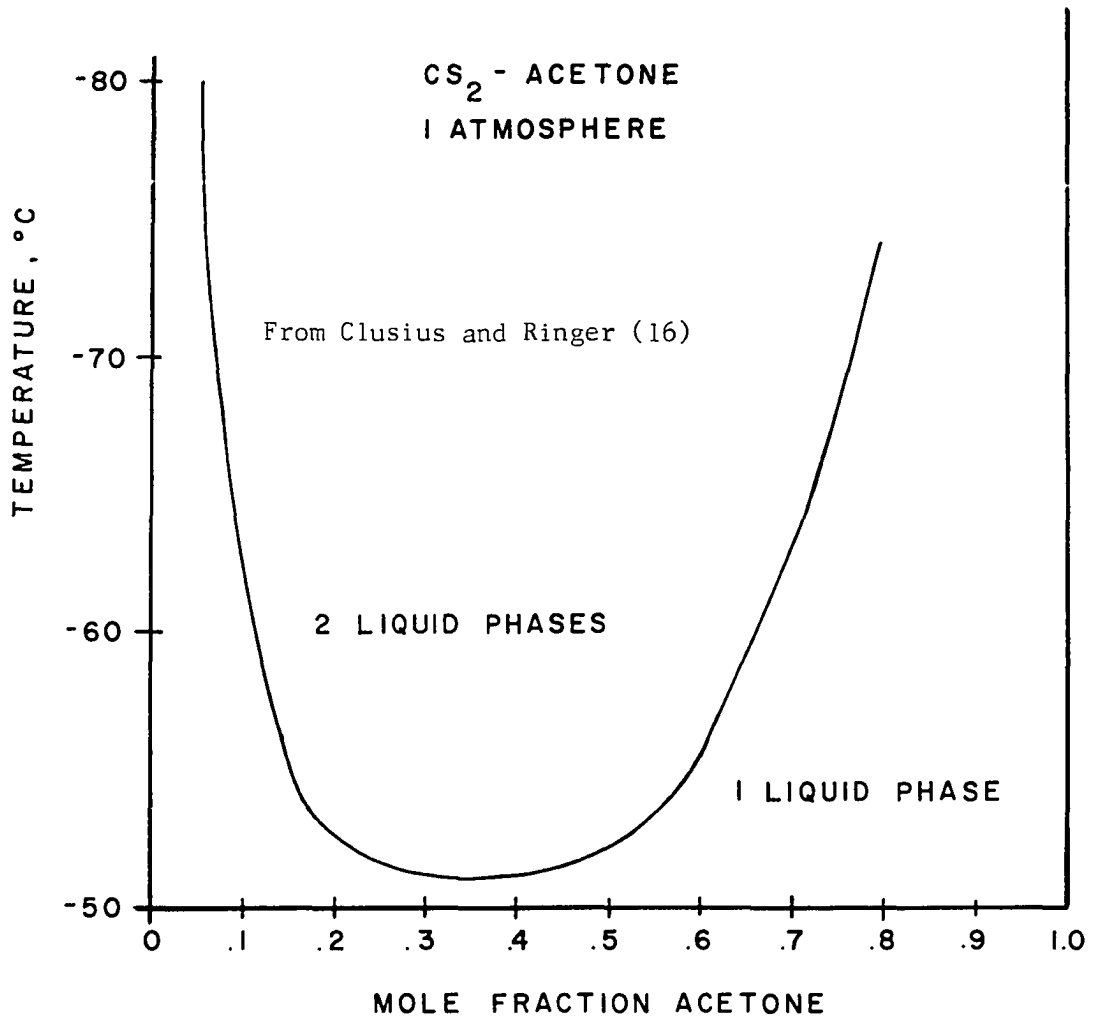


Figure 26.--Isobaric Phase Behavior

CHAPTER IX

CONCLUSIONS

The agreement between the predicted phase diagram for the system acetone-carbon disulfide at 0°C and the experimental points extrapolated to that same temperature (Figure 25) seem to indicate, neglecting the possibility of fortuitous error cancellations, rather acceptable results. As determined in "Error Analysis," the expected accuracy in the change in volume on mixing was from one to five percent. The prediction, based in part on this term, deviates from the observed behavior by an average of three percent in pressure. If the activity data of Zawidzky (48), heat of mixing data of Schmidt (36), and specific heat data of Staveley (41), are all considered perfect, the error in the prediction can be assumed to be completely the fault of the measurements made in this investigation. However, as seen from the scatter in the heat of mixing data (Appendix III), a final judgment of the accuracy of the data must await a more precise means of ascertaining the free energy diagram at 0°C and one atmosphere. With this stipulation, the contributions of the work may be listed as follows:

- 1) The fractional change in volume with pressure for one binary liquid system at one temperature has been obtained to 85,000 psi over the entire range of composition.
- 2) A method has been described which allows the use of this

data, along with solution behavior and density data at one atmosphere, in predicting the isothermal liquid-liquid phase diagram of the system or;

- 3) If the isothermal phase diagram is available, permits a check on the accuracy of the thermodynamic data.
- 4) The isothermal liquid-liquid phase diagram for the system has been obtained and found to compare favorably with the prediction.

TABLE OF NOMENCLATURE

a	= defined by Equation 93.
\bar{a}_i	= activity of component i (See Equation 9)
\bar{a}_1	= activity of component 1
\bar{a}_2	= activity of component 2
A_i	= i^{th} coefficient
A	= coefficient
b	= defined by Equation 93
B	= coefficient
C	= coefficient
$(C_p)_i$	= molal specific heat of pure component i , cal./mole $^{\circ}\text{K}$.
$(C_p)_m$	= molal specific heat of mixture, cal./mole $^{\circ}\text{K}$.
ΔC_p^m	= molal change in specific heat on mixing, cal./mole $^{\circ}\text{K}$.
$\Delta \bar{C}_p^m$	= average molal change in specific heat on mixing, cal./mole $^{\circ}\text{K}$.
D	= coefficient
E	= coefficient
f	= function
f_i°	= fugacity of pure component i
\bar{f}_i	= fugacity of component i in solution
G_i	= molal free energy of pure component i
\bar{G}_i	= partial molal free energy of component i in solution
G_1	= molal free energy of pure component 1

\bar{G}_1	= partial molal free energy of component 1 in solution
\underline{G}_2	= molal free energy of pure component 2
\bar{G}_2	= partial molal free energy of component 2 in solution
\underline{G}_1'	= molal free energy of pure component 1 referred to phase 1
\bar{G}_1'	= partial molal free energy of component 1 in solution in phase 1
\underline{G}_1''	= molal free energy of pure component 1 referred to phase 2
\bar{G}_1''	= partial molal free energy of component 1 in solution in phase 2
\underline{G}_2'	= molal free energy of pure component 2 referred to phase 1
\bar{G}_2'	= partial molal free energy of component 2 in solution in phase 1
\underline{G}_2''	= molal free energy of pure component 2 referred to phase 2
\bar{G}_2''	= partial molal free energy of component 2 in solution in phase 2
\underline{G}_m	= molal free energy of mixture
$\Delta \underline{G}^m$	= molal change in free energy on mixing
ΔG^m	= total change in free energy on mixing
$(\Delta \underline{G}^m)'$	= molal change in free energy on mixing in phase 1
$(\Delta \underline{G}^m)''$	= molal change in free energy on mixing in phase 2
\underline{H}_i	= molal enthalpy of pure component i
\bar{H}_i	= partial molal enthalpy of component i in solution
$\Delta \underline{H}^m$	= molal change in enthalpy on mixing
K	= bellows constant, cc/ohm (See Equation (57))
L	= length of bellows, in.
N_1	= moles of component 1
N_2	= moles of component 2
P	= pressure, psi.
P_o	= initial pressure, psi.

ΔP	= change in pressure, psi.
q	= defined by Equation (64)
Q	= defined by Equation (64)
r	= resistivity of Karma wire, ohms/in.
R_1, R_2, R_3	= constant value resistors, ohms
R_s	= resistance of Karma wire segment as measured, ohms
$R_w - R_w'$	= slide wire rheostat
R	= gas constant
$\Delta_p R_s$	= change in resistance of Karma wire segment during pressure change P , ohms.
T	= temperature, °K.
V	= volume, cc.
V^0	= volume of bellows at one atmosphere, cc.
\underline{V}_i	= molal volume of pure component i at pressure P , cc.
\bar{V}_i	= partial molal volume of component i in solution at pressure P ., cc.
\underline{V}_1	= molal volume of pure component 1 at pressure P , cc.
\bar{V}_1	= partial molal volume of component 1 in solution at pressure P ., cc.
\underline{V}_2	= molal volume of pure component 2 at pressure P , cc.
\bar{V}_2	= partial molal volume of component 2 in solution at pressure P ., cc.
\underline{V}_m	= molal volume of mixture at pressure P , cc.
\underline{V}_m^0	= molal volume of mixture at 1 atmosphere, cc.
\underline{V}^0_{ace}	= molal volume of pure acetone at one atmosphere, cc.
$\underline{V}^0_{CS_2}$	= molal volume of pure CS_2 at one atmosphere, cc.
(V/V^0)	= volume occupied by mass of mixture at pressure P which occupied unit volume at one atmosphere.
$(\Delta \underline{V}^m)^0$	= molal change in volume on mixing at one atmosphere, cc.

$\Delta \underline{v}^m$	= molal change in volume on mixing at pressure P, cc.
$\Delta_p(V/V^0)$	= fractional change in volume during pressure change P.
$\Delta_p(V/V^0)'$	= fractional change in volume during pressure change P as reported in the literature
W	= weight of sample, g
X	= mole fraction
X_i	= mole fraction component i
X_1	= mole fraction component 1
X_2	= mole fraction component 2
X_1'	= mole fraction component 1 in phase 1
X_1''	= mole fraction component 1 in phase 2
X_2'	= mole fraction component 2 in phase 1
X_2''	= mole fraction component 2 in phase 2
X'	= mole fraction of total system existing as phase 1
X''	= mole fraction of total system existing as phase 2
$(MW)_{ace}$	= molecular weight of acetone, g
$(MW)_{CS_2}$	= molecular weight of carbon disulfide, g
β_s	= adiabatic compressibility (See Equation (94))
β_t	= isothermal compressibility (See Equation (93))
δ	= error
$\bar{\gamma}$	= activity coefficient (See Equation (1))
ρ	= density, g./cc.
ρ^0	= density at one atmosphere, g./cc.

LITERATURE CITED

1. Adams, L. H. Jour. Am. Chem. Soc., LIII, 1931, p. 3769.
2. Adams, L. H. Jour. Am. Chem. Soc., LIV, 1932, p. 2229.
3. Alders, L. Liquid-Liquid Extraction. New York: Elsevier, 1955.
4. Babb, S. E., Jr. ASME Winter 1962 Meeting, to be published.
5. Balanchandran, C. G. Jour. Indian Inst. Sci., XXXVIII A, 1956, p. 10.
6. Benedict, M., Webb, G. B. and Rubin, L. C. Chem. Eng. Prog., XLVII, 1951, p. 449.
7. Bridgman, P. W. Proc. Am. Acad. Arts Sci., XLVII, 1912, p. 439.
8. _____. Proc. Am. Acad. Arts Sci., XLIX, 1913, p. 1.
9. _____. Proc. Am. Acad. Arts Sci., LVIII, 1923, p. 166.
10. _____. Proc. Am. Acad. Arts Sci., LXVI, 1931, p. 185.
11. _____. Proc. Am. Acad. Arts Sci., LXVII, 1931, p. 1.
12. _____. Proc. Am. Acad. Arts Sci., LXXVII, 1949, p. 129.
13. _____. The Physics of High Pressure. New York: Macmillan, 1931, p. 39.
14. _____. Proc. Am. Acad. Arts Sci., LXXIV, 1940, p. 21.
15. _____. Jour. Chem. Phys., IX, 1941, p. 794.
16. Clusius, K. and Ringer, W. Zeit. Physik. Chem., CLXXXVII A, 1940, p. 186.
17. Cutler, W. G., et. al. Jour. Chem. Phys., XXIX, 1958, p. 727.
18. Eduljee, H. E., Newitt, D. M. and Weale, K. E. Jour. Chem. Soc., Part IV, 1951, p. 3086.
19. Faust. Zeit. Physik. Chem., LXXXX, 1912, p. 97.

20. Findlay, A. Phase Rule. New York: Dover, 1951, p. 101.
21. Gibson, R. E., and Loeffler, O. H. Jour. Phys. Chem., XLIII, 1939, p. 207.
22. Griswold, J. and Buford, C. B. Ind. and Eng. Chem., XLI, 1949, p. 2347.
23. Harwood Engineering Company, company publication.
24. Hougen, O. A., Watson, K. M. and Ragatz, R. A. Chemical Process Principles. Pt. 2. 2nd ed. New York: Wiley, 1959.
25. Mathieson, A. R. Jour. Chem. Soc., CLXI, 1958, p. 4444.
26. Mickley, H. S., Sherwood, T. K. and Reed, C. E. Applied Mathematics in Chemical Engineering. New York: McGraw-Hill, 1957, p. 54.
27. Moelwyn-Hughes, E. A. Physical Chemistry. New York: Pergamon, 1957.
28. Pitzer, K. S. and Hultgren, G. O. Jour. Am. Chem. Soc., LXXX, 1958, p. 4793.
29. Poulter, T. C. Phys. Rev., XXXV, 1930, p. 297.
30. Powers, J. E. Chemist Analyst, XLIX, 1960, p. 54.
31. Prigogine, I. and Defay, R. Chemical Thermodynamics. New York: Longmans-Green, 1954, p. 289.
32. _____. Chemical Thermodynamics. New York: Longmans-Green, 1954, p. 290.
33. Reamer, H. H., Berry, V. and Sage, B. H. Jour. Chem. Eng. Data, VI, 1961, p. 184.
34. Rowlinson, J. S. Liquids and Liquid Mixtures. London: Butterworth, 1959, p. 136.
35. _____. Liquids and Liquid Mixtures. London: Butterworth, 1959, p. 160.
36. Schmidt, G. C. Zeit. Physik. Chem., CXXI, 1926, p. 221.
37. Seitz, W. and Lechner, G. Annalen der Physik, XLIX, 1916, p. 93.
38. Singh, H. and Seth, R. S. Ann. Physik, V, 1959, p. 53.
39. Sokollu, A. Fen Faklute Univ. Istanbul, XVI A, 1951, p. 162.
40. Springer, R. and Roth, H. Monatsch, LVI, 1930, p. 1.

41. Staveley, L. A. K., et. al. Trans. Far. Soc., LI, 1955, p. 323.
42. Timmermans, J. Journal de Chimie Physique, XX, 1923, p. 491.
43. _____. Physico-Chemical Constants of Binary Systems in Concentrated Solutions. New York: Interscience, 1959.
44. van Itterbeck, A. and Verhaegen, L. Proc. Phys. Soc., LXII B, 1949, p. 800.
45. Vecino and Varona. Anales Soc. Espan. fis. quim, XI, 1913, p. 498.
46. Washburn, E. W. International Critical Tables. 1st ed. New York: McGraw-Hill, 1928.
47. Winnick, J. and Powers, J. E. A. I. Ch. E. Journal, VII, 1961, p. 303.
48. Zawidzky, J. V. Zeit. Physik. Chem., XXXV, 1900, p. 154.

References to Table 2

49. Bredig, G. and Bayer, R. Zeit. Physik. Chem., CXXX, 1927, p. 15.
50. Brown, I. Austr. Journal Sci. Res., V, 1952, p. 530.
51. Brown, I., Fock, W., and Smith, F. Austr. Journal Chem., IX, 1956, p. 364.
52. Brown, I. and Smith, F. Austr. Journal Chem., VII, 1954, p. 264.
53. _____. Austr. Journal Chem., VIII, 1955, p. 501.
54. _____. Austr. Journal Chem., VIII, 1955, p. 62.
55. _____. Austr. Journal Chem., XII, 1959, p. 407.
56. Harms, H. Zeit. Physik. Chem., B, LIII, 1943, p. 280.
57. Joukovsky, N. I. Bull. Soc. Chem. Belg., XLIII, 1934, p. 397.
58. Kremann, R., Meingast, R. and Gugl, F. Monatsch, XXXV, 1914, p. 1235.
59. Neparko, E., Ph.D. Thesis, University of Oklahoma, 1960.
60. Parks, G. S. and Chaffe, C. S. Jour. Phys. Chem., XXXI, 1927, p. 439.
61. Phibbs, M. K. Jour. Phys. Chem., LIX, 1955, p. 346.

62. Peel, J. B., Madgin, W. M. and Briscoe, H.V.A. Jour. Phys. Chem., XXXII, 1928, p. 285.
63. Poppe, G. Bull. Soc. Chem. Belg., XLIV, 1935, p. 640.
64. Sieg, L., Crutzen, J. L. and Jost, W. Zeit. Elektro-Chem., LV, 1951, p. 199.
65. Timmermans, J. Arch. Nierland Sci., VI, 1922, p. 147.
66. Timmermans, J. and Kohnstamm, P. Verslag Akad. Weten., XXI, 1912, p. 783.
67. Zawidzky, J. V. Zeit. Physik. Chem., XXXV, 1900, p. 154.

APPENDIX I

ERROR ANALYSIS

Using the technique outlined by Mickley, Sherwood and Reed (26), for calculating the error in the function;

$$Q = f(q_1, q_2, \dots, q_n) \quad (64)$$

$$\Delta Q = \left(\frac{\partial f}{\partial q_1}\right)_{q_2 \dots q_n} \Delta q_1 + \left(\frac{\partial f}{\partial q_2}\right)_{q_1, q_3 \dots q_n} \Delta q_2 + \dots + \left(\frac{\partial f}{\partial q_n}\right)_{q_1 \dots q_{n-1}} \Delta q_n \quad (65)$$

where: ΔQ = Error in Q.

Δq_i = Error in variable q_i .

the error in each of the reported quantities can be estimated.

PVT Measurements

I. Bellows Linearity

The ratio of change in volume to change in length of the syphon bellows was obtained by measuring the change in height of the liquid in a capillary as the bellows was compressed with a micrometer. The ratio can be expressed in terms of the measured variables:

$$\left(\frac{dV}{dL}\right)_B = \left(\frac{dV}{dL}\right)_C \frac{dL_c}{dL_m} \quad (66)$$

where: $\left(\frac{dV}{dL}\right)_B$ = ratio of volume change to length change of bellows, cc/in.

$\left(\frac{dV}{dL}\right)_C$ = ratio of change in volume to change in height of liquid in capillary, cc/in.

$\frac{dL_c}{dL_m}$ = ratio of change in height of liquid in capillary to change in length of micrometer, in/in.

The maximum possible error in these measurements is written:

$$\delta \left(\frac{dV}{dL} \right)_B = \left(\frac{dV}{dL} \right)_c \delta \left(\frac{dL_c}{dL_M} \right) + \frac{dL_c}{dL_M} \delta \left(\frac{dV}{dL} \right)_c \quad (67)$$

where the terms can be broken down to:

$$\delta \left(\frac{dL_c}{dL_M} \right) = \frac{1}{dL_M} \delta (dL)_c + \frac{dL_c}{(dL)_M^2} \delta (dL)_M \quad (68)$$

$$\text{and, } \delta \left(\frac{dV}{dL} \right)_c = \frac{1}{dL_c} \delta (dV)_c + \frac{dV_c}{(dL)_c^2} \delta (dL)_c \quad (69)$$

For a compression of the bellows of 0.10 in, or about 10% of its maximum:

$$dL_M = 0.10 \text{ in}; \quad dL_c = 15 \text{ in}; \quad dV_c = 0.4 \text{ cc}$$

$$\delta \left(\frac{dL_c}{dL_M} \right) = 1 \times 10^{-1} + (15/1 \times 10^{-2})(1 \times 10^{-4}) = 0.25 \text{ in/in}$$

$$\delta \left(\frac{dV}{dL} \right)_c = \frac{1}{15} \times 0.001 + \frac{0.4}{225} \times 0.01 \cong 8 \times 10^{-5} \text{ cc/in}$$

$$\left(\frac{dV}{dL} \right)_c = 2.76 \times 10^{-2} \text{ cc/in}$$

$$\frac{dL_c}{dL_M} = 150 \text{ in/in}$$

$$\text{So; } \delta \left(\frac{dV}{dL} \right)_B \cong 0.02 \text{ cc/in} \cong 0.5\%$$

II. Mole Fraction, (X):

The mole fraction of samples prepared by the method of Powers

(30) was calculated as:

$$X_{ACE} = \frac{W_{ACE}/(MW)_{ACE}}{\left[W_{CS_2}/(MW)_{CS_2} \right] + \left[W_{ACE}/(MW)_{ACE} \right]} \quad (70)$$

$$\delta X_{ACE} = \frac{W_{ACE}/(MW)_{ACE}}{\left\{ \left[W_{CS_2}/(MW)_{CS_2} \right] + \left[W_{ACE}/(MW)_{ACE} \right] \right\}^2} \delta \left[\frac{W_{CS_2}}{(MW)_{CS_2}} \right] \quad (71)$$

$$+ \frac{W_{CS_2}/(MW)_{CS_2}}{\left\{ \left[W_{CS_2}/(MW)_{CS_2} \right] + \left[W_{ACE}/(MW)_{ACE} \right] \right\}^2} \delta \left[\frac{W_{ACE}}{(MW)_{ACE}} \right]$$

where: W_{ace} = weight of sample of acetone.

W_{CS_2} = weight of sample of CS_2 .

Since two weighings on an analytical balance of 0.1 mg precision were necessary and the weight of an average sample was 4g.;

$$\Delta X_{ACE} = \frac{4/76}{(4/76 + 4/58)^2} \times \frac{0.0002}{58} + \frac{4/58}{(4/76 + 4/58)^2} \times \frac{0.0002}{76} = 2.4 \times 10^{-5}$$

III. Average Molecular Weight, (\overline{MW}).

The average molecular weight of any sample was calculated as:

$$\overline{MW} = X_{ACE} (MW)_{ACE} + (1 - X_{ACE}) (MW)_{CS_2} \quad (72)$$

So, the maximum error is predicted by:

$$\Delta (\overline{MW}) = (MW)_{ACE} \Delta X_{ACE} + (MW)_{CS_2} \Delta (1 - X_{ACE}) = 3.2 \times 10^{-3} \text{ g./mole}$$

IV. Density Determinations, (ρ^0)

$$\rho^0 = \frac{\text{Weight of Sample } (W_s)}{\text{Volume of Pycnometer } (V_p)} \quad \text{g./cc} \quad (73)$$

So that;

$$\Delta \rho^0 = \left(\frac{\partial \rho^0}{\partial W_s} \right) \Delta W_s + \left(\frac{\partial \rho^0}{\partial V_p} \right) \Delta V_p \quad (74)$$

a) The samples in the pycnometer agreed in weight within 0.001g:

$$\Delta W_s = 0.001 \text{ g.} \quad (75)$$

b) The volume of the pycnometer was determined by the weight of distilled water it held:

$$V_p = \frac{W_{H_2O}}{\rho_{H_2O}^0} \quad \text{cc} \quad (76)$$

$$\Delta V_p = \left(\frac{\partial V_p}{\partial W_{H_2O}} \right) \Delta W_{H_2O} + \left(\frac{\partial V_p}{\partial \rho_{H_2O}^0} \right) \Delta \rho_{H_2O}^0 \quad (77)$$

The calibration samples agreed in weight to 0.0005g. and the density of water is assumed known as 0.99987 g/cc (46):

$$\Delta V_p = 5 \times 10^{-4} \text{ cc} \quad (78)$$

Equation (74) becomes:

$$\begin{aligned}\delta\rho^{\circ} &= \frac{1}{V_p} \times 0.001 + \frac{W_s}{V_p^2} \times 5 \times 10^{-4} \\ &= 1 \times 10^{-4} + 5 \times 10^{-5} = 1.5 \times 10^{-4} \text{ g./cc}\end{aligned}$$

V. Error in Density of Bellows Samples

The density of each sample used in the PVT measurements was determined from the curve obtained from the density experiment and the calculated mole fraction of the bellows sample. The effect of the latter is shown as:

$$\left(\frac{\partial\rho^{\circ}}{\partial X}\right) = 0.5 \text{ g./cc} \quad (79)$$

And since the mole fraction can be determined to $\pm 2.4 \times 10^{-5}$:

$$\delta\rho^{\circ} = \left(\frac{\partial\rho^{\circ}}{\partial X}\right) \delta X = 0.5 \times 2.4 \times 10^{-5} = 1.2 \times 10^{-5} \quad (80)$$

or only about 10% of the error in the density determinations.

VI. Initial Volume of Bellows, (V°):

$$V^{\circ} = W_s / \rho^{\circ} \quad (81)$$

$$\delta V^{\circ} = \frac{1}{\rho^{\circ}} \delta W_s + \frac{W_s}{(\rho^{\circ})^2} \delta \rho^{\circ} \quad (82)$$

The weight of the sample in the bellows requires two weighings, so that;

$$\delta V^{\circ} = 1 \times 2 \times 10^{-4} + 3 \times 7.5 \times 10^{-5} = 4.25 \times 10^{-4} \text{ cc}$$

where the density is assumed known to half the error of each experimental sample due to smoothing.

VII. Molal Volume at 1 atmosphere, (V_m°):

$$\underline{V_m^{\circ}} = \overline{MW} / \rho^{\circ} \quad (83)$$

$$\int V_m^0 = \frac{1}{\rho^0} \int (MW) + \frac{MW}{(\rho^0)^2} \int \rho^0 = 8 \times 10^{-3} \text{ cc/mole} \quad (84)$$

VIII. Volume of Bellows at Pressure, P (V):

$$\int V = \left(\frac{\partial V}{\partial L} \right) \int L \quad \text{cc} \quad (85)$$

a) Resistance of Karma wire section (R_s)

$$R_s = \frac{R_1 (R_w + R_3)}{R_1 + R_2 + R_3 + (R_w + R_w')} \quad \text{ohms} \quad (86)$$

$$\int R_s = \frac{R_1 \int R_w}{R_1 + R_2 + R_3 + (R_w + R_w')} \quad (87)$$

where $\int R_w = 0.0017 \text{ ohms}$

$$\int R_s = 5 \times 10^{-5} \text{ ohms}$$

b) Length of Bellows (ΔL):

$$\int \Delta L = \frac{\int \Delta R_s}{r} = 7.5 \times 10^{-5} \text{ in}$$

where $r =$ resistivity of Karma (approx. $8 \Omega/\text{ft.}$)

So that;

$$\int V = 4 \text{ cc/in}^* \times 7.5 \times 10^{-5} \text{ in} = 3 \times 10^{-4} \text{ cc}$$

Incorporating the effect of pressure;

$$\frac{\partial \Delta R_s}{\partial P} \cong 2 \times 10^{-6} \text{ ohms/psi}$$

using an average compressibility in the low pressure range where the error is greatest.

In this range, the Heise gauge is used to measure pressure to

± 50 psi, so:

$$\int R_s = \left(\frac{\partial R_s}{\partial P} \right) \int P = 2 \times 10^{-6} \times 50 = 1 \times 10^{-4} \text{ ohm} \quad (88)$$

*As determined in calibration of bellows with micrometer and capillary tube (See Chapter V).

This corresponds to an error in length of 1.5×10^{-4} in. and volume of 6×10^{-4} cc. The total maximum error in the volume of the bellows at any pressure is then:

$$\delta V = 3 \times 10^{-4} + 6 \times 10^{-4} = 9 \times 10^{-4} \text{ cc}$$

IX. Fractional Change in Volume at Pressure P, (V/V^0) :

$$\begin{aligned} \delta(\Delta_P V/V^0) &= \frac{1}{V^0} \delta(\Delta_P V) + \Delta_P V \left[\frac{1}{(V^0)^2} \right] \delta V^0 \\ &= \frac{1}{3} \times 0.0009 + 1 \times \frac{1}{9} \times 4.25 \times 10^{-4} \\ &= 3.5 \times 10^{-4} \text{ cc/cc} \end{aligned} \quad (89)$$

Using the large value of lcc for $\Delta_P V$.

X. Change in Volume on Mixing, (ΔV^m) :

$$\begin{aligned} \Delta V^m &= \underline{V}_M (V/V^0) - X_{ACE} \underline{V}_{ACE} (V/V^0)_{ACE} - (1 - X_{ACE}) \underline{V}_{CS_2} (V/V^0)_{CS_2} \quad (90) \\ \delta \Delta V^m &= (V/V^0) \delta \underline{V}_M + \underline{V}_M \delta (V/V^0) + X_{ACE} \underline{V}_{ACE} \delta (V/V^0)_{ACE} \\ &\quad + \underline{V}_{ACE} (V/V^0)_{ACE} \delta X_{ACE} + X_{ACE} (V/V^0)_{ACE} \delta \underline{V}_{ACE} + (1 - X_{ACE}) \underline{V}_{CS_2} \delta (V/V^0)_{CS_2} \\ &\quad + (1 - X_{ACE}) (V/V^0)_{CS_2} \delta \underline{V}_{CS_2} + \underline{V}_{CS_2} (V/V^0)_{CS_2} \delta (1 - X_{ACE}) \quad (91) \\ &= 0.082 \text{ cc/mole} \end{aligned}$$

which is about the same as the maximum deviation of the points shown on Figures 18 and 19 from the smooth curves. These points were calculated directly from the unsmoothed (V/V^0) vs P data.

Temperature variation during any trial was not considered because no appreciable hysteresis was noted. That is, points taken during increasing pressure lay on the same line as points taken during decreasing pressure. If the temperature did change during any run enough to cause a measureable error, this reproducibility would, in all probability, have not occurred.

Visual Observation

The observed phase separation data are affected only by errors in temperature, pressure and composition. Since the temperature was measured directly, it was probably not in error by more than 0.5°F. This would cause an error in the pressure of separation of about 600 psi. The pressure was measured to within 100 psi, so the total effect of temperature and pressure variation was no greater than 700 psi.

The effect of composition is more difficult to ascertain. The presence of water would certainly cause a decrease in the pressure of separation, while presence of a hydrocarbon soluble in both CS₂ and acetone would cause an increase in the pressure (20). Because the amount of impurities would not have been the same in any sample, some idea of the error can be obtained from the manner in which the data fit a smooth curve, pressure and temperature variation considered non-existent. Since the data do seem to fit within 1000 psi, the effect of composition is probably about the same as the effect of the other two variables.

APPENDIX II

CONSISTENCY OF ACTIVITY DATA

The data reported by Zawidzky (48) for the system acetone-carbon disulfide at 35.17°C and one atmosphere is shown in Table 13 as columns 1-3. The activities were calculated from the data as:

$$\bar{a}_i = P_i / P_i^0 \quad (92)$$

where: P_i = partial pressure of component i (calculated assuming ideal behavior in the vapor phase).

P_i^0 = vapor pressure of pure component i at the temperature of the system.

The thermodynamic consistency of this data were checked using the method illustrated by Rowlinson (35), whereby the logarithm of the ratio of the activity coefficients is plotted against mole fraction. The difference between the positive and negative areas give at least a qualitative indication of the consistency of the data.* As shown in Figure 27, the areas are as identical as can be determined graphically on 8½x11 paper. Enlargement of the graph would be of little value as the test itself is not perfectly rigorous (35).

*Consistent data yield equal areas.

TABLE 13

ACTIVITY DATA AT 1 ATMOSPHERE
 CS₂ -- ACETONE
 35.17°C
 Zawidzky Z.P.C. 35, 129, (1900)

X_1^*	P_{ace}	P_{cs_2}	$\ln \bar{a}_2$	$\ln \bar{a}_1$	$X_1 \ln \bar{a}_1 + X_2 \ln \bar{a}_2$
1.0000	343.8	0			
0.9376	331.0	110.7	-1.533	-0.0375	-0.1308
0.9330	327.8	119.7	-1.455	-0.0472	-0.1415
0.9289	328.7	123.1	-1.427	-0.0445	-0.1428
0.8788	313.5	191.7	-0.9840	-0.0918	-0.1999
0.8670	308.3	206.5	-0.9096	-0.1085	-0.2150
0.8143	295.4	258.4	-0.6854	-0.1513	-0.2505
0.8009	290.6	271.9	-0.6345	-0.1677	-0.2606
0.7915	283.4	283.9	-0.5902	-0.1932	-0.2760
0.7239	275.2	323.3	-0.4614	-0.2222	-0.2882
0.7131	274.2	328.7	-0.4447	-0.2258	-0.2886
0.6498	263.9	358.3	-0.3585	-0.2640	-0.2971
0.6449	262.1	361.3	-0.3503	-0.2709	-0.2991
0.5942	254.5	379.6	-0.3008	-0.3003	-0.3005
0.5859	253.0	382.1	-0.2942	-0.3062	-0.3012
0.5526	250.2	390.4	-0.2727	-0.3173	-0.2973
0.5470	247.6	394.2	-0.2630	-0.3278	-0.2984
0.5067	242.8	403.2	-0.2406	-0.3473	-0.2947
0.5026	242.1	404.1	-0.2383	-0.3503	-0.2946
0.4298	232.6	419.4	-0.2011	-0.3902	-0.2824
0.4270	232.2	420.3	-0.1989	-0.3920	-0.2814
0.3876	227.0	426.9	-0.1833	-0.4146	-0.2730
0.3854	225.9	427.7	-0.1815	-0.4195	-0.2732
0.3839	225.5	428.1	-0.1806	-0.4213	-0.2730
0.3287	217.0	438.0	-0.1577	-0.4597	-0.2570
0.3287	217.6	437.3	-0.1593	-0.4570	-0.2572
0.2780	207.7	446.9	-0.1375	-0.5035	-0.2392
0.2803	207.1	447.5	-0.1363	-0.5063	-0.2400
0.1720	180.2	464.9	-0.0980	-0.6455	-0.1922
0.0809	123.4	490.7	-0.0440	-1.024	-0.1233
0.0758	120.3	490.0	-0.0455	-1.050	-0.1216
0.0650	109.4	491.9	-0.0416	-1.144	-0.1133
0.0593	103.5	492.0	-0.0414	-1.200	-0.1101
0.0451	85.9	496.2	-0.0329	-1.386	-0.0939
0.0380	73.4	500.8	-0.0237	-1.544	-0.0815
0.0308	62.0	502.0	-0.0213	-1.713	-0.0734
0.0000	0.0	512.3			

*Component 1 refers to acetone.

TABLE 14
CONSISTENCY OF ACTIVITY DATA

$X_{CS_2}(2)$	$X_{ace}(1)$	$\ln X_{CS_2}$	$\ln X_{ace}$	$(\ln \bar{\gamma}_2 X_2 - \ln \bar{\gamma}_1 X_1)$	$\ln \bar{\gamma}_2 / \bar{\gamma}_1$
.0670	.9330	-2.703	- .069	-1.4080	1.226
.1212	.8788	-2.112	- .129	- .8922	1.091
.1857	.8143	-1.685	- .205	- .5341	.946
.2761	.7239	-1.287	- .323	- .2392	.725
.3502	.6498	-1.050	- .431	- .0945	.5245
.4058	.5942	- .902	- .520	- .0005	.3815
.4530	.5470	- .792	- .603	.0648	.254
.4974	.5026	- .698	- .688	.1120	.122
.5730	.4270	- .557	- .851	.1931	- .101
.6161	.3839	- .484	- .957	.2407	- .232
.6713	.3287	- .399	-1.112	.2977	- .415
.7197	.2803	- .329	-1.272	.3700	- .573
.8280	.1720	- .189	-1.760	.5475	-1.0235
.9242	.0758	- .079	-2.580	1.0045	-1.4965
.9470	.0593	- .061	-2.827	1.1586	-1.607
.9620	.0380	- .039	-3.270	1.5203	-1.711
.9692	.0308	- .031	-3.480	1.6917	-1.757

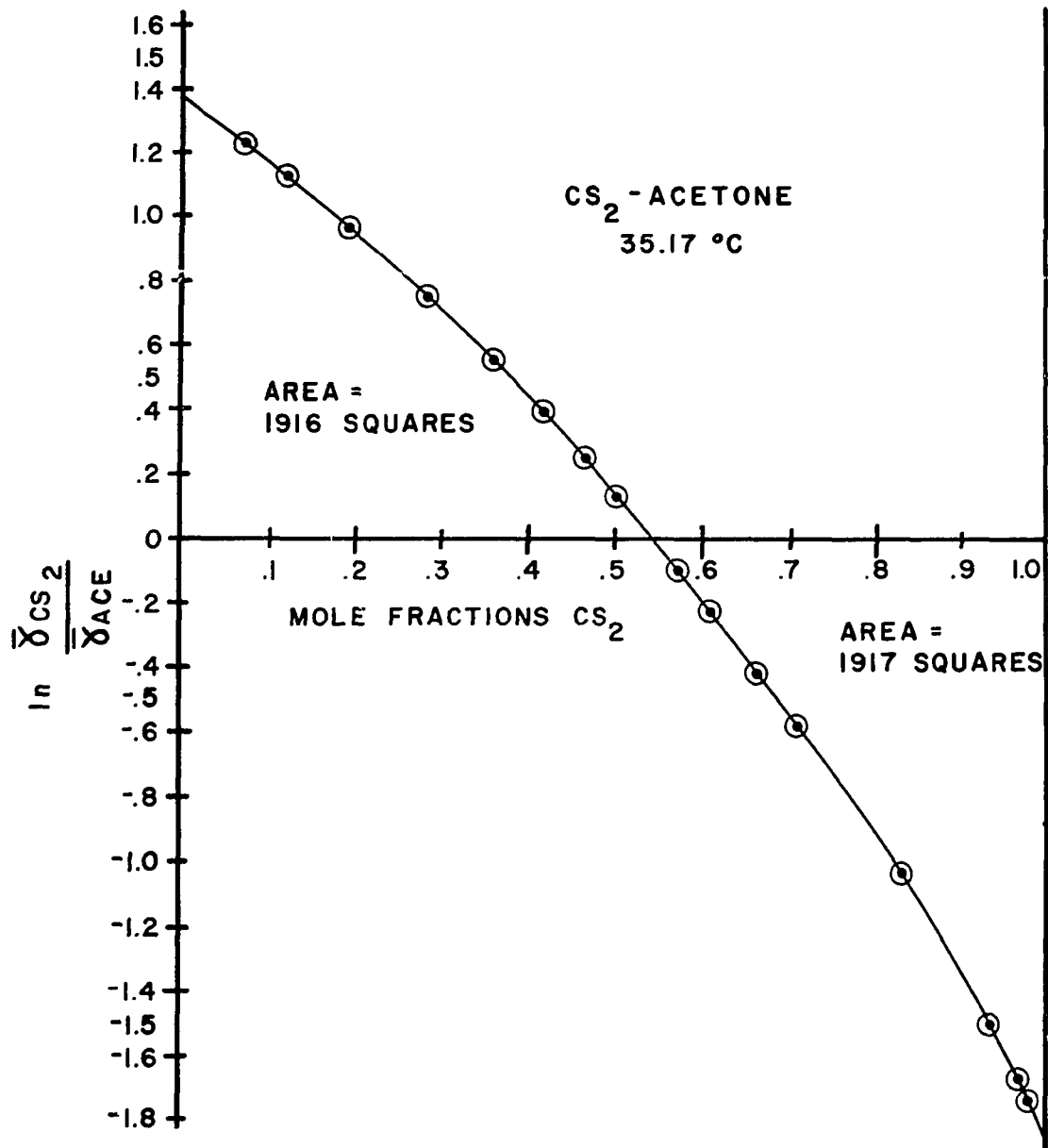


Figure 27.--Consistency of Activity Data

APPENDIX III

CONVERSION OF FREE ENERGY DIAGRAM

As mentioned previously, 0°C was chosen as the temperature at which to predict the liquid-liquid phase behavior of the system acetone-carbon disulfide in order to lower the pressure required for separation to within the limits of the visual observation equipment. To make such a prediction, as is explained in Chapter II, the change in free energy on mixing of the system need be accurately known at this same temperature and some low pressure. Unfortunately there exist no such data. Therefore, the accurate* data at 35.17°C (48), (Table 13), were converted by use of the enthalpy of mixing data of Schmidt (36) at 16°C, the specific heat data of Staveley (41) at 20°, 30° and 40°C., and the relation:

$$\left[\frac{\Delta G^m}{RT} \right]_{0^\circ\text{C.}} - \left[\frac{\Delta G^m}{RT} \right]_{35.17^\circ\text{C.}} = \int_{308.17^\circ\text{K.}}^{273^\circ\text{K.}} \left[\frac{(\Delta H^m)_{16^\circ\text{C.}} + (\Delta \bar{C}_P^m)(T-289)}{RT^2} \right] dT \quad (38)$$

The values of $(\Delta H^m)_{16^\circ\text{C}}$ used were obtained by fitting Schmidt's data by a least squares method. The resultant curve, along with the experimental points is shown as Figure 28. A fifth degree polynomial seemed to afford the best curve. It is of interest to note that the same degree equation was necessary to adequately fit the change in

*See Appendix II.

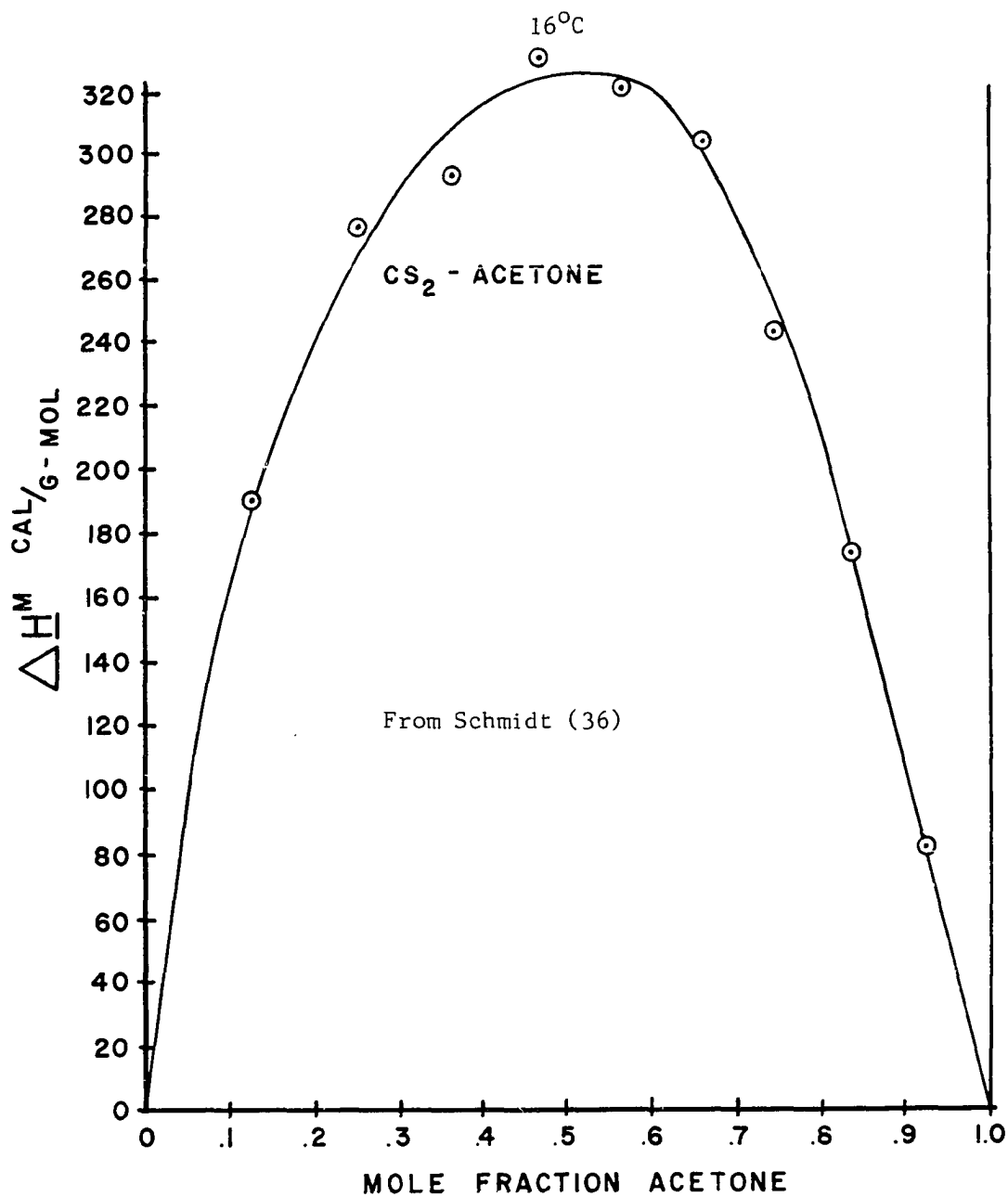


Figure 28.--Heat of Mixing

volume on mixing data at one atmosphere.

The values used for $\Delta \bar{C}_p^m$ were the arithmetic average from 40°C to 0°C (See Figures 31, 32, and 33). The difference in the change of free energy calculated in this manner and that calculated using an expression for $\Delta \bar{C}_p^m$ of the form:

$$\Delta \bar{C}_p^m = a + bT \quad (93)$$

is found to be less than 0.1%* in the worst cases.

Equation (38) was integrated at each 0.1 increment in mole fraction and a smooth curve drawn (Figure 34). This curve was then added to the free energy of mixing curve at 35.17°C. The results are tabulated in Table 15. Column 2 shows the data for the free energy diagram at 35.17°C, column 3 the results of the integration of Equation (38) from 35.17°C to 0°C., and column 4 the data for the diagram at 0°C.

*The exact error in the calculation is:

$$\int_{T_1}^{T_2} \left\{ \frac{(\Delta H^m)_{T_3} + \left[\frac{(\Delta C_p^m)_{T_2} + (\Delta C_p^m)_{T_1}}{2} \right] (T - 289)}{RT^2} \right\} dT - \int_{T_1}^{T_2} \left[\frac{(\Delta H^m)_{T_3} + \int_{T_3}^T (a + bT) dT}{RT^2} \right] dT$$

$$= \frac{b}{2R} \left[(T_2 + T_1) \ln \frac{T_2}{T_1} + T_3 \left(\frac{T_1}{T_2} - \frac{T_2}{T_1} - \frac{T_3}{T_2} + \frac{T_3}{T_1} \right) + T_1 - T_2 \right] \quad (94)$$

At X=0.5, this amounts to -0.00005 or about 0.1% (See Table 15).

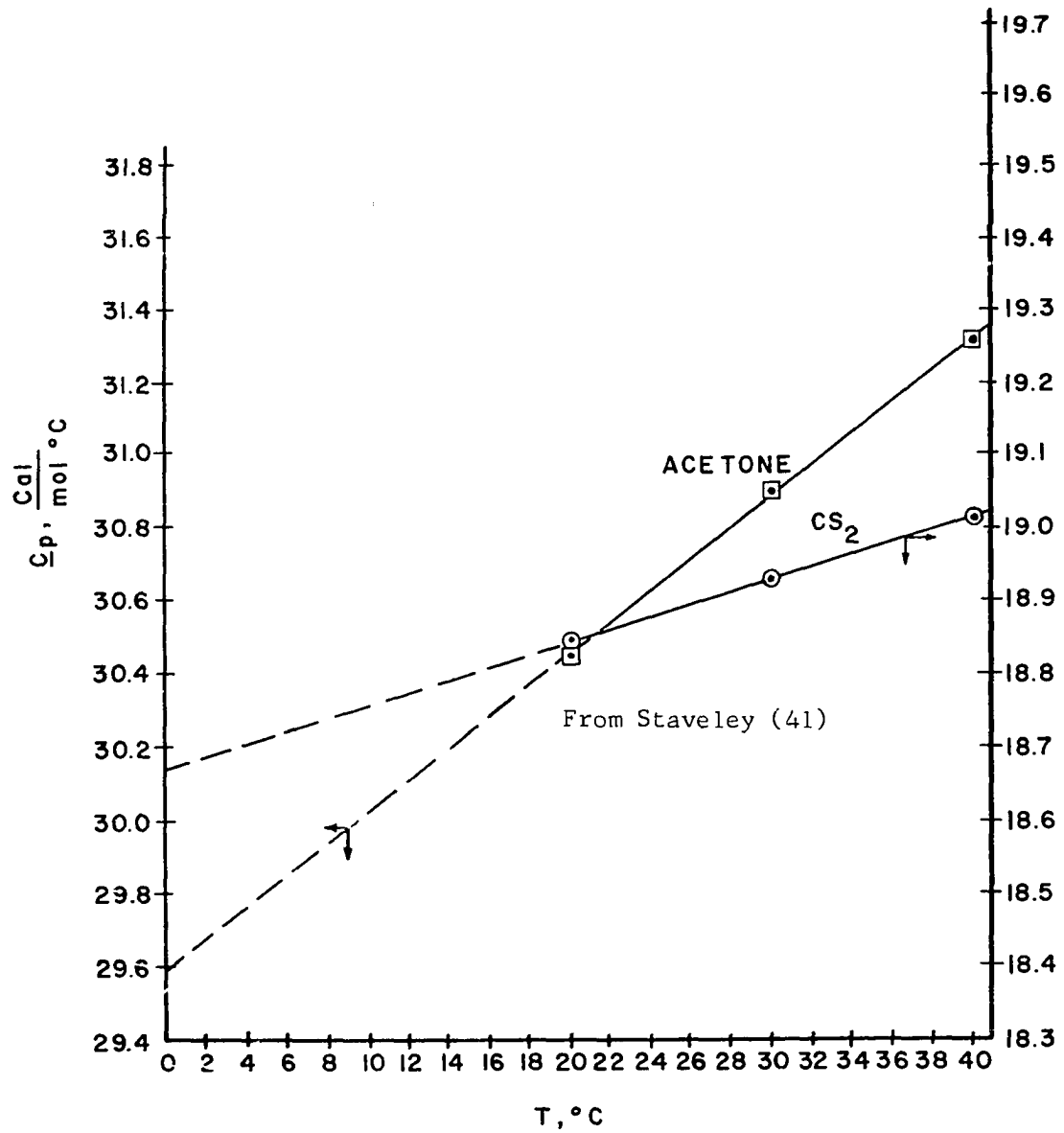


Figure 29.---Specific Heats as Functions of Temperature

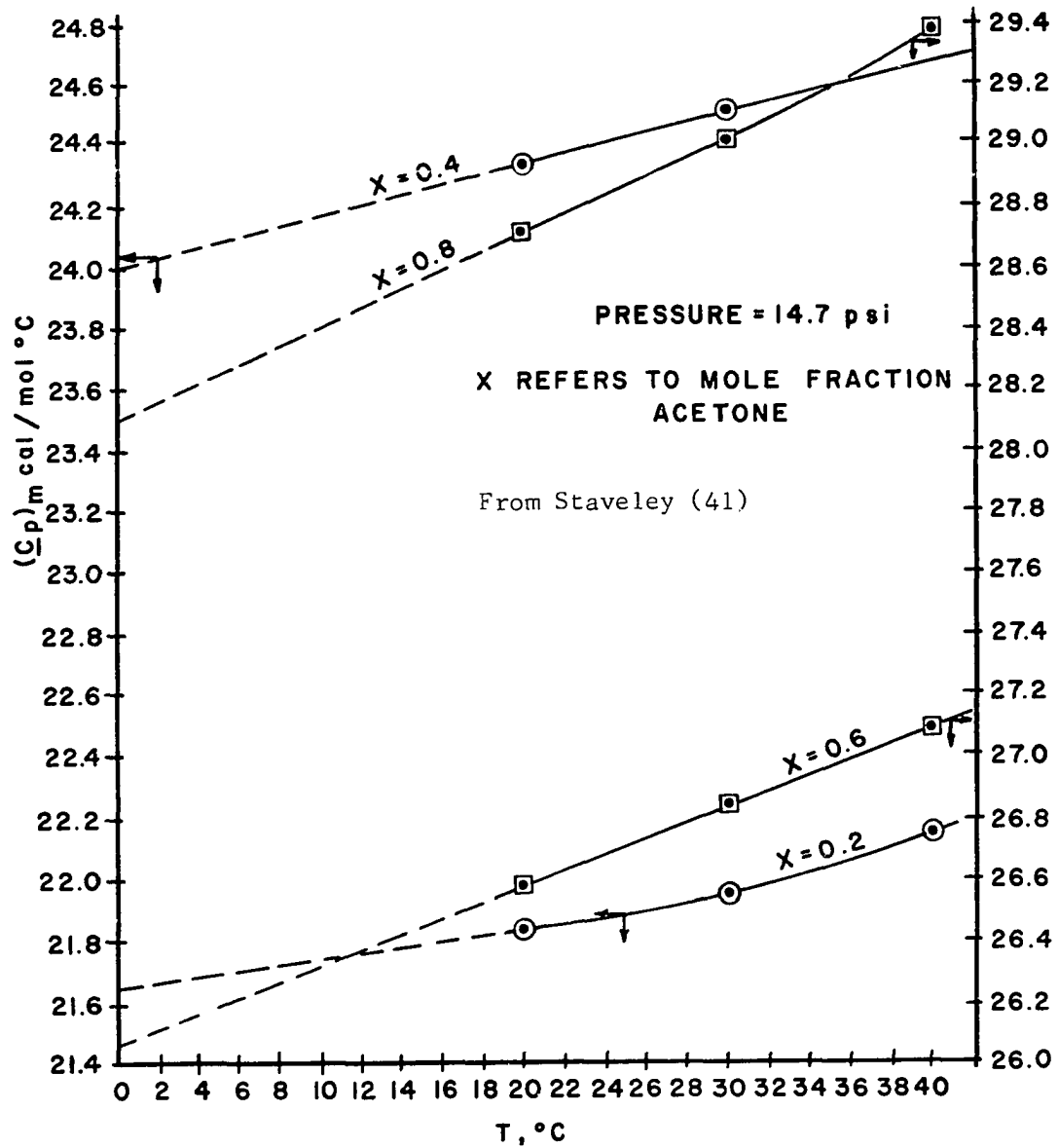


Figure 30.--Specific Heats as Functions of Temperature

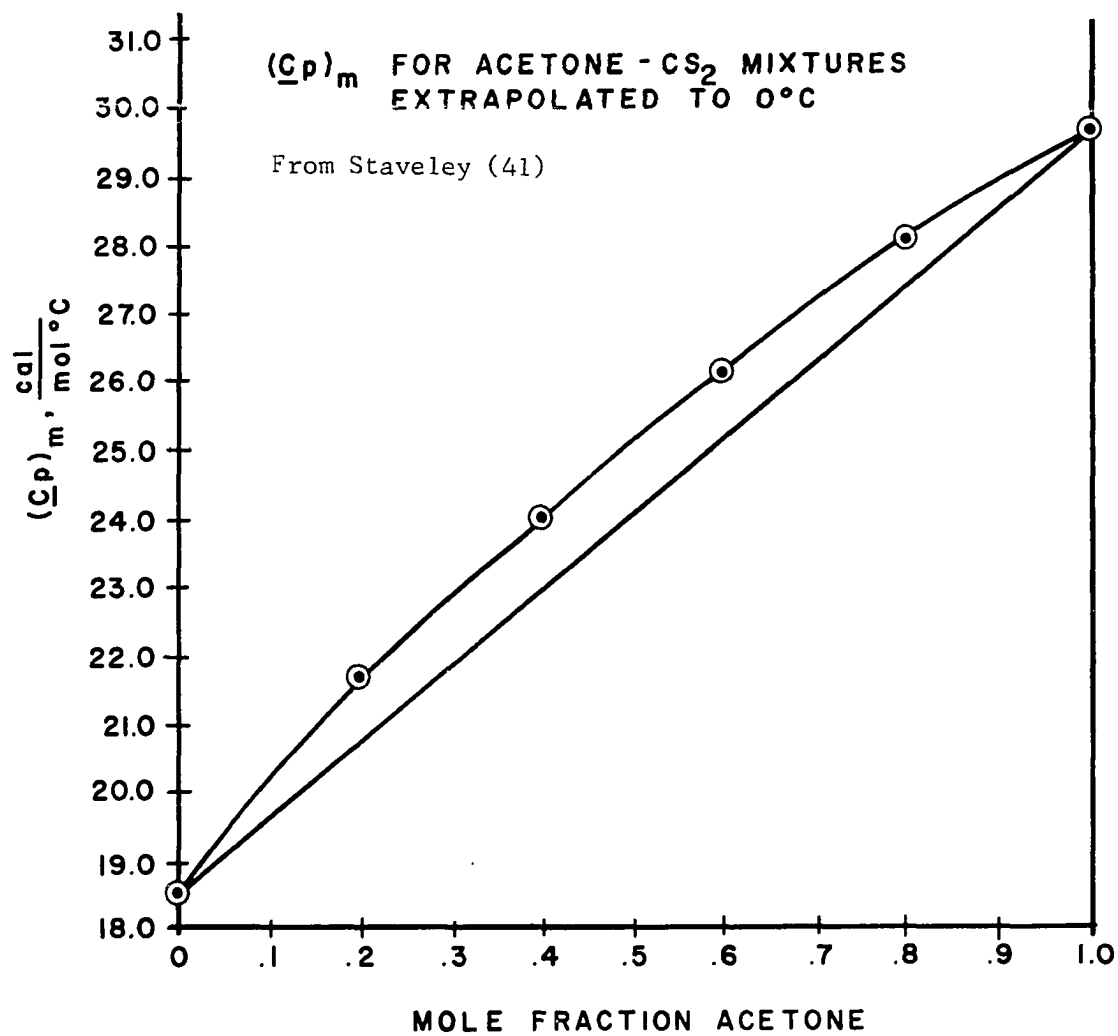


Figure 31.--Specific Heats as Functions of X

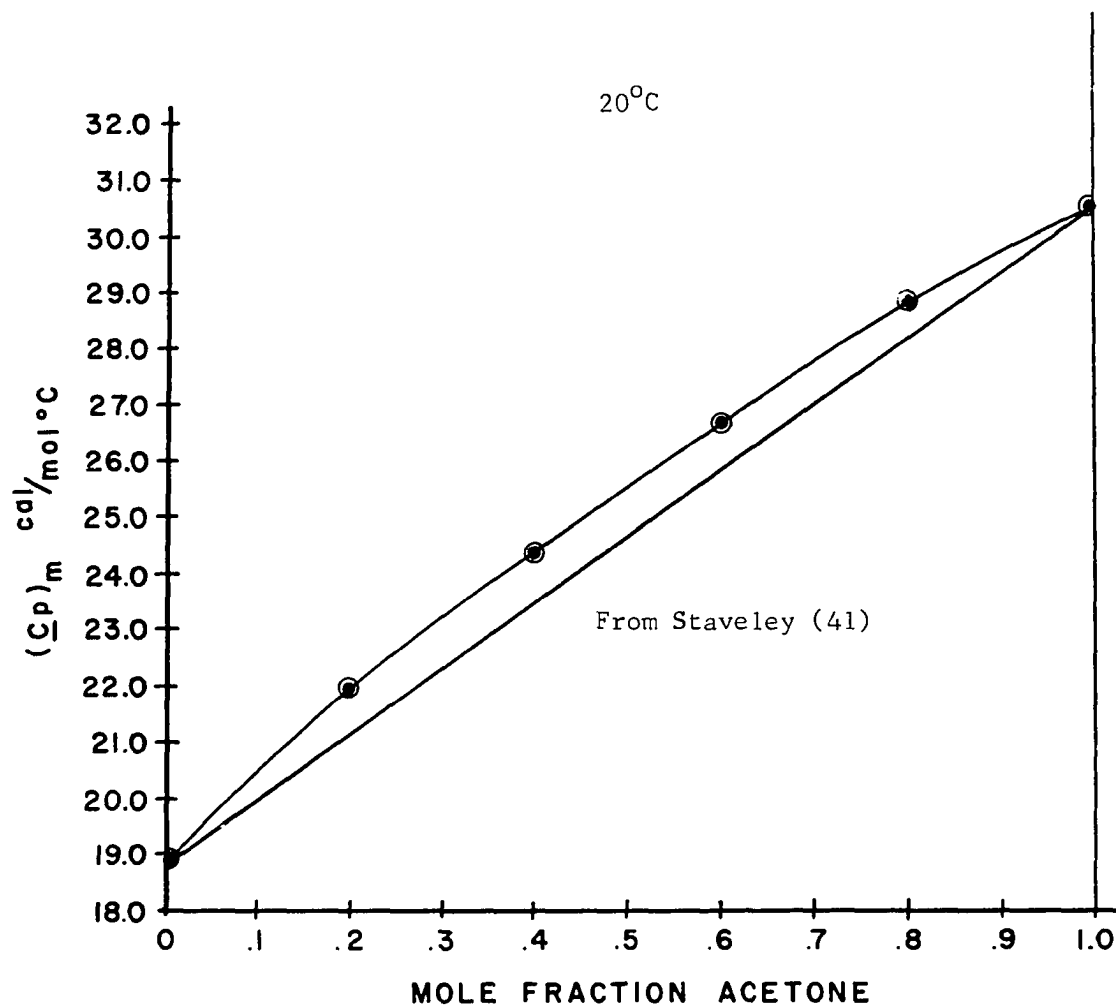


Figure 32.--Specific Heats as Functions of X

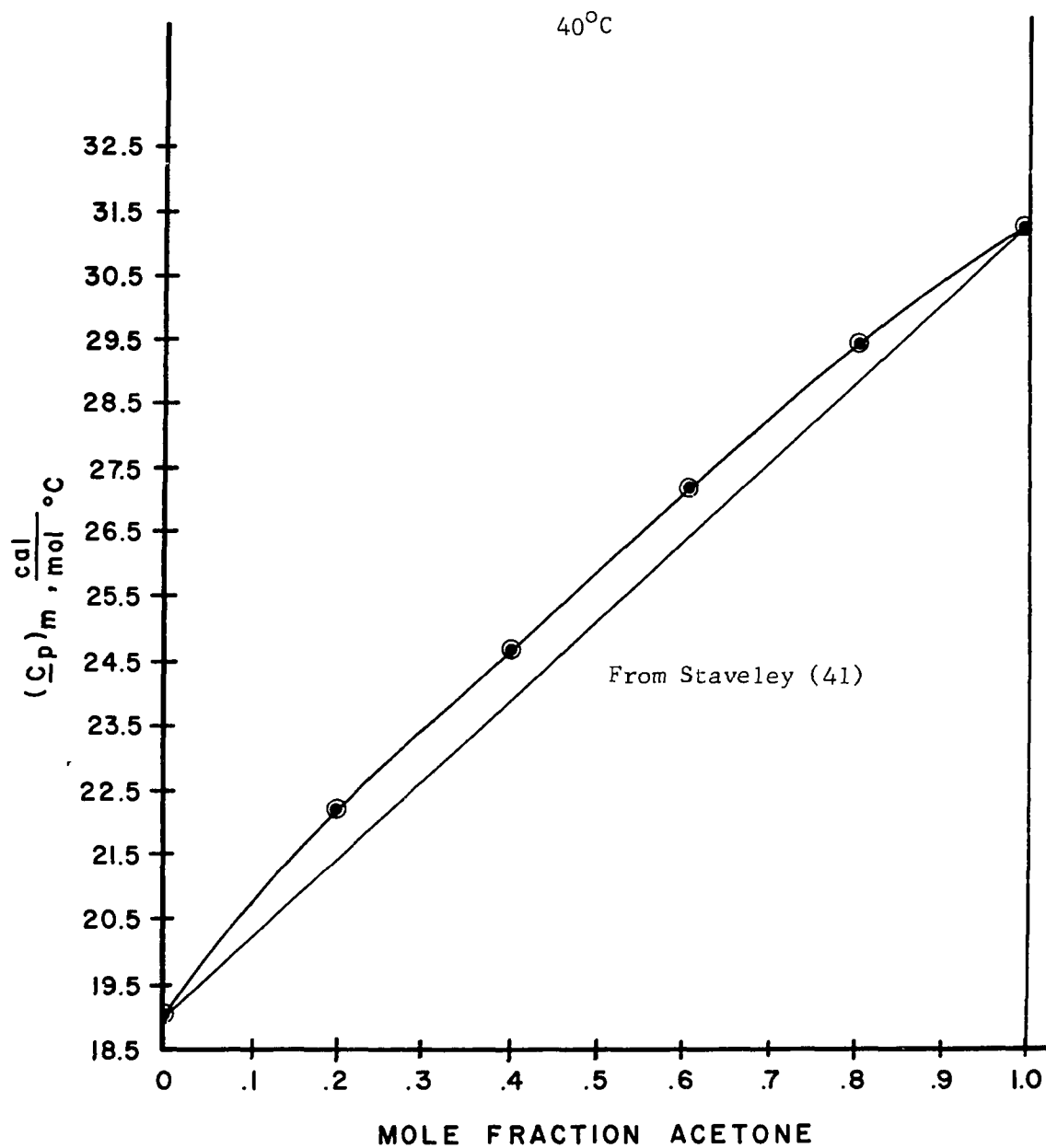


Figure 33.--Specific Heats as Functions of X

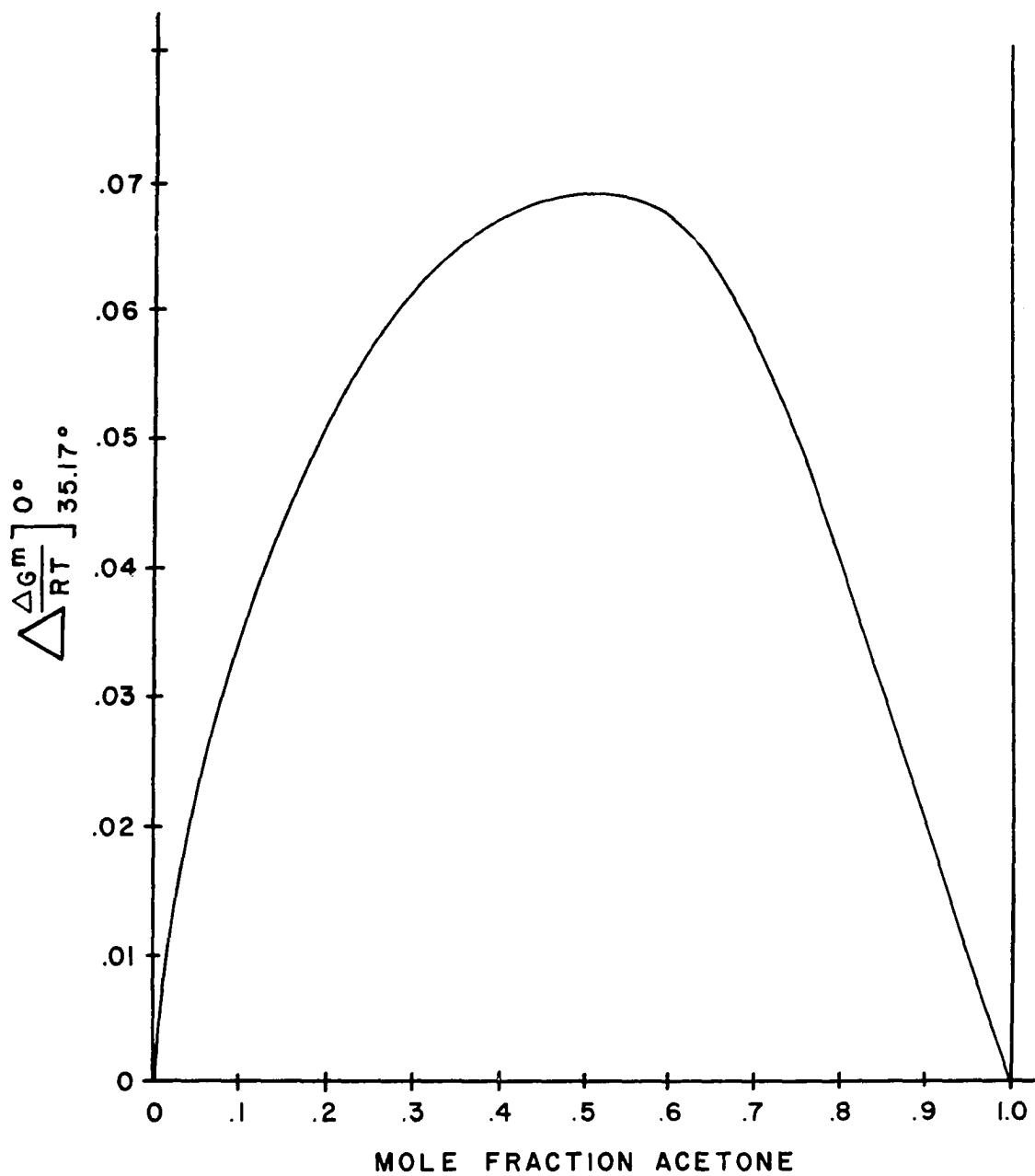


Figure 34:--Change in Free Energy from 35.17 to 0°C

TABLE 15

CONVERSION OF FREE ENERGY DIAGRAM TO 0°C

x_{ace}	$-\left(\frac{\Delta G^m}{RT}\right)_{35.17^\circ\text{C.}}$	$\Delta\left(\frac{\Delta G^m}{RT}\right)_{35.17^\circ\text{C.}}^{0^\circ}$	$-\left(\frac{\Delta G^m}{RT}\right)_{0^\circ\text{C.}}$
.10	0.1420	0.0350	0.1070
.12	0.1569	0.0393	0.1176
.14	0.1703	0.0431	0.1272
.16	0.1828	0.0464	0.1364
.18	0.1946	0.0493	0.1453
.20	0.2050	0.0516	0.1534
.22	0.2147	0.0538	0.1609
.24	0.2237	0.0556	0.1681
.26	0.2323	0.0575	0.1748
.28	0.2405	0.0592	0.1813
.30	0.2479	0.0607	0.1872
.32	0.2546	0.0621	0.1925
.34	0.2609	0.0634	0.1975
.36	0.2666	0.0646	0.2020
.38	0.2719	0.0656	0.2063
.40	0.2767	0.0666	0.2101
.42	0.2813	0.0675	0.2138
.44	0.2853	0.0683	0.2170
.46	0.2887	0.0689	0.2198
.48	0.2918	0.0694	0.2224
.50	0.2943	0.0696	0.2247
.52	0.2964	0.0696	0.2268
.54	0.2982	0.0694	0.2288
.56	0.2996	0.0692	0.2304
.58	0.3008	0.0690	0.2318
.60	0.3012	0.0683	0.2329
.62	0.3008	0.0672	0.2336
.64	0.2994	0.0657	0.2337
.66	0.2978	0.0641	0.2337
.68	0.2955	0.0622	0.2333
.70	0.2924	0.0602	0.2322
.72	0.2882	0.0574	0.2308
.74	0.2831	0.0546	0.2285
.76	0.2764	0.0514	0.2250
.78	0.2687	0.0478	0.2209
.80	0.2592	0.0441	0.2151
.90	0.1795	0.0220	0.1575

APPENDIX IV

COMPARISON OF COMPRESSIBILITY CURVE

Because the isothermal compressibility is defined as

$$\beta_T = -\frac{1}{V} \left(\frac{\partial V}{\partial P} \right)_T \quad (95)$$

it would be expected that a minimum in the (V/V^0) data would occur at approximately the same mole fraction as a maximum in the compressibility curve and vice versa. Such is found to be the case if the data is compared to the results of Sokollu (39). Although the quantity reported by Sokollu is the adiabatic compressibility:

$$\beta_s = -\frac{1}{V} \left(\frac{\partial V}{\partial P} \right)_s \quad (96)$$

the difference between the two (41);

$$\beta_T - \beta_s = \frac{T}{C_p V} \left(\frac{\partial V}{\partial T} \right) \quad (97)$$

is nearly constant for the system acetone-carbon disulfide (41). Therefore, a plot of the adiabatic compressibility versus mole fraction will have essentially the same shape as that of the isothermal compressibility.

At a composition of approximately 80 mole percent acetone, the (V/V^0) data (Figure 17) show a definite minimum. The compressibility data of Sokollu (Figure 35) at one atmosphere show a large maximum near

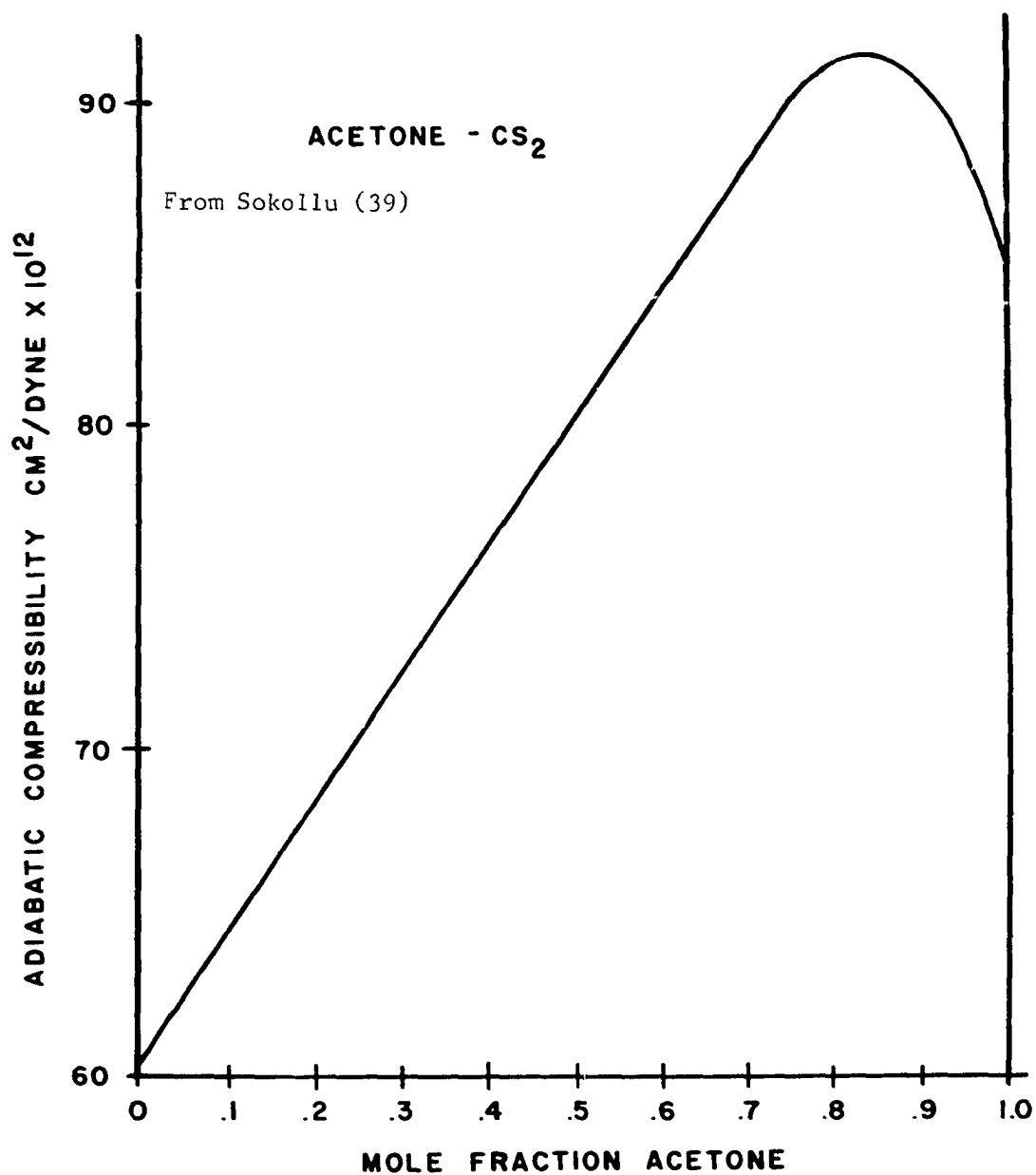


Figure 35.--Adiabatic Compressibility

this same concentration. The data of Staveley (41), on the other hand, do not show a maximum compressibility at any concentration. He does mention that some data in this region of concentration were thrown out. It is possible that these data would cause the maximum obtained by Sokollu. The absence of the minimum in the (V/V^0) curves at 20,000 psi (Table 8) undoubtedly results from the smoothing.

The curves above 70,000 psi are not as accurate as those below because the samples rich in acetone were not compressed to more than 85,000 psi. For this reason, the (V/V^0) vs. P curves for these samples are probably not well established at the high pressures and hence, the (V/V^0) vs X curves will be in error.

APPENDIX V

FREE ENERGY CURVES AND ACTIVITIES

The activities of the system acetone-carbon disulfide were calculated at five pressures, 14.7, 25,000, 50,000, 75,000 and 100,000 psi, by fitting the free energy curve at each pressure with a 10th order polynomial and making use of Equations (45), (51) and (54):

$$\frac{\Delta G^M}{RT} = \sum A_i X_2^{(i-1)} \quad (45)$$

$$\ln \bar{a}_1 = - \sum_{i=3}^M (i-2) A_i X_2^{(i-1)} \quad (51)$$

$$\ln \bar{a}_2 = \sum_{i=2}^M (i-1) A_i X_2^{(i-2)} - \sum_{i=3}^M (i-2) A_i X_2^{(i-1)} \quad (54)$$

The results are listed as Table 16.

TABLE 16

COEFFICIENTS OF FREE ENERGY POLYNOMIAL AND ACTIVITIES AT 0°C

I. P = 1 atmosphere

A ₁	=	0
A ₂	=	-2.10869
A ₃	=	18.8372
A ₄	=	-125.272
A ₅	=	530.306
A ₆	=	-1452.35
A ₇	=	2621.25
A ₈	=	-3100.89
A ₉	=	2314.19
A ₁₀	=	-988.125
A ₁₁	=	184.163

X_{ace}	$\ln \bar{a}_{cs2}$	$\ln \bar{a}_{ace}$
0.00	0.0000	-∞
.05	-.0241	-.9642
.10	-.0523	-.6172
.15	-.0639	-.5179
.20	-.7384	-.4705
.25	-.8665	-.4265
.30	-.1028	-.3840
.35	-.1199	-.3483
.40	-.1365	-.3206
.45	-.1524	-.2990
.50	-.1685	-.2812
.55	-.1860	-.2654
.60	-.2066	-.2499
.65	-.2345	-.2340
.70	-.2772	-.2132
.75	-.3488	-.1867
.80	-.4691	-.1522
.85	-.6658	-.1100
.90	-.9863	-.0661
.95	-1.5272	-.0228
1.00	-∞	0.0000

TABLE 16--Continued

 II. P = 25,000 psi

A ₁	=	0
A ₂	=	-1.91798
A ₃	=	19.8937
A ₄	=	-139.645
A ₅	=	619.321
A ₆	=	-1791.23
A ₇	=	3436.54
A ₈	=	-4338.30
A ₉	=	3461.11
A ₁₀	=	-1580.15
A ₁₁	=	314.384

<u>X_{ace}</u>	<u>ln \bar{a}_{cs2}</u>	<u>ln \bar{a}_{ace}</u>
0.00	0.0000	-∞
.05	-.0244	-.7407
.10	-.0486	-.4171
.15	-.0585	-.3440
.20	-.0637	-.3190
.25	-.0705	-.2957
.30	-.0793	-.2726
.35	-.0884	-.2535
.40	-.0973	-.2387
.45	-.1063	-.2266
.50	-.1157	-.2161
.55	-.1260	-.2070
.60	-.1381	-.1978
.65	-.1569	-.1875
.70	-.1889	-.1717
.75	-.2439	-.1516
.80	-.3295	-.1277
.85	-.4570	-.0988
.90	-.6801	-.0664
.95	-1.1906	-.0310
1.00	-∞	0.0000

TABLE 16--Continued

III. P = 50,000 psi

A ₁	=	0
A ₂	=	-1.71900
A ₃	=	18.2978
A ₄	=	-121.553
A ₅	=	501.472
A ₆	=	-1341.369
A ₇	=	2370.95
A ₈	=	-2750.82
A ₉	=	2015.57
A ₁₀	=	-846.212
A ₁₁	=	155.383

<u>x_{ace}</u>	<u>ln \bar{a}_{cs2}</u>	<u>ln \bar{a}_{ace}</u>
.00	0.0000	-∞
.05	-.0233	-.6112
.10	-.0470	-.2933
.15	-.0556	-.2289
.20	-.0574	-.2199
.25	-.0596	-.2124
.30	-.0638	-.2015
.35	-.0687	-.1913
.40	-.0733	-.1836
.45	-.0779	-.1773
.50	-.0836	-.1710
.55	-.0914	-.1641
.60	-.1019	-.1561
.65	-.1167	-.1478
.70	-.1396	-.1365
.75	-.1789	-.1219
.80	-.2487	-.1024
.85	-.3691	-.0758
.90	-.5804	-.0461
.95	-.9625	-.0156
1.00	-∞	0.0000

TABLE 16--Continued

IV. P = 75,000 psi

A ₁	=	0
A ₂	=	-1.53600
A ₃	=	15.9011
A ₄	=	-93.5653
A ₅	=	320.689
A ₆	=	-650.349
A ₇	=	725.121
A ₈	=	-282.613
A ₉	=	-246.969
A ₁₀	=	309.867
A ₁₁	=	-96.5463

<u>X_{ace}</u>	<u>ln \bar{a}_{cs2}</u>	<u>ln \bar{a}_{ace}</u>
.00	0.0000	-∞
.05	-.0216	-.5279
.10	-.0455	-.2093
.15	-.0538	-.1468
.20	-.0530	-.1501
.25	-.0515	-.1554
.30	-.0524	-.1531
.35	-.0546	-.1484
.40	-.0565	-.1453
.45	-.0583	-.1429
.50	-.0622	-.1386
.55	-.0705	-.1312
.60	-.0828	-.1221
.65	-.0970	-.1138
.70	-.1125	-.1061
.75	-.1386	-.0966
.80	-.2011	-.0787
.85	-.3382	-.0500
.90	-.5679	-.0175
.95	-.7934	.0000
1.00	-∞	0.0000

TABLE 16--Continued

V. P = 100,000 psi

A ₁	= 0
A ₂	= -1.48010
A ₃	= 16.6617
A ₄	= -100.969
A ₅	= 353.968
A ₆	= -735.511
A ₇	= 848.097
A ₈	= -369.867
A ₉	= -238.518
A ₁₀	= 334.640
A ₁₁	= -107.022

<u>x_{ace}</u>	<u>ln a_{cs2}</u>	<u>ln a_{ace}</u>
.00	0.0000	- ∞
.05	-.0222	-.4378
.10	-.0454	-.1260
.15	-.0517	-.0775
.20	-.0485	-.0920
.25	-.0447	-.1055
.30	-.0429	-.1103
.35	-.0417	-.1127
.40	-.0397	-.1161
.45	-.0378	-.1187
.50	-.0394	-.1170
.55	-.0473	-.1099
.60	-.0613	-.0996
.65	-.0777	-.0900
.70	-.0940	-.0819
.75	-.1179	-.0731
.80	-.1734	-.0573
.85	-.2953	-.0318
.90	-.4885	-.0042
.95	-.6163	.0000
1.00	- ∞	0.0000

APPENDIX VI

UNSUCCESSFUL SEALING PROCEDURES

Several other sealing methods were attempted before Poulter's (29) was decided upon. A number of "O" rings were used in attempting to seal in the manner of Winnick and Powers (47), whereby the "O" ring makes the actual seal with the sapphire and pressure cell wall (See Figure 36a). Five different compounds were tried: Neoprene, Silicone, Thiokol, Viton and Teflon. The first four did not seal due to their rapid dissolution in the acetone-carbon disulfide mixture. The Teflon ring never seemed to make a seal due to its "cold-flow" or plastomeric behavior. A Teflon covered Silicone "O" ring was then tried, but it too failed to make a seal either at the sapphire or cell wall (See Figure 36b).

To eliminate this problem, a seal was designed which would not require the use of an "O" ring. As shown in Figure 36c) two copper rings were constructed for each sapphire which would act to make an unsupported area seal, the initial seal being obtained by driving the end plugs firmly into the rings and steel inner plug. This seal proved effective to about 50,000 psi above which pressure leakage occurred.

Other seals utilizing the same principle were attempted, as shown in Figure 36d) and e), also with unsuccessful results. Those rings with large angle S (See Figure 36d) and hence high mechanical

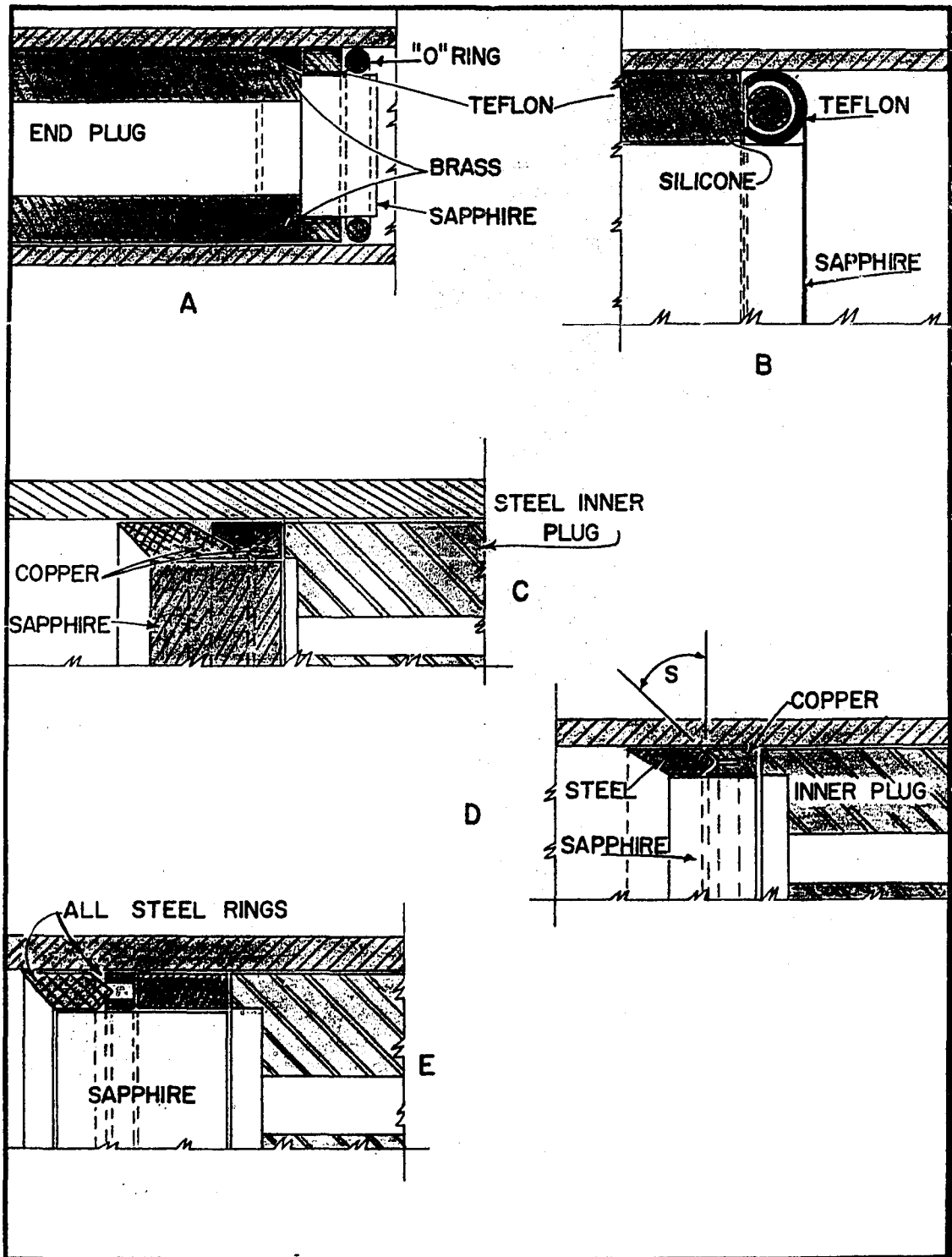


Figure 36.--Unsuccessful Sealing Devices

advantage, would break the sapphire under pressure while those with smaller angles would not affect a seal. There undoubtedly is some configuration which would allow a non-"O" ring seal to be made; however, it would seem to be a problem which only costly trial and error procedures can solve.